OMICS COMPARISON OF TWO COMMON BEAN GENOTYPES AND STUDY OF *pvSPS4* KNOCKDOWN IN COMPOSITE PLANTS UNDER SALINE CONDITIONS

by

Harun Niron

B.S., Molecular Biology and Genetics, Boğaziçi University, 2012

M.S., Molecular Biology and Genetics, Boğaziçi university, 2015

Submitted to the Institute for Graduate Studies in
Science and Engineering in partial fulfillment of
the requirements for the degree of
Doctor of Philosophy

Graduate Program in Molecular Biology and Genetics

Boğaziçi University

2021

ACKNOWLEDGEMENTS

Initially I would like to express my special thanks to my supervisor Prof. Müge Türet for her guidance, valuable critics, and encouragement during this study. I am thankful for her invaluable support in both academic and personal conditions, and I am particularly grateful for her complete trust in me.

I would also like to thank members of the thesis committee, Asst. Prof. Igor Kryvoruchko and Asst. Prof. Emrah Nikerel for their constructive feedback throughout my study. I am also thankful to additional committee members, Prof. Yelda Özden Çiftçi and Asst. Prof. Steven Footitt, for taking their time to evaluate this thesis.

I enjoyed being part of the MBG family at Bogazici University. I am lucky to have known Prof. Esra Battaloğlu, Prof. Arzu Çelik and Assoc. Prof. Stefan H. Fuss for their support, mentoring and friendship along the way. I am grateful to Ümit Bayraktar, Aslı Gündoğdu and Cenan Özbakır as they dealt with all my problems during these years. I would like to express my gratitude to my previous colleague Dr. Mahmut Can Hız for his scientific contribution to my career and to İsmail Tuğberk Kaya for his friendship and support. I also made great friends during my study and would like to thank all: Nazmiye Özkan, Seden Tezel, Yiğit Kocagöz, Mehmet Can Demirler, Barış Can Mandacı, Aysu Alkiraz, Zeynep Dokuzluoğlu, Sinay Mollamustafaoğlu, Dr. Aslı Uğurlu and Dr. Burçak Özeş.

I would like to express my special thanks to my family, especially to my mother Hülya Niron, for their endless love and support. I could not finish this extensive and intense study without them. I am also grateful for having my close friend Mehmet Debbağ by my side throughout this journey as his support and friendship was invaluable. I also would like to thank Boğaziçi University Scientific Research Projects (BAP 14925 and BAP 16842) for supporting this study.

Finally, I would like to express my sincere gratitude for my colleague, friend, and dear wife, Dr. Ayşe Candayan. Her love made life much colorful, simpler, and joyful. Her presence was enough for me to smile during the most challenging periods, and she was always successful in comforting me. I am extremely lucky to have you and your love in my life.

ABSTRACT

OMICS COMPARISON OF TWO COMMON BEAN GENOTYPES AND STUDY OF *pvSPS4* KNOCKDOWN IN COMPOSITE PLANTS UNDER SALINE CONDITIONS

Soil salinity is an abiotic stress factor that limits global agricultural output. Common bean is an important protein source in developing countries, however sensitive to salinity. To understand the underlying mechanism of salt stress responses, transcriptomics, metabolomics, and ionomics analyses were performed on both salt-tolerant and susceptible common bean genotypes under saline conditions. Transcriptomics revealed enhanced photosynthesis together with active carbon and amino acid metabolism in the tolerant genotype. Metabolomics revealed increased carbohydrate and amino acid metabolism in the tolerant genotype. Ion content comparison indicated that the tolerant genotype blocked the accumulation of Na^+ in the leaves. The results of this omics study have demonstrated the differences in contrasting genotypes and provided information on the novel mechanisms salt tolerance to pinpoint genes with high potential for functional analyses. Stress-related carbohydrate metabolism is a dynamic network and disruptions in this system can have negative effects on tolerance. Sucrose phosphate synthase (SPS) enzymes operate in the sucrose synthesis pathway and have significant roles in sugar metabolism. This study has focused on the function of SPS homolog, *pvSPS4*, in the roots of salt-tolerant common bean under salt stress. Composite common bean plants with *pvSPS4* knockdown roots exhibited sensitivity to salinity. Disturbed root carbohydrate and ion balance resulted in a reduction in photosynthesis together with osmoregulation and antioxidant capability. These results indicate that *pvSPS4* is an important gene for carbohydrate balance regulation in the salt-stress response in the common bean root tissues.

ÖZET

TUZ STRESİ ALTINDA İKİ FASÜLYE GENOTİPİNİN OMİKS KARŞILAŞTIRMASI VE KOMPOZİT FASÜLYEDE *pvSPS4* GENİNİN SUSTURULMASININ İNCELEMESİ

Toprak tuzluluğu, küresel tarımsal üretimi sınırlayan önemli bir stres faktörüdür. Fasulye, tuzluluğa duyarlı olmakla birlikte gelişmekte olan ülkelerde önemli bir protein kaynağıdır. Tuz stresi tepkilerinin altında yatan mekanizmayı anlamak için, tuzlu koşullar altında hem tuza dayanıklı hem de duyarlı fasulye genotipleri üzerinde transkriptomik, metabolomik ve iyonomik analizler yapıldı. Transkriptomik analiz, tuzlu koşullarda dayanıklı genotipin daha aktif karbon ve amino asit metabolizmaları ile birlikte artmış fotosentez sergilediğini göstermiştir. GC-MS ile metabolit analizi, toleranslı genotipte artan şeker içeriği ile etkin amino asit ve karbonhidrat metabolizmasını işaret etmiştir. İyon içeriği karşılaştırması, toleranslı genotipin yapraklarda Na^+ birikimini engellediğini göstermiştir. Bu omik çalışmasının sonuçları, zıt genotiplerdeki farklılıkları göstermiş ve fonksiyonel analizler için yüksek potansiyele sahip genleri saptamak için tolerans mekanizmaları hakkında bilgi sağlamıştır. Strese bağlı karbonhidrat metabolizması dinamik bir ağdır ve bu sistemdeki aksamaların tolerans üzerinde olumsuz etkileri olabilir. Sükroz fosfat sentaz (SPS) enzimleri, sükroz sentezi yolağında çalışır ve şeker metabolizmasında önemli rollere sahiptir. Çalışma, tuz stresi altında, tuza dayanıklı fasulye genotipinin köklerinde SPS homologu *pvSPS4*'ün işlevine odaklanmıştır. *pvSPS4* anlatımı azaltılmış köklere sahip kompozit fasulye bitkileri, tuzluluğa karşı hassasiyet sergilemiştir. Bozulmuş kök karbonhidrat ve iyon dengesi, ozmoregülasyon ve antioksidan kapasitesi ile birlikte fotosentezde bir azalma ile sonuçlanmıştır. Sonuçlarımız, *pvSPS4*'ün, kök dokularında tolerans açısından, karbonhidrat dengesi regülasyonu için önemli bir gen olduğunu ima etmektedir.

TABLE OF CONTENTS

LIST OF FIGURES

LIST OF TABLES

LIST OF SYMBOLS

%	Percent
°C	Degree Celcius
A	Absorbance
dS	deciSiemens
g	Gram
h	Hour
mg	Milligram
min	Minutes
ml	Milliliter
mM	Millimolar
s	Second
μg	Microgram
μl	Microliter

LIST OF ACRONYMS/ABBREVIATIONS

APS	Ammonium Persulfate
APX	Ascorbate Peroxidase
BSA	Bovine Serum Albumin
CAT	Catalase
cDNA	Complementary Deoxyribonucleic Acid
chl a	Chlorophyll a
chl b	Chlorophyll b
CO_2	Carbon Dioxide
DADM	Differentially Accumulated/Depleted Metabolites
DEG	Differentially Expressed Gene
dH_2O	Distilled Water
DNA	Deoxyribonucleic Acid
dNTP	Nucleoside Triphophate Mixture
EC	Electrical Conductivity
EDTA	Ethylenediaminetetraacetic Acid
EL	Electrolyte Leakage
ELISA	Enzyme-Linked Immunosorbent Assay
FC	Fold Change
FDR	False Discovery Rate
FW	Fresh Weight
GC	Gas Chromatography
GMO	Genetically Modified Organism
GO	Gene Ontology
HCl	Hydrochloric Acid
ID	Identification Number
ihpRNA	Intron Containing Hairpin RNA
IL	Ispir Leaf
IR	Ispir Root

KEGG	Kyoto Encyclopedia of Genes and Genomes
LB	Luria-Bertani
LC	Liquid Chromatography
Misc.	Miscellaneous
MS	Mass Spectrometry
MSTFA	N-Methyl-N-(Trimethylsilyl)-Trifluoroacetamide
NaCl	Sodium Chloride
NRT	Nitrate Transporter
ns	Not Significant
PBS	Phosphate Buffered Saline
PCA	Primary Component Analysis
PCR	Polymerase Chain Reaction
PEP	Phosphoenolpyruvate
ppt	Parts Per Thousand
PVDF	Polyvinylidene Fluoride
pvNRT1	*Phaseolus vulgaris* Nitrate Transporter 1
pvSPS4	*Phaseolus vulgaris* Sucrose Phosphate Synthase 4
QC	Quality Control
qPCR	Quantitative Polymerase Chain Reaction
Ri	Root Inducing
RIN	RNA Integrity Number
RNA	Ribonucleic Acid
RNAi	Ribonucleic Acid İnterference
RNA-seq	RNA Sequencing
RT-qPCR	Reverse Transcription-Quantitative PCR
RWC	Relative Water Content
SDS	Sodium Dodecyl Sulfate
SDS-PAGE	Sodium Dodecyl Sulfate-Polyacrylamide Gel Electrophoresis
SEM	Standard Error of Mean
SPP	Sucrose Phosphatase
SPS	Sucrose Phosphatase Synthase

T	Temperature
TBE	Tris Borate EDTA
TBS	Tris Buffered Saline
TBS-T	Tris Buffered Saline with Tween-20
T-DNA	Transfer Deoxyribonucleic Acid
TEMED	Tetramethyl Ethylenediamine
TL	TR43477 Leaf
TMCS	Trimethylchlorosilane
TR	TR43477 Root
UDP	Uridine Diphosphate
WB	Western Blot

1. INTRODUCTION

A soil is considered saline if it contains enough soluble salt to have detrimental effects on the growth of crop plants. Saline soil is roughly defined as soil with electrical conductivity of saturated extract (EC_e) equal or higher than 4 dS m^{-1} [1]; but the majority of common crop yields display reduction even at lower EC_es [2, 3].

Salt accumulation has become one of the most imminent agricultural threats in recent years. It is estimated that nearly 20% of cultivated and 33% of irrigated farmland has been affected globally [4] (Figure 1.1) and, these percentages are expected to increase annually through diverse causes; such as excessive evaporation, improper irrigation or inadequate precipitation. Projections demonstrate that, at this rate, the amount of salt-affected arable farmlands will reach 50% by 2050 [2]. The scene becomes more disturbing considering that many agriculturally significant products such as rice, maize, potato, tomato, and legumes are rather susceptible to salinity [5]. Furthermore, predictions indicate that by the year 2050, the human population will surpass 9 billion, which will escalate the demand for an increase in food production up to 70% [6]. All these forecasts establish the importance of enhanced agricultural productivity for the sustainability of human life on Earth.

Although various salts contribute to soil salinity, sodium chloride (NaCl) is the most significant. Elevated NaCl disrupts diverse systems necessary for consistent plant growth and development [4, 7]. It leads to two types of generalized stress for plants: osmotic and ionic stress. Osmotic stress is induced by decreased water potential and water availability for the plant. Ionic stress, on the other hand, is caused by toxic ion accumulation over time [8]. These stress factors create a network of restraints on survival, not just with ion toxicity and water retention, but also with nutrient and metabolic imbalances that collectively become a physiological response [9].

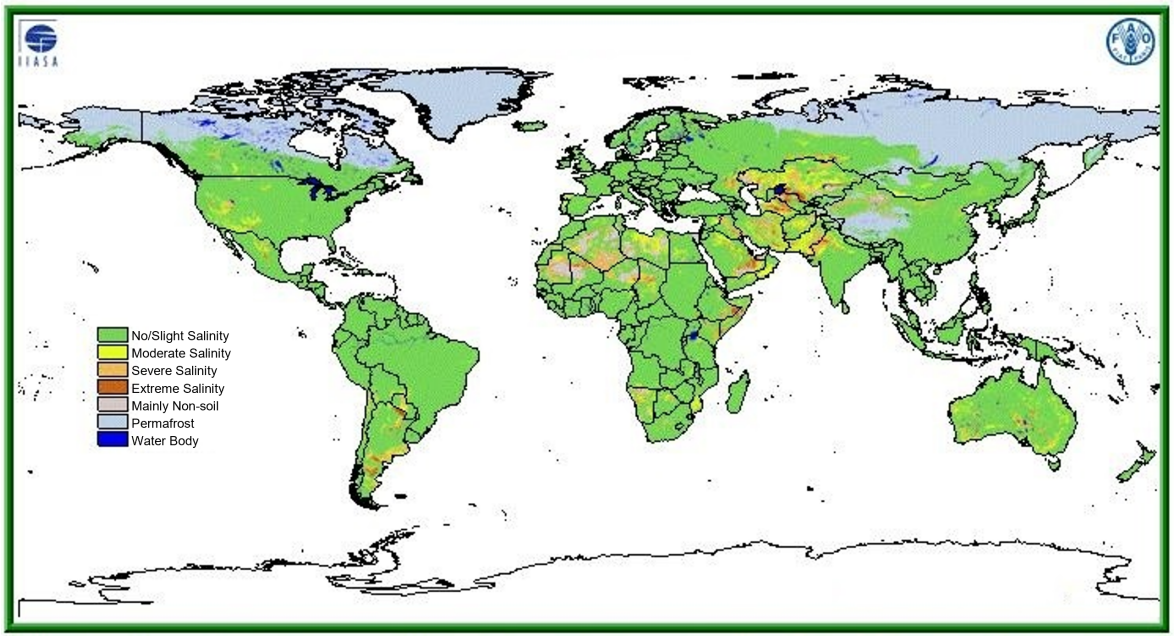

Figure 1.1. Global soil salinity map displaying the affected areas such as Middle East and South East Asia. Reproduced with permission from FAO of UN - Harmonized World Soil Database v 1.2.

Understanding this response is a laborious task and requires a comprehensive strategy against these stress factors. Essentially plants employ water homeostasis control and adjustment of osmotic balance, salt exclusion, sequestration, oxidative protection, regulation of potassium exchange, biochemical responses, and growth regulation to cope with salt stress [3, 4, 9, 10]. As there is a complex network of connections between these systems, tolerance to salt can be defined as a character driven by genetic interactions involving the regulation of thousands of genes [11, 12]. This complexity can be reduced by making a comparison among species and varieties of plants that have evolved distinct mechanisms to tolerate salinity. Though there are very similar strategies involved among tolerant and susceptible plants, differential regulation of the responses can point out the key elements of the salt tolerance mechanisms [13].

Common bean (*Phaseolus vulgaris* L.) is a grain legume with substantial agricultural importance. As a rich source of vitamins, minerals, and dietary proteins it is essential nutrient for human consumption, especially for the developing countries.

It represents approximately half of the produced and consumed grain legumes in the world [14]. However, common bean is fairly susceptible to salt stress; this crop can suffer nearly 20% yield loss even in slightly saline soil with 1 dS m^{-1} EC_e [15]. This inconvenience can be mitigated by using salt-tolerant varieties of common bean such as the variety Ispir [16], but this solution may not be sustainable against increasing soil salt content.

1.1. Comparative Transcriptome, Metabolome, and Ionome Study

Transcriptome analysis of common bean (Ispir variety) by our group was the first publication on the omics-based approach on common bean under salt stress [17]. This study provided an important database for the wider community, and contributed to our general knowledge of stress-related genes, particularly in legumes.

It is crucial to remember that the phenotype is the outcome of the blending of dynamic interactions and regulation between various factors such as DNA, RNA, proteins, and metabolites together with the influence of the environment. This is why genome-scale and transcriptome-based studies demand complementary studies such as proteomics and metabolomics to form reliable descriptions of distinct phenotypes [18] (Figure 1.2). In this context, while gene and protein expression exhibit the capacity and inclination of a plant in response to environmental conditions, metabolite content forms the link between expression and environment [18].

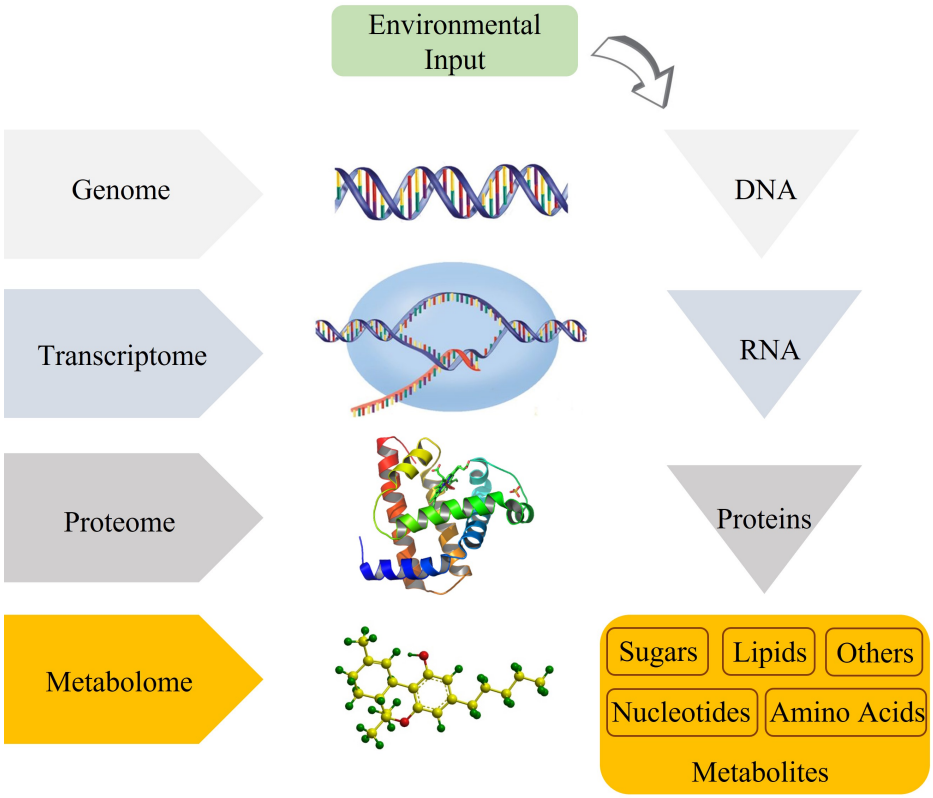

Figure 1.2. Relationship of omics with generic elements and environment.

Metabolomics deals with the detection, measurement, and evaluation of the small molecules (low molecular weight metabolites) in an organism depending on the functions of time, developmental stage, and conditions [19]. However, metabolomics, even with the state-of-the-art technologies, is difficult because of the numerous small molecules with variable frameworks and chemical features. For example, *Arabidopsis thaliana* possesses more than 5000, mostly unidentified metabolites. Unlike transcriptomics, in metabolomics, there is no specific way for the identification and quantification of all metabolites. The focus and coverage of the technique depend on the combination of suitable extraction, separation and detection (usually mass-spectrometry) methodologies [20]. The selection for the specific class of metabolites depends on the separation procedure. For plant samples, gas chromatography (GC) is preferred for the detection of the primary metabolites such as amino acids and sugars [21]. However, liquid chromatography (LC), with its flexibility, can be modified to detect various metabolite groups, and is mainly used for the analysis of the secondary metabolites [19].

Another concern in metabolomics studies is the data analysis procedure; the metabolites should be annotated for meaningful results. There are a handful of public databases [22, 23] for GC-MS data so primary metabolite annotation is considered quite reliable at this point. On the contrary, no inclusive database is available for the annotation of secondary metabolites [24, 25].

In any given situation, the metabolite content of a plant is associated with the gene expression profile. The function of a metabolic pathway requires both the activity of the enzymes, the supply of precursor and intermediate compounds. The product can yield a bioactive molecule such as a signaling compound, a structural component, an antioxidant, a hormone, and so on. The study of the metabolome, together with a gene expression profile can be a useful instrument for the evaluation of the signaling, defense, structural and other systems used in plant tolerance to stressful conditions [26, 27]. Examples of the practical use of metabolomics in studies of heavy-metal [28], UV-light [29], drought [30], alkali [31] and salt stresses [32, 33] together with studies on the effect of *Pseudomonas syringae* pv. [34] and thrips [35] have proven metabolomics to be a useful technique for the characterization of both abiotic and biotic tolerance mechanisms in plants. Moreover, studies with genetically modified wheat [36], tomato [37] and tobacco [33] have indicated its importance in the assessment of GM crops.

In addition to transcriptomics and metabolomics, a comparative study of plant-environment interaction can be augmented by the addition of an ionomics analysis. The ionome of an organism represents the mineral composition and inorganic constituents in a given condition. The ionome can be considered the inorganic branch of the metabolome. Ionome analysis (ionomics), produces a qualitative and a quantitative report of the elemental composition [38]. Comparative ionomics in our case highlights the adjustments and differences in elemental composition in these salt tolerant and susceptible common bean genotypes. It is well known that the regulation of Na^+ and K^+ homeostasis [39] and Ca^{2+} signaling [40] are important in salt stress tolerance. Also, other major ions such as Mg^{2+} [41] and Fe^{2+} [42] are shown to possess regulatory roles in abiotic stress tolerance as well as their roles in the primary metabolism.

The aforementioned transcriptome study of two varieties of common bean with differing salt tolerance manifests high ambiguity due to insufficient number of biological replications. Thus, in the first part of this study, we repeated this study with enough biological replicates and combined it with metabolomics and ionomics studies on the root and leaf tissues of these two common bean varieties under salt stress. The results were mapped on the common bean metabolic network to further investigate novel tolerance pathways (Figure 1.3).

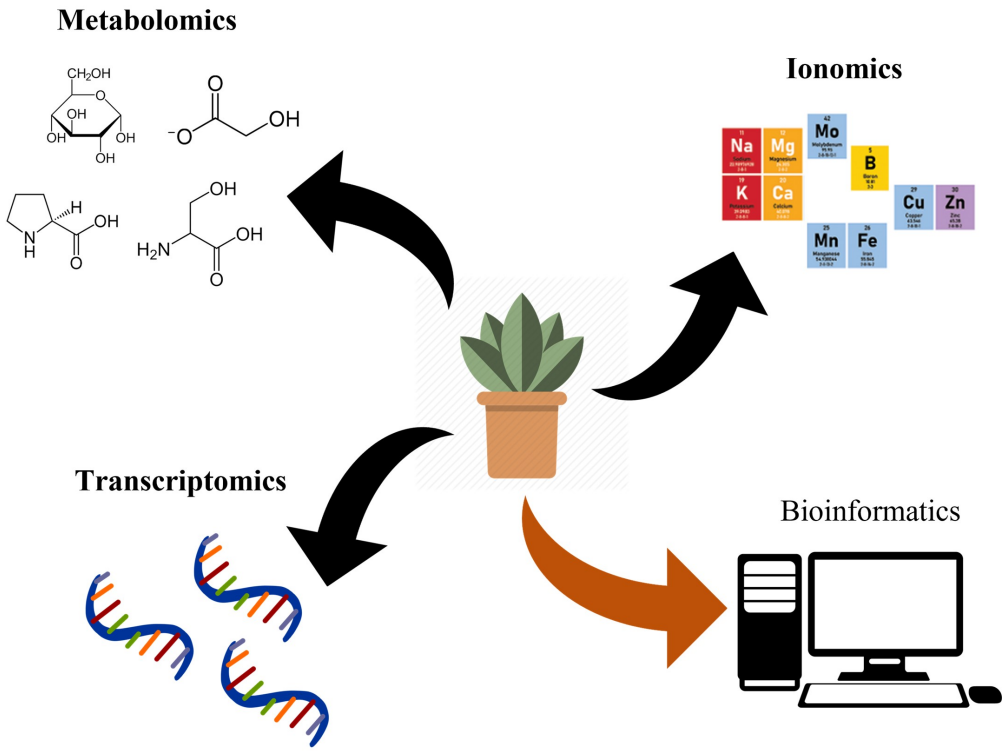

Figure 1.3. The overall structure of the omics study.

The focus of the metabolomics analysis was on the primary metabolites not just due to the aforementioned reliability and ease of this kind of analysis, but because any variation in the primary metabolism constitutes a significant factor in tolerance. Actually, primary metabolites like amino acids, sugars, sugar-alcohols, and most of the molecules in the photosynthesis pathway are actively regulated during salt stress; biosynthesis and catalysis of these metabolites creates a complex regulatory network that may provide fundamental information about the salt tolerance mechanisms [43].

Moreover, the obtained results shed light on the selection of candidate salt-responsive genes for further functional studies.

1.2. Role of *Sucrose Phosphate Synthase 4* in Root Tissues Under Salt Stress Conditions

Environmental stresses like drought, salinity, extreme temperatures, insufficient light, and pathogens may cause a significant reduction in photosynthetic capacity in plant sugar-exporting (source) tissues which results in decreased soluble sugar supply to the sugar-importing (sink) tissues [44, 45]. Stress-related sugar metabolism is a highly dynamic process. Changes in CO_2 assimilation, leading to fluctuations in soluble carbohydrate content, disrupt the source-sink carbon partitioning and the regulation of this requires the activation or deactivation of many proteins and genes [46,47]. Since source-sink partitioning is directly related to the distribution of energy and resources over the plant, it is a key component of stress tolerance [48, 49]. Moreover, since soluble carbohydrates have roles as primary messengers and regulate the expression of numerous genes, the interruption of CO_2 assimilation and partitioning may result in extensive complications for the plant [50–52].

Sucrose is the main output of photosynthetic CO_2 assimilation. It can be directly consumed by glycolysis for energy production or translocated through phloem within the plant to the sink tissues. Sucrose is the most abundant soluble storage carbohydrate and it also functions as a signaling molecule that regulates metabolism [53]. Plants utilize around 80% of the CO_2 that is assimilated during the photosynthetic process for sucrose synthesis. This is essential for development as sucrose is the main element for carbon transport from source to sink organs [54] to be utilized for metabolic maintenance, cell wall synthesis, respiration, or starch production for later use [55, 56].

Sucrose not only acts as an energy and signaling element for the the plants but also functions as an osmolyte during water stress to prevent cellular damage. Thus, regulation of sucrose transport and distribution is crucial for stress response [47, 57].

The concentration of sucrose in phloem sap, the main form of transported carbon, is affected by abiotic stresses [46]. In Arabidopsis, a boost in the phloem sap sucrose concentration seen under drought and saline conditions serves to maintain the water potential under such osmotic stress [58,59]. Maintenance of sucrose homeostasis among tissues in crop plants is proposed to have great potential for sustaining growth and development under stress conditions [60]. In agreement with this, studies demonstrated the prioritized partitioning of carbon assimilates to root tissues in the initial phases of water stress [61].

Synthesis of sucrose is catalyzed by *sucrose phosphate synthase* (SPS) and *sucrose phosphatase* (SPP) enzymes. This process is restricted to plants, cyanobacteria, and proteobacteria. SPS performs the reversible transfer of a glycosyl group from an activated donor sugar, uridine diphosphate glucose, to an acceptor fructose-6'-phosphate molecule in the first step of the sucrose synthesis pathway. The resulting sucrose-6'-phosphate molecule, is then dephosphorylated to produce sucrose through an irreversible reaction by SPP [62] (Figure 1.4). The SPS catalyzed reaction is a rate-limiting step in sucrose synthesis [63, 64]. This enzyme has a central role in carbon partitioning between starch synthesis and the accumulation of soluble sugars in numerous physiological processes [65–68] as well as sucrose translocation from the source to sink tissues [69].

Plants possess multiple homologs of SPS, and their expression depends on tissue type, developmental stage, and environmental conditions [68,70,71]. Also, the activity of SPS may increase [72] or a decrease [73] under salt stress depending on the species or genotype. While SPS activity in wheat [74], and rice leaves [75] increases in drought stress, in soybean SPS activity has demonstrated both increase and decrease depending on the developmental stages, tissues, and SPS homologs [76]. Another study with cold-stressed maize also displayed the genotype dependency of the SPS regulation [77]. This range of variability suggests a wide functional and regulatory activity for SPS homologs.

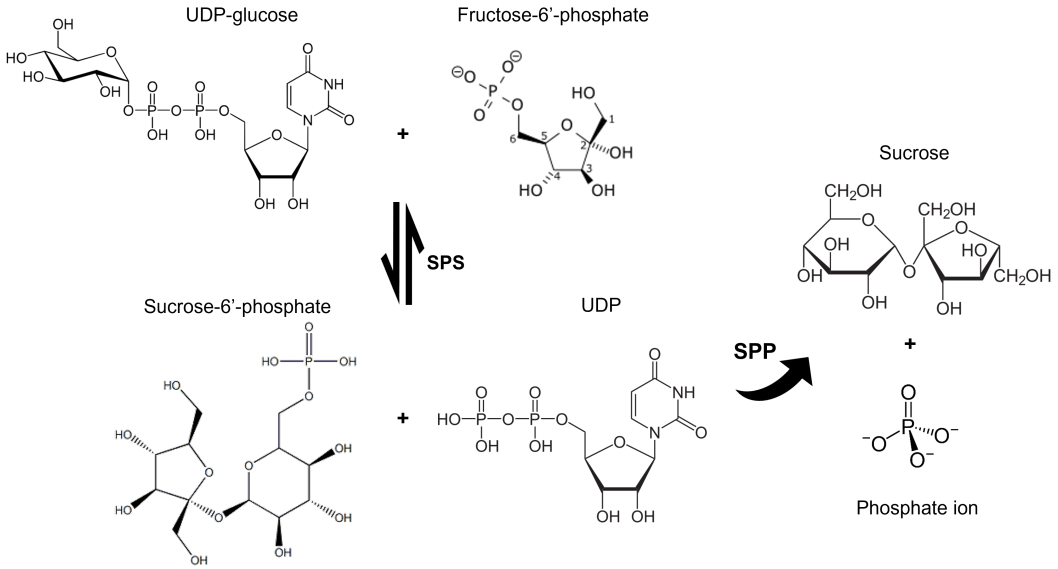

Figure 1.4. Synthesis of sucrose molecule by SPS and SPP enzymes.

There has been extensive research on the function and regulation of SPS genes in photosynthetic tissues [63, 65, 68]. However, the role of SPS enzymes in non-photosynthetic tissues, such as roots, where sucrose is imported, is not yet clear. SPS may have two possible roles in these tissues: It may take part in the sucrose re-synthesis following import through apoplastic cleavage to glucose or fructose or it may be directly engaged in the sugar regulatory cycle with the coordination of sucrose/starch balance [67]. Either case has significant potential to directly connect with stress tolerance pathways; thus, further attention is required for a better understanding of the role of SPS in plant root metabolism as well as stress tolerance.

Agrobacterium rhizogenes mediated hairy root transformation is particularly convenient for plant species that are hard to transform with *Agrobacterium tumefaciens* as it yields high transformation rates in shorter periods compared to the latter. *A. rhizogenes* is a gram-negative soil bacterium that promotes stable introduction of a T-DNA region into the plant genome using a root-inducing (Ri) plasmid. Root locus (*rol*) genes that are introduced in to the T-DNA region, such as *rolA*, *rolB*, *rolC* and *rolD*, induces hairy root formation at infection site [78]. This method can be used for generation of wild-type shoot transgenic root composite plants for further analysis [79].

The newly emerged hairy roots are generally non-chimeric and quite similar to wild-type roots in the phenotypic and structural sense. They develop with a high rate of plagiotropic root development through lateral branching [80, 81].

The *A. rhizogenes* mediated hairy-root transformation procedure is a rapid, easy, and efficient system that can be readily applied to Phaseolus genus subspecies [82, 83]. Furthermore, the great advantage is that it enables direct investigation of roots as they are the first organ interact with salt in the soil. Since different tissues respond differently to salinity, this methodology, by modifying the root but not shoot genome, offers a reliable and fast approach to evaluate the effect of a root-exclusive genetic modification on the whole plant under saline conditions. In the second part of this study, we took advantage of this methodology to elucidate the effect of common bean *SPS4* (*pvSPS4*) knockdown in the root tissues of Ispir genotype under salt tolerance.

2. PURPOSE

Natural plant varieties give us a chance to compare and understand the diverse responses of plants to environmental signals such as abiotic stress factors. The main purpose of this project was to compare the tolerance response of two common bean genotypes under salt stress to unravel novel salt tolerance mechanisms. A multi-omics-based approach was chosen combining transcriptomics, metabolomics and ionomics to give a broad overview of the impact of salt stress on diverse metabolic pathways at multiple levels. To provide this perspective for the interpretation of the mechanism behind distinct phenotypes, the omics datasets were overlayed to metabolic pathways maps demonstrating the differentially enriched pathways on both expressional and metabolic levels to illuminate the regulatory pathways important in salt tolerance.

The secondary aim of this study was to identify the role of root-specific, salt-responsive, sugar metabolism gene *pvSPS4*, that was uncovered in the omics part, in the tolerance mechanism. The knockdown study, utilizing the *A. rhizogenes* mediated hairy root transformation, provided clues on the function of this sucrose metabolism gene in the root tissues under salinity stress. Furthermore, the results also contributed to the general literature about the functioning of SPS genes in non-photosynthetic tissues.

3. MATERIALS

3.1. General Enzymes, Kits, and Reagents

Enzymes, kits and reagents used in this study are listed in Table 3.1.

Table 3.1. List of general enzymes, kits, and reagents.

Name	Model
Plasmid Extraction	740615 Nucleospin Plasmid Quickpure, Macherey-Nagel, DE
cDNA Synthesis	K1622, First Strand cDNA Synthesis, Thermo Scientific, US
DNA Ladder	SM0311, GeneRuler 1 kb DNA Ladder, Fermentas, US
DNA Loading Dye	B7021S, Fermentas, US
LR Clonase	11791, Gateway LR Clonase II Enzyme Mix, Life Technologies, US
BP Clonase	11789, Gateway BP Clonase II Enzyme Mix, Life Technologies, US
qPCR Master Mix	K0221, Maxima SYBR Green/ROX qPCR Master Mix, Thermo Scientific, US
DNA Polymerase	EP0711, DreamTaq Green DNA Polymerase, Thermo Scientific, US
	F-530S, Phusion High-Fidelity DNA Polymerase, Thermo Scientific, US
dNTPs	10mM PCR Nucleotide Mix, Promega, US
RNA Extraction	15596-026, TRIzol Reagent, Invitrogen, US
	74904, RNeasy Plant Mini Kit, Qiagen, US
Gel Extraction Kit	K0691, Genejet Gel Extraction Kit, Thermo Scientific, US
Glucose/Sucrose Assay Kit	MBS841570, Mybiosource, US
SPS ELISA Kit	MBS269987, Plant Sucrose Phosphate Synthase ELISA Kit, Mybiosource, US
WB luminol reagents	ECLP0250, ECL Pico, Expedeon, UK
	34095, SuperSignal West Femto Maximum Sensitivity Substrate Thermo Scientific, US
Protease inhibitor cocktail tablets	11873580001, Roche, US

3.2. Chemicals, Plastics, and Glassware

Chemicals were acquired from either Alfa-Aesar (US), Merck (DE), Duchefa (NL), or Sigma-Aldrich (US) if not specified otherwise; mini-centrifuge tubes and tips from Axygen (US), 50 and 15ml centrifuge tubes from CAPP (DE) sterile plates from Interlab (DE). Glasswares were purchased from VWR (US). Sterilization for all glassware, tips, and tubes was performed by autoclaving at 121°C for 20 min before use.

3.3. Equipment

The equipment used in this study is listed in Table 3.2.

Table 3.2. List of equipment used in omics and physiological studies.

Name	**Model**
Agarose Gel Electrophoresis	Minicell Primo EC320 Electrophoretic Gel System, Thermo Scientific, US
Autoclaves	Model MAC-601, Eyela, JP
	Model ASB260T, Astell, UK
Balances	AY123, Satorius, DE
Centrifuges	5453000 MiniSpin Plus Benchtop Centrifuge, Eppendorf, DE
	Allegra X-22, Beckman, US
	J2-MC Centrifuge, Beckman, US
	J2-21 Centrifuge, Beckman, US
Deep Freezers (-20°C)	A2021-D, Arçelik, TR
Deep Freezers (-80°C)	Forma 860-ULT, Thermo Scientific, US
Ice Machine	Scotsman Inc. AF20, IT
Magnetic Stirrer	0004810000 IKA RCT basic Safety Control, DE
Scanner	GT-20000 Scanner, Epson, JP
	C1000 Thermal Cycler, Bio Rad, US
Thermal Cycler	Runik Thermal Cycler, Sacem Life Technologies, TR
Incubator	EN500 Nüve, TR
Microwave	MD55I, Arçelik, TR

Table 3.2. List of equipment used in omics and physiological studies. (cont.)

Name	**Model**
Gel documentation systems	Gel Doc XR System, Bio Rad, US
	SynGene, Bio Rad, US
Micro-centrifuge	Himac CT15RE, Hitaci Koki, JP
Microplate Reader	680, Bio Rad, US
Oven	Gallenkamp 300, UK
pH Meter	HI 83141, Hanna, US
Pipettes	Pipetman Classic, Gilson, US
Power Supply	164-5050 PowerPac Basic, Bio Rad, US
	EC250-90, Thermo Scientific, US
Refrigerator (4°C)	MFAA1, Hotpoint Ariston, IT
Rotors	JS-7.5 Beckman, US
	JA-14 Beckman, US
Spectrophometer	DU-730 UV/Vis Spectrophotometer, Beckman, US
	NanoDrop1000, Thermo Scientific, US
Vortex	NM110, Nüve, TR
Gartengold Torf	Substrate1, SAB, DE
Plant Growth Chamber	JSPC-960, JSR, KR
Real Time PCR System	PikoReal96, Thermo Scientific, US
Vacuum-concentrator	Savant DNA120 SpeedVac Concentrator, Thermo Scientific, US
Gas Chromatography (GC)	6890 N Network GC system, Agilent, US
Mass Spectrometer for GC	5973 Inert Mass Selective Detector, Agilent, US
ICP-MS	7700 Series ICP-MS, Agilent, US
ICP-OES	700 Series ICP-OES, Agilent, US
Blotting Apparatus	Mini Trans-Blot Cell, Bio-Rad, US
Electrophoresis System	Mini-Protean III Cell, Bio-Rad, US
Fluorescence Microscope	Observer Z1, Zeiss, DE
Conductivity Meter	Aquapro, HM Digital, US

3.4. Buffers and Solutions

Buffers and solutions used in this study are listed in Table 3.3.

Table 3.3. Buffers and solutions for cloning and molecular analyses.

Name	Content
LB Medium	10g/L Tryptone
	5g/L NaCl
	5g/L Yeast Extract
LB Agar	10g/L Tryptone
	5g/L NaCl
	5g/L Yeast Extract
	15g/L Agar
Spectinomycin	50mg/ml in ddH_2O
Gentamicin	30mg/ml in ddH_2O
6x Protein Sample Buffer	300mM Tris-HCl (pH 6.8)
	12mM EDTA
	60% glycerol
	12% SDS
	6% β-mercaptoethanol
	0.04% bromophenol blue
30% Acrylamide-Bisacrylamide Solution	29% acrylamide
	1% N,N'-methylenebisacrylamide
Ammonium Persulfate (APS)	10% APS (w/v) in dH_2O
Blocking Buffer	1-5% skim milk powder or BSA in TBS-T
Running Buffer	25mM Tris
	250mM Glycine
	0.2% SDS
Tris Buffer Saline (TBS)	20mM Tris-HCl (pH 8.0)
	150mM NaCl
TBS with Tween-20 (TBS-T)	0.1% Tween-20 in 1X TBS
Transfer Buffer	25mM Tris
	200mM Glycine
	20% Methanol

Table 3.3. Buffers and solutions for cloning and molecular analyses. (cont.)

Name	**Content**
Running Gel for Western Blotting	10% Acrylamide:Bisacrylamide (37.5:1)
	375mM Tris-HCl (pH 8.8)
	0.1% TEMED
	0.1% SDS
	0.1% APS
Stacking Gel for Western Blotting	4.5% Acrylamide:Bisacrylamide (37.5:1)
	125mM Tris-HCl (pH 6.8)
	0.1% TEMED
	0.1% SDS
	0.1% APS
Agarose Gel for Separation of DNA (1%)	1% (w/v) agarose in 0.5X TBE Buffer
	0.2 μg/ml Ethidium Bromide
Tris-Boric Acid-EDTA (TBE) Buffer (10X)	20mM EDTA (pH 8.3)
	0.89 M Tris-Base
	0.89 M Boric Acid
Phosphate Buffer Saline (PBS) pH 7.0 (100mM)	61:39 - Na_2HPO_4:NaH_2PO_4 (100mM)
Phosphate Buffer Saline (PBS) pH 7.8 (100mM)	91.5:8.5 - Na_2HPO_4:NaH_2PO_4 (100mM)
Acidic Ninhydrin	1.25g ninhydrin
	30ml glacial acetic acid
	20ml 6M orthophosphoric acid

Plant nutrient solutions used for hydroponics system are listed in Table 3.4 (Modified Hoagland solution) and Table 3.5 (B&D solution).

Table 3.4. Ingredients of modified Hoagland solution.

Macronutrients	**Concentrations (nM)**
$MgSO_4$	1.4
KH_2PO_4	0.02
$CaNO_3$	2.8
KNO_3	1.8

Table 3.4. Ingredients of modified Hoagland solution. (cont.)

Micronutrients	**Concentrations (nM)**
H_3BO_3	0
$MnSO_4$	1.1
$CuSO_4$	0.2
$NaMoO_4$	0.1925
$ZnSO_4$	0.5
$NaFe_3$ EDDHA	1

Table 3.5. Ingredients of B&D solution used for composite plant growth.

Macronutrients	**Concentrations (nM)**
$CaCl_2$	1
$KHPO_4$	0.5
Micronutrients	**Concentrations (uM)**
$MgSO_4$	250
K_2SO_4	250
$C_6H_5FeO_7$ (Ferric Citrate)	10
H_3BO_3	2
$ZnSO_4$	0.5
$CuSO_4$	2
$CoSO_4$	0.1
$NaMoO_4$	0.1
$MnCl_2$	1
Nitrogen Supplement	**Concentration (mM)**
KNO_3	8, 4 or 2

3.5. Biological Material

3.5.1. Plant Material

Phaseolus vulgaris L. (Ispir and TR43477 genotypes) seeds were supplied by Prof. Yıldız Dasgan from Çukurova University.

3.5.2. Bacterial Strains

Escherichia coli, DH5α strain was used for cloning experiments. *Agrobacterium rhizogenes*, K599 strain (supplied by Dr. Vojta Hudzieczek, Masaryk University, CZ) that is resistant to streptomycin (100µg/ml) and chloramphenicol (5µg/ml) was used for hairy-root transformation experiments.

3.5.3. Vectors

Gateway cloning vectors used in the knockdown study and their specifications are listed in Table 3.6.

Table 3.6. Specifications of Gateway cloning vectors.

Gateway Donor Vector	
Name	pDONR207
Application	Gateway Vector Transfer
Species	N/A
Bacterial Selection	Gentamycin (15µg/ml)
Type	Gateway Donor
Promoter	N/A
Supplied by	Dr. Giorgia Batelli, CNR-IGV, IT
Gateway Destination Vector	
Name	pK7GWIWG2_II-RedRoot
Application	Silencing (RNAi)
Species	Plant
Bacterial Selection	Spectinomycin (E.coli - 50µg/ml / A. rhizogenes - 150µg/ml)
	Fluorescence Reporter (dsRED)
Type	Gateway Destination
Promoter	35S
Supplied by	Dr. Roger Y. Tsien, HHMI, US

3.5.4. Primers

Primers used in RT-qPCR verification of RNA-seq analysis are listed in Table 3.7.

Table 3.7. Primer list for RT-qPCR verification of RNA-seq.

Transcript	**Sequence**	**Amplicon Size**	**Annealing Temperature (°C)**
Phvul.001G195700	TCTTGCCTTGATCTTCGG	172	53
	AGGTTTGAATAGAGGATGTG		
Phvul.002G027900	ACTCCAACAAACTCGAAACA	234	55
	CACATACCACTCGGACCA		
Phvul.008G170800	TGATCCCATTGCAAATCC	151	53
	TCCCCCCATAAAACCAAC		
Phvul.009G105300	CTCCACCTTTTCCACCAAC	157	56
	CTTCCCACTACTCCTATTCC		
Phvul.006G159600	GCTATGGTTCCAGCTTTT	120	54
	AGTTATTGGGGTTGGGTT		
Phvul.001G083000	CTCCTTTATCGCCTTCCT	230	54
	ACTTCCGCATTACCAACA		
Phvul.004G117100	GCCTTCTCTTTTACCTTCT	102	53
	ACACCACCATAATCCTCA		
Phvul.003G229500	GCTAGCTGTTCCATTTACGCAGAGT	100	60
	AGCTGCCGTAGAGTTTGATTGCACC		
Phvul.001G181100	GCAGCTCCCAACCACTGACTAC	186	58
	CCATCCAACCAAAGATCAACGCCCA		
Phvul.005G051600	AACCATGCCTTCACCAGCTTCAAAT	107	60
	AGGTTGTGGGAGAAGAAGATGTGGA		
Phvul.008G011000 (Actin-11)	TGCATACGTTGGTGATGAGG	190	58
	AGCCTTGGGGTTAAGAGGAG		

Primers used in cloning for the knockdown study are listed in Table 3.8.

Table 3.8. Gene-specific primers for the Gateway cloning. Asterisk displays the end of the Gateway adaptor sequence.

Gene	**Sequence**	**Amplicon Size**	**Annealing Temp. (°C)**
pvSPS4	GGGGACAAGTTTGTACAAAAAAGCAGGCTTC *ACCTCTCCCATGTTGAACA	280	72
	GGGGACCACTTTGTACAAGAAAGCTGGGTC *TCAGCAGCAACTACCACA		
pvNRT1	GGGGACAAGTTTGTACAAAAAAGCAGGCTTC *TCCACTAATTGCCTCAAACC	288	72
	GGGGACCACTTTGTACAAGAAAGCTGGGTC *GTCCACAGCTTCAGTAACA		
Human *ferritin*	GGGGACAAGTTTGTACAAAAAAGCAGGCTTC *TTACTGCTTTCACCTGCC	268	72
	GGGGACCACTTTGTACAAGAAAGCTGGGTC *CCAGCGGTGAATGTATGT		

Primers used in RT-qPCR verification of knockdown are listed in Table 3.9.

Table 3.9. Primer list for RTq-PCR verification of knockdown.

Transcript	**Sequence**	**Amplicon Size**	**Annealing Temp. (°C)**
Phvul.003G164000.1 (pvNRT1)	AGATCCAAAACTGGCGGTTG TGGCAGATGCATGACTGAGA	126	58
Phvul.005G002600.1 (pvSPS4)	GCAACTTTGGTCGGAGGATG GCTAGAGCACGAGCAAGTTC	153	59
Phvul.006G031700.1 (pvSPS3)	GCATTTCAACCCCACCAAGT TCTGGGTTTCCTCCCATTCC	194	58
Phvul.003G170100.1 (pvSPS1)	GCTATGGGAGATCCATGCCT CGAGGGTTGGTAAAGAAGCG	172	58

Primers used in vector sequencing are listed in Table 3.10.

Table 3.10. List of vector sequencing primers.

Vector	**Sequence**	**Annealing Temp. (°C)**
pDONR207	TCGCGTTAACGCTAGCATGGATCTC	49
	GTAACATCAGAGATTTTGAGACAC	

4. METHODS

4.1. Plant Growth, Salt-Stress Application, and Sample Collection

Ispir (salt-tolerant) and TR43477 (salt-susceptible) genotypes of common bean were grown, and salt-treated in hydroponic conditions to collect tissue samples. Seeds were sterilized in a 5% hypochlorite solution for 5min and then washed with distilled water. Germination was performed in vermiculite-containing plug trays under a 16-h light/8-h dark photoperiod at 24°C/20°C cycle with 50-70% relative humidity. Trays were irrigated daily with 1X Hoagland nutrient solution [84] until the plants reached to fully expanded foliage stage. Five seedlings from each variety were transferred to the hydroponics system. Salt treatment was carried on in the same conditions as in the transcriptome study on salt-tolerant common bean performed by Hiz *et al.* (2014) [17] to obtain correlated results. Gradual step acclimation method was employed to prevent osmotic shock [85]. After five days post-transfer hydroponics system, the plants were subjected to gradual NaCl treatment starting with 50mM first day, increased to 100mM on the second day, and set to 125mM on the third day. In total, the plants were grown under 125mM NaCl for three days before they were sacrificed for tissue sample collection.

4.2. RNA-sequencing and Transcriptome Analysis

4.2.1. RNA Extraction and Quality Assessment

Total RNA extractions for RNA-sequencing analysis were carried out with 100mg homogenized tissue, using RNeasy Plant RNA extraction kit according to the manufacturer's instructions. Quantification and qualification of the sample RNAs were performed with spectrophotometer as explained by Barbas *et al.* (2007) [86]. Quality and integrity of the RNA samples were also determined by 1% denaturing agarose gel electrophoresis with 5µl of sample.

4.2.2. Library Preparation and Illumina Sequencing

Preparation of cDNA library from total RNA and the RNA-sequencing were outsourced to Macrogen Inc. Truseq stranded mRNA kit (Illumina, US) was used for poly(A+) enrichment and cDNA library construction according to manufacturer instructions. Second strands were synthesized via DNA polymerase I and after PCR purification, Illumina sequencing adapters were ligated to the fragments, which will then be selectively enriched by PCR. The obtained paired-end library was sequenced using NovaSeq 6000 system.

4.2.3. Raw Data Mapping and Differential Expression Analysis

RNA-sequencing raw data read files were subjected to quality control (QC) analysis with FastQC tool [87]. According to the QC results the raw reads were trimmed via Trimmomatic software [88].

Genome indexing and paired read alignment were performed using the HISAT2 tool [89] using *Phaseolus vulgaris* genome v.2.1 as reference. Obtained SAM files were converted to sorted BAM files with Samtools [90]. The BAM files were utilized for differential expression analysis; first, the transcripts were assembled, and the read counts were determined with Seqmonk v.1.44.0 tool. The obtained read counts were used with EdgeR tool [91] for differential expression analysis. Differentially expressed genes (DEGs) were selected from all genes with a filter of $|\log_2 \text{fold change}| > 1$ and false discovery rate (FDR) < 0.01. DEGs were further subjected to filtering for the generation of a list of candidate genes for functional analysis by the means of an intensity difference analysis through Seqmonk v.1.44.0 tool which not only filters through fold change and FDR but also the amounts of initial raw read counts and the depth of change among the samples.

4.2.4. Verification of Expression Levels with RT-qPCR Analysis

Ten genes were selected for the RT-qPCR analysis: The procedure was carried out with 10ng of cDNA, produced with First Strand cDNA Synthesis kit (Thermo Scientific, US) according to manufucturer's instructions, from the roots of both genotype, for each reaction. Three experimental replicates were performed for three biological replicates. PikoReal 96 Real-time PCR system (Thermo Fisher Scientific, DE) was utilized for the experiment. Actin-11 (GenBank: CV529679.1) gene of common bean was used as the reference gene as it was reported to preserve a stable expression level under salt treatment in common bean [92]. Relative expression levels were calculated by the $2^{\Delta\Delta}$Ct method [93]. The correlation between RNA-seq and RT-qPCR results was calculated with Pearson correlation coefficient.

4.2.5. Gene Ontology (GO) and KEGG Pathway Enrichment Analyses

Gene ontology IDs for the transcripts were obtained using the Biomart tool [94]. GO enrichment analysis was performed with the GO-IDs of DEGs via AgriGO v2.0 tool [95]. KEGG pathway enrichment analysis was performed with the transcript IDs via PlantGSAE tool [96] In both enrichment analyses, the enriched terms were subjected to multi-test adjustment with Benjamini-Hochberg method [97], and those with FDR<0.05 were selected.

4.3. Metabolic Content Analysis – Untargeted Metabolomics

4.3.1. Extraction of Metabolites

The metabolite extraction procedure was performed as described by Lisec *et al.*, (2006) [98]. Roughly 100mg of flash-frozen and ground tissue samples were mixed with 60µl of water containing ribitol as an internal standard for MS data optimization. The samples were mixed with 0.3ml of methanol and 0.1ml of chloroform and vortexed for 5min followed by incubation at 70°C for 10min, and then centrifugation at 15.000g.

Supernatants were collected into glass tubes and were dried in a vacuum-dryer system. Following desiccation, samples were incubated for 2h at 37°C with 80µl of methoxamine hydrochloride. Derivatization for GC was performed with 1% trimethylchlorosilane (TMCS) in N-Methyl-N-(trimethylsilyl)-trifluoroacetamide (MSTFA) (100µl) at 70°C for 1h [98].

4.3.2. Gas Chromatography Coupled Mass-Spectrometry

Derivatized samples were injected in 1ul aliquots into Agilent 8990N GC-MS system and separation was performed with a non-polar capillary column. Helium was used as a carrier gas and the flow rate was 1.0mL/min. The initial temperature was 60 $^\circ$C; rising 8 $^\circ$C/min to 125 $^\circ$C, 4 $^\circ$C/min to 210 $^\circ$C, 5 $^\circ$C/min to 270 $^\circ$C, and 10 $^\circ$C/min to 305. Finally, the temperature stayed at 305 $^\circ$C for 3min. The ion source was operating at 260 $^\circ$C. Full scan mode with the default conditions was used. The reading rate was 20 spectrum/s.

4.3.3. MS Data Collection and Analysis

For GC-MS data processing, such as chromatogram alignment, peak extraction, normalization, and annotation, the in-house MassHunter WorkStation with MSD ChemStation DA software (Agilent, USA) was utilized. Compound identification was performed by using the Wiley7n, Nist98, and W9N11 libraries. For software-suggested annotations, a 90% similarity ratio was taken into consideration and final compound annotations were selected under manual curation. The data normalization was carried out with the software's default choices. Principal component analysis was performed with XLSTAT software (Addinsoft Corporation, USA) (Addinsoft, 2019) for dimensionality reduction of normalized data. Through univariate analysis (two-sample t-test), differentially accumulated/depleted metabolites (DADMs) were determined by statistical significance of $p<0.05$.

4.4. Ion Content Analysis - Ionomics

4.4.1. Heavy Metal Extraction

Flash-frozen ground leaf and root tissue samples of five control and salt-treated biological replicates were dried at 80°C in the oven and 100mg sample was combined with 10ml HNO_3 and 5ml H_2O_2 in 50ml Falcon tubes. The digestion was carried out by heating the samples at 100°C for 10min, then at 150°C for 15min, and at 180°C for 15min. Solutions were then made up to 25ml with dH_2O.

4.4.2. ICP-MS and ICP-OES Measurements

Inductively coupled plasma-mass spectrometry (ICP-MS) and inductively coupled plasma - optical emission spectrometry (ICP-OES) analyses were outsourced to Yildiz Teknik University Merkez laboratories. Measurement conditions were set as described by Mihaylova *et al.* (2013) [99]. Analysis was performed for 10 ions namely sodium, iron, calcium, potassium, magnesium, manganate, aluminum, zinc, copper, and molybdenum. ICP-MS was used to measure concentrations of six ions (B, Mn, Fe, Cu, Zn, Mo) and concentrations of four other ions (Na, K, Mg, Ca) were determined by ICP-OES. Differential accumulation/depletion was defined with two-sample t-test with a statistical significance of $p<0.05$. Statistical significance of difference among the responses of the genotypes was calculated by two-way ANOVA with replication ($p<0.05$) using Excel Analysis ToolPak add-inn (Microsoft, 2019).

4.5. Transcriptomics – Metabolomics - Ionomics Data Integration

Collectively transcriptomics, metabolomics, and ionomics data from Ispir and TR43477 common bean genotypes were integrated on KEGG mapper [100, 101]. The complete data set was used for a pathway-based integration to generate a representative map of molecular mechanisms of salt tolerance. Enriched pathways were the focus of candidate gene selection for functional analysis.

4.6. Photosynthetic Pigment Measurement

Chlorophyll and carotenoid contents of the leaves were determined as described by Warren, (2008) [102]. One ml methanol was added to 100mg ground leaf sample, incubated for 2min at 950rpm in a shaking incubator, and then centrifuged to obtain the supernatant. This procedure was repeated twice, and the supernatants were combined in a separate tube. Technical triplicates of samples (200µl) were put in 96-well microplates. Specific absorbance (A) values (A_{652}, A_{665} and A_{470}) were measured using methanol as reference. Values were corrected by dividing by path length (˜0.56) and applied to separate equations to estimate chlorophyll a , chlorophyll b and carotenoid contents of the leaves:

$$\text{chl } a \text{ (µg/mL)} = -8.0962 \text{ x } A_{652} + 16.5169 \text{ x } A_{665} \quad (4.1)$$

$$\text{chl } b \text{ (µg/mL)} = 27.4405 \text{ x } A_{652} - 12.1688 \text{ x } A_{665} \quad (4.2)$$

$$\text{Total carotenoids (µg/mL)} = (1000 \text{ x } A_{470} - 1.91 \text{ x chl } a - 95.15 \text{ x chl } b) \text{ / } 225. \quad (4.3)$$

4.7. Functional Analysis with Selected Candidate Gene

4.7.1. Gateway Cloning of Gene Specific Parts

Sequences of the selected candidate genes were analyzed for distinct, gene-specific 150-400bp sites for RNA interference (RNAi) in the NCBI database. Selected sites were amplified using gene-specific primers containing *attB* adapter sequences for Gateway Cloning (Table 3.10). The resulting *attB* linked sequences were first inserted to Gateway donor vector pDONR207 through a BP reaction. The obtained entry clones were transformed to *E. coli* DH5α strain by $CaCl_2$ chemical transformation method. The bacterial colonies carrying the entry clone were selected both by antibiotic resistance and colony PCR approach. Following the liquid culture growth of the bacteria, the entry vectors were purified with Nucleospin Plasmid Quickpure plasmid extraction kit according to the manufacturer's instructions.

Gene sequences inside entry clones were transferred to a plant-specific RNAi Gateway destination vector (pK7GWIWG2_II-RedRoot - RedRoot thereafter) through an LR reaction. The insertion was in two directions with a linker between insertions (promoter::sequence::intron-linker::CGTA) to produce an intron-containing hairpin RNA (ihpRNA) for the use of host RNAi machinery. Obtained expression vectors were first transformed to *E. coli* DH5α strain, selected, amplified, and purified as described above. The purified expression vectors then transformed to *Agrobacterium rhizogenes* K599 strain by $CaCl_2$ chemical transformation to be employed for the production of transgenic hairy roots on Ispir genotype plantlets.

4.7.2. Plant Growth, Hairy Root Induction, and Salt Treatment Conditions

Ispir genotype common bean growth was performed as described by Estrada-Navarrete *et al.*, (2007) [82] with minor modifications. Surface sterilized seeds (with 96% ethanol and 5% hypochlorite) were germinated on UV sterilized petri dishes with ddH_2O soaked – autoclaved napkins at 24°C for 2 days. Seedlings were transferred to vermiculite-pots saturated with half-strength Broughton and Dilworth (B&D - supplemented with 4mM KNO_3) solution and grown for about 5 days until the emergence of cotyledons. At this point, the pods were soaked with full-strength B&D (Supplemented with 8mM KNO_3) solution as a preparation for hairy root induction.

For the hairy root induction, *A. rhizogenes* colonies were grown on LB-agar plates, dislodged with 2ml dH_2O and a spreading rod, and transferred to microcentrifuge tubes. Plantlets were infected with the help of a needle and a syringe on the shoots, 2cm above the primary root growth zone, through 4-5 micro-injections. For the growth of hairy roots, the pots were transferred to transparent containers that ensured a humidity level above 95%. The leaves were sprayed with B&D (Supplemented with 8mM KNO_3) every two to three days to keep the humidity levels high. After 18-21 days post-transformation, plants with sufficiently developed hairy roots had their primary roots removed. Plants then were transferred to 15cm diameter pots with B&D (Supplemented with 8mM KNO_3) saturated vermiculite and the leaves were sprayed.

The plants were grown in transparent containers for another three weeks to facilitate root growth, before removing the lid of the containers. Plants were irrigated with half-strength B&D (Supplemented with 2mM KNO_3) and grown for another week without containers. After this point, the above-mentioned procedure (section 4.1) was followed for salt treatment.

The RedRoot vector carries a dsRED reporter linked to 35S constitutive promoter, so the initial affirmation of plasmid insertion to the genome of the hairy roots was performed by imaging the red fluorescence. The knockdown pattern under salt stress conditions was verified by RT-qPCR and Western blotting analyses as described in the following sections. As most of the cotyledons fell off or in a necrotic phase due to the stress induced by the hairy-root trasformation methodology, they were not used as samples in this study.

4.7.3. Measurement of Gene Expression with RT-qPCR

Total RNA extractions for RT-qPCR analysis were performed with 0.1g homogenized root tissue, using Tri Reagent© (Sigma, US) according to the manufacturer's instructions. Quantification and qualification of the RNA samples were performed with spectrophotometer [86] and 1% denaturing agarose gel electrophoresis. RT-qPCR was carried out as described in section 4.2.4.

4.7.4. Measurement of Protein Levels with ELISA and Western Blotting

Crude root protein extracts to be used in enzyme-linked immunosorbent assay (ELISA) and Western blotting (WB) experiments were prepared by throughly mixing 0.1g ground root tissue with 150µl pH 7.8 100mM PBS (supplemented with Roche cOmplete™ Proteinase Inhibitor and 0.1mM EDTA) and collecting the supernatants through centrifugation (20min at 13.000g, 4°C). Sample protein concentrations were determined with Pierce™ BCA Protein Assay Kit (Thermo Scientific, US) according to the manufacturer's instructions.

WB was performed with 25μg of protein. Proteins were separated according to their sizes with SDS-PAGE (10% polyacrylamide) and transferred into a PVDF membrane. The membrane was incubated in blocking solution (4% skimmed milk dissolved in TBS-T) for 1h at room temperature and then incubated in primary antibody (Anti-SPSc – 1:1000 in 4% skimmed milk-TBS-T; or Anti-Actin – 1:5000 in 4% skimmed milk-TBS-T) solution at 4°C overnight. The next day, the membranes were washed three times with TBS-T and incubated in secondary antibody of goat anti-rabbit IgG HRP conjugate (1:3000 in 4% skimmed milk-TBS-T) solution for 1 hour at room temperature before visualization using a luminol working solution (ECL Pico for Actin; Supersignal West Femto for pvSPS4). The bands were visualized with SynGene documentation system and relative intensities were measured manually with ImageJ software [103].

The ELISA for the measurement of Putative SPS1A (Phvul.003G170100) levels were performed with 750µg protein using MyBioSource Plant Sucrose Phosphate Synthase SPS ELISA Kit (MBS269987) according to manufacturer's instructions. The standard SPS sample of the kit (*Solanum tuberosum* SPS1A–UniProtKB_Q43845) was also used in WB experiments as negative control.

4.7.5. Physiological Analyses

Three individual leaf photos (from first and second trifoliate) were taken for leaf area calculations. Leaf area measurements were performed by ImageJ software [103]. Then, to measure relative water content (RWC) and electrolyte leakage (EL), five separate leaf discs (Diameters of 1.5cm for RWC and 1.0cm for EL) were taken from various leaves of the plants.

RWC was measured by an equation defined by Barrs & Weatherley, (1962). The discs were first weighed for fresh weight, then incubated in dH_2O (upper surface in contact with water) for four hours and weighed for turgor weight. Dry weights were measured after overnight incubation at 80°C oven.

To measure EL, the leaf sections were incubated in ddH_2O for 30min to eliminate sectioning-related leakage; dried and transferred to 5ml ddH_2O in 50ml falcon tubes with closed cap to prevent evaporation. Increase in the electrical conductivity of the water was measured with a conductivity meter at 2nd, 4th, and 8th hours after sectioning.

4.7.6. Proline Content Measurement

Leaf and root proline contents were determined by acidic-ninhydrin based colorimetric assay developed by Bates *et al.*, (1973) [104] which depends on the red color formation by a chemical reaction between ninhydrin and proline in and acidic environment; proline content of the samples was estimated by use of spectrophotometry and a standard curve. Briefly, 100mg of ground sample was mixed with 500µl 3% sulfosalicylic acid and then centrifuged. Hundred µl of the supernatant was added to the reaction mixture in a separate tube consisting of 100µL 3% sulfosalicylic acid, 200µL glacial acetic acid, and 200µL acidic ninhydrin. The tube lid was perforated, the mixture was incubated at 96°C for an hour, and then the reaction was terminated by incubation on ice for 5min. The sample was mixed with 1ml toluene in a glass tube, vortexed for 10sec, and the A_{520} was measured with a quartz cuvette using toluene as reference. To calculate proline concentration as milligram per gram fresh weight (mg/g FW), A_{520} readings were inserted into the equation derived from the proline standard curve.

4.7.7. Photosynthetic Pigment Measurement

Chlorophyll contents of the leaves were determined as described in section 4.6.

4.7.8. Antioxidant Enzyme Activities

Approximately 100 mg ground leaf tissue sample was thoroughly homogenized with vortex in ice-cold 1ml of 100mM PBS (pH 7.8 supplemented with 0.1mM EDTA).

After centrifugation at 13.000g for 20min at 4°C, the supernatant was divided into 100ul aliquots of crude extracts and stored at -80°C for further use. The concentration of the crude protein was spectrophotometrically calculated using the Warburg-Christian formula [105]:

$$\text{Protein concentration (mg/ml)} = (1.55 \text{ x A280}) - (0.76 \text{ x A260}). \quad (4.4)$$

Catalase (CAT) activity was determined by following the decomposition of H_2O_2 as a decrease in absorbance at 240nm in UV/Vis spectrophotometer (Aebi, 1984). Reaction solution was prepared by adding 77.5µl 30% H_2O_2 to 50ml PBS (pH 7.0, 100mM). 50µl crude extract was mixed thoroughly with 1ml reaction solution in a 1.5ml tube; the solution was transferred to a quartz cuvette and the change of A_{240} every 10sec for 2min was recorded. Ascorbate peroxidase (APX) activity was calculated by measuring the drop in A_{290} as a result of the oxidation of ascorbate in the reaction. The reaction solution was prepared by mixing 15ml PBS (pH 7.0) and 100µl 100mM ascorbate. Assay mixture was prepared in a 1.5ml tube with 90µl crude extract, 10µl 0.5mM H_2O_2, and 900µl reaction solution. Next, the assay mixture was transferred to a quartz cuvette for dynamic measurement of A_{290} for 3min at 15sec intervals. The basal level of ascorbate oxidation was also measured using PBS (pH 7.0) instead of crude extract. The mean changes in A_{240} (ΔA_{240}) and A_{290} (corrected by subtracting the mean basal value; ΔA_{290}) were used in equations below to calculate the CAT and APX activities respectively:

$$\text{CAT activity (unit/mg protein)} = \Delta\text{A240 x (V/Vt)/(0.1 x t)/Cp} \quad (4.5)$$

$$\text{APX activity (unit/mg protein)} = \Delta\text{A290 x (V/Vt)/(2.8 x t)/Cp} \quad (4.6)$$

where:

- V: Total volume of crude extract
- Vt: Volume of used crude extract
- t: Reaction time (min)
- Cp: Crude protein concentration (mg/ml)

- 0.1: A unit of CAT is defined as the quantity that causes 0.1 decrease of OD_{240} per minute
- 2.8: Extinction coefficient for reduced ascorbate (mM^{-1} cm^{-1}).

4.7.9. Root Glucose and Sucrose Content Measurement

Root soluble carbohydrates were extracted with 96% ethanol as described by Maness (2010) [106]. Hundred mg ground root tissue was thoroughly mixed with 1ml 96% ethanol and incubated for 30 min at 85°C. The solution was centrifuged at 10.000g for 10min, the supernatant was collected to another tube. This procedure was repeated three times for a tissue sample and supernatants were combined. The ethanol was removed with a vacuum-drier and the extracts were solved in 150μl dH_2O for further analysis.

The colorimetric measurement of glucose and sucrose contents was performed with Mybiosource Glucose and Sucrose Assay Kit (MBS841570) using 10μl of sample according to manufacturer's instructions. Glucose levels were measured by exploiting the reaction of oxidized glucose with resorufin, a compound that can be detected at A_{570} by colorimetric measurement [107]. Sucrose content was measured by converting the sucrose to glucose using invertase enzyme [108], to measure total glucose level as described above. The sucrose level was then calculated by subtracting the first measured glucose amount from the total glucose amount.

4.7.10. Tissue Ion Content Measurement with ICP-OES

The remaining tissue samples were collected separately in 50ml tubes and dried in 80°C oven for three days. ICP-OES measurements of four ions (Na, Ca, Mg and K) were outsourced to Yildiz Technical University Merkez laboratories and performed as described in section 4.4.

4.7.11. Statistical Analyses

Statistical analysis was performed using Graphpad Prism version 9.1.2 for Windows (GraphPad Software, San Diego, California USA). RT-qPCR for *pvSPS4* knockdown was examined with One-Way ANOVA (Brown-Forsythe and Welch test) and multiple comparisons were done with Dunnet's T3. RT-qPCR for *SPS* homologs and WB were analyzed with parametric t-test due to the relative nature of measurements. Evaluation of other physiological, molecular and ion content measurements were done with 2-Way-ANOVA. Multiple comparisons for control vs salt treatment conditions were implemented with Sidak's test and presented with black outlines. Control vs control and treatment vs treatment comparisons between lines were done with Tukey's test: Control comparisons were presented with blue outlines and treatment comparisons were presented with ruby outlines (*-$p<0.05$, **-$p<0.01$, ***-$p<0.005$, ****-$p<0.001$). Correlations of the responses of the lines to salt stress was assessed with Spearman's Rank Order correlation.

5. RESULTS

5.1. Transcriptomics

5.1.1. RNA Extraction and Quality Control

The quality of the extracted RNA was initially tested with agarose gel electrophoresis (Figure 5.1). The results displayed intact 28S and 18S bands for all samples, thus demonstrated that the RNA samples were not degraded.

The sample quality together with the quantity was also checked with Nanodrop 2000 spectrophotometer. $OD_{260/280}$ and $OD_{260/230}$ values (Table 5.1) demonstrated the purity of the samples except for $OD_{260/280}$ values for the leaves of the TR43477: These values were closer to 1.8 which indicated slight DNA contamination [86]. Since the samples were purified one more time with salt-ethanol precipitation and the integrity analysis with Agilent 2100 bioanalyzer (Agilent, US) analysis demonstrated a RIN$\geq$7.4 for all samples, they were considered to be ready for library preparation for RNA-seq.

5.1.2. Raw Reads: Statistics, QC Analysis, and Trimming

The RNA-seq of 24 samples generated more than 935 million reads in total with Illumina adapters for paired ends of the reads. After adapter removal, those reads had presented an average Q30 (Quality score - probability of an incorrect base call 1 in 1000 times) of 95.14% with the lowest being 94.34% (Table 5.2).

Primary trimming was performed for the left-most 13 bases of each read due to high variability in per base sequence content (Figure 5.2). Next, the reads were subjected to a sliding-window analysis (5 bases with a Phred score of 25). After the trimming procedures, the minimum read length was set to 35, and reads below that length were removed from the data.

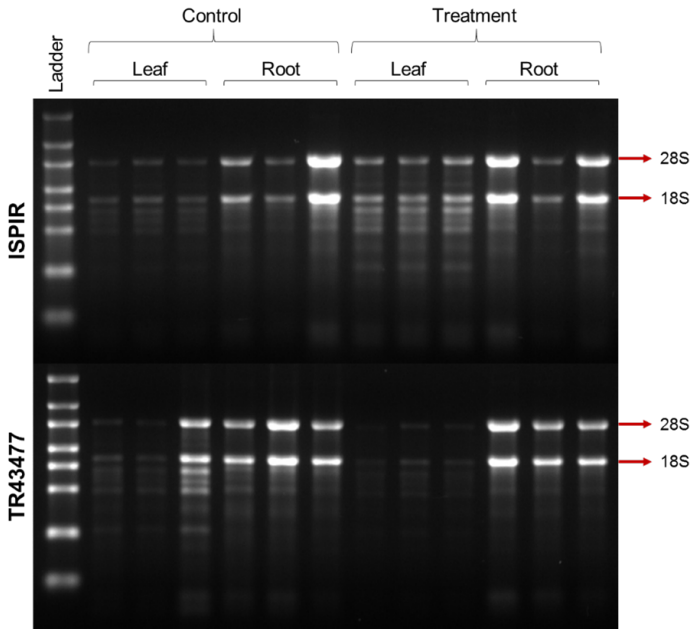

Figure 5.1. Agarose gel electrophoresis results of RNA samples. Intact 28S and 18S bands indicate a reliable quality for all samples.

Table 5.1. Spectrophotometric quality control of RNA samples from the leaf and root tissues of genotypes.

		CONTROL			**TREATED**			
	Sample no.	Conc.(ng/ul)	260/280	260/230	Conc.(ng/ul)	260/280	260/230	
Ispir	1	77.7	2.12	2.17	200	2.15	2.44	LEAVES
	2	88.7	2.1	2.15	228.1	2.11	2.49	
	3	81.7	2.12	2.28	244.5	2.14	2.34	
TR43477	1	83	2.18	2.4	174.2	1.86	2.44	
	2	66.8	2.11	2.19	106.3	1.83	2.38	
	3	314.9	2.12	2.51	83.4	1.77	2.38	
		Conc.(ng/ul)	260/280	260/230	Conc.(ng/ul)	260/280	260/230	
Ispir	1	189.3	2.15	2.56	378.2	2.1	2.39	ROOTS
	2	122.5	2.16	1.82	116.4	2.15	2.26	
	3	396	2.1	2.54	300.3	2.13	2.43	
TR43477	1	235.4	2.13	2.48	327.5	2.12	2.46	
	2	328.7	2.13	2.53	223.2	2.14	2.39	
	3	241.5	2.14	2.38	204.8	2.14	2.21	

Table 5.2. Raw read statistics for RNA-seq. C - control; T - treatment.

Sample	**Total Bases**	**Read Count**	**GC (%)**	**(%)**	**Q20) (%)**	**Q30 (%)**
Ispir_LeafC_1	3343001020	33099020	45.44	54.57	98.41	95.2
Ispir_LeafC_2	5302372336	52498736	45.45	54.55	98.32	94.9
Ispir_LeafC_3	5317031476	52643876	45.76	54.24	98.25	94.77
Ispir_RootC_1	3390577878	33570078	45.37	54.63	98.37	95.17
Ispir_RootC_2	3246379572	32142372	45.29	54.71	98.33	95.05
Ispir_RootC_3	3551236154	35160754	45.75	54.25	98.44	95.35
Ispir_LeafT_1	3053973360	30237360	45.7	54.3	98.18	94.72
Ispir_LeafT_2	4908335986	48597386	45.95	54.05	98.36	95.02
Ispir_LeafT_3	3074807236	30443636	46.01	53.99	98.56	95.58
Ispir_RootT_1	3094850888	30642088	45.69	54.31	98.22	94.79
Ispir_RootT_2	3551804380	35166380	45.27	54.73	98.48	95.39
Ispir_RootT_3	3387507478	33539678	45.43	54.58	98.28	94.95
TR43_LeafC_1	3392535460	33589460	45.42	54.58	98.46	95.34
TR43_LeafC_2	3247383714	32152314	45.67	54.33	98.63	95.74
TR43_LeafC_3	3713945134	36771734	46.22	53.78	98.49	95.37
TR43_RootC_1	3346787914	33136514	45.46	54.54	98.44	95.34
TR43_RootC_2	4326666886	42838286	45.71	54.29	98.31	95.07
TR43_RootC_3	3710713336	36739736	45.68	54.32	98.4	95.24
TR43_LeafT_1	3221677194	31897794	45.1	54.9	98.4	95.15
TR43_LeafT_2	4061372004	40211604	44.97	55.03	98.37	95.15
TR43_LeafT_3	3824157344	37862944	45.24	54.76	98.52	95.45
TR43_RootT_1	3852252514	38141114	45.56	54.44	98.43	95.31
TR43_RootT_2	6770562068	67035268	45.39	54.61	98.09	94.34
TR43_RootT_3	5822458504	57648104	45.31	54.7	98.32	94.94

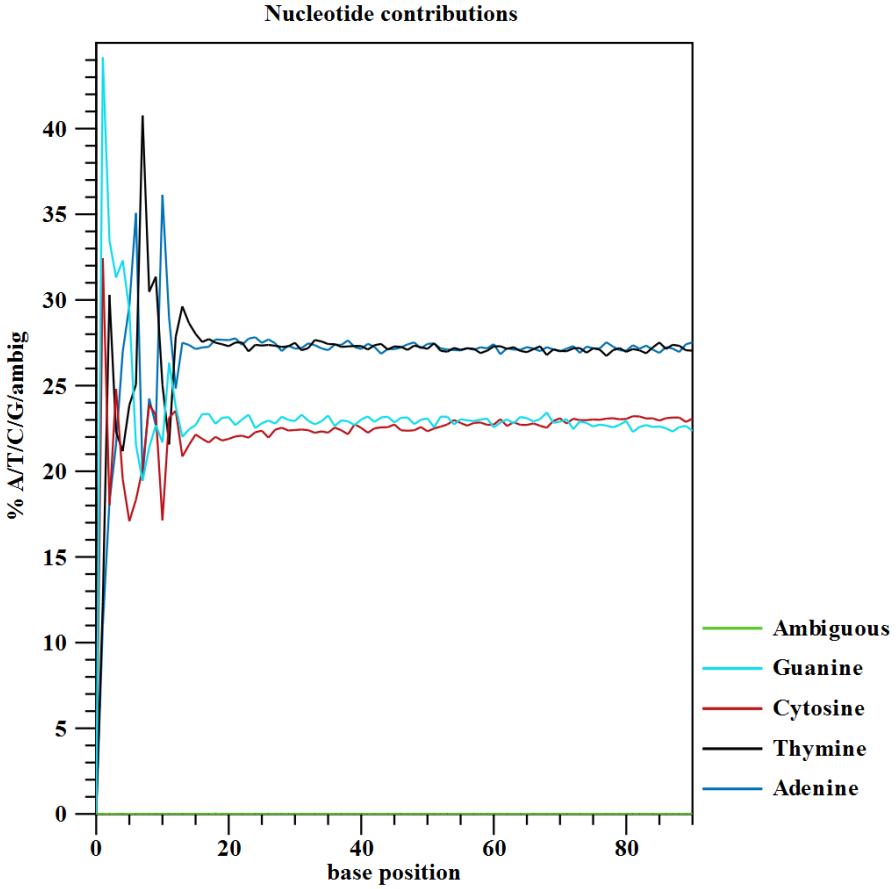

Figure 5.2. Representative per base sequence content graph. The first 13 bases displayed high variability, thus trimmed for further analyses.

5.1.3. Raw Read Mapping and DEG Analysis

On average the mapping has produced 89.05% concordant alignment and 96.28% overall alignment to the reference genome (Table 5.3). The greatest number of DEGs was observed for tolerant genotype leaves with 3072 genes while roots of the susceptible genotype displayed the lowest number of DEGs with 910 genes (Table 5.4). On the other hand, intensity difference analysis -which has selected the genes with the highest difference based on the mapped read number, gene length, FDR, and fold change value (Figure 5.3) has yielded a different result: Roots of the susceptible genotype had the highest number with 329 while the leaves of the susceptible genotype displayed the lowest number of DEGs of 206 (Full list of intensity filtered genes for leaf and root tissues can be found in Table A1 and Table A2 respectively).

Table 5.3. Statistics for trimmed read mapping to the *P.vulgaris* L. reference genome.

			Paired read count	**Concordant alignment (%)**	**Overall alignment (%)**
ISPIR	**LEAF**	Control_1	15492583	92.1	97.99
		Control_2	24501307	89.49	97.34
		Control_3	24519671	92.88	97.92
		Treatment_1	14073496	91.15	97.25
		Treatment_2	22721821	90.4	97.52
		Treatment_3	14335336	92.2	97.85
	ROOT	Control_1	15713485	87.87	96.25
		Control_2	15019777	89.31	95.87
		Control_3	16496524	89.15	96.94
		Treatment_1	14253723	85.57	96.5
		Treatment_2	16537801	90.26	96.95
		Treatment_3	15648266	90.55	97.33
TR43477	**LEAF**	Control_1	15753609	88.56	95.54
		Control_2	15196921	90.44	96.38
		Control_3	17281002	88.51	96.04
		Treatment_1	14931185	88.2	95.71
		Treatment_2	18796243	88.77	95.67
		Treatment_3	17793700	88.73	95.66
	ROOT	Control_1	15559453	87.59	95.64
		Control_2	20006512	87.48	95.5
		Control_3	17229757	86.48	93.65
		Treatment_1	17897796	87.2	95.25
		Treatment_2	31045673	86.69	94.3
		Treatment_3	26924512	87.62	95.72

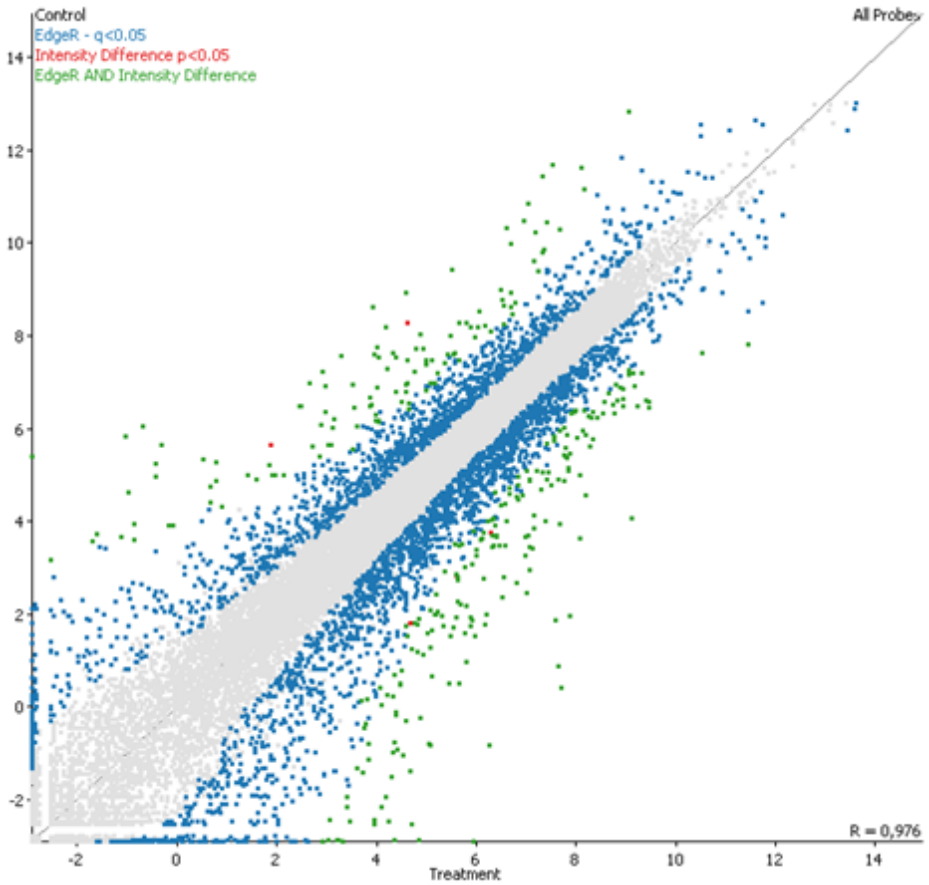

Figure 5.3. Scatter plot illustration of DEG filtration. Blue dots depict the conventional selection, while the red dots indicate the DEGs that were selected with intensity difference filtration. Green dots display the common elements in both lists.

Comparison of the conventional DEG lists has shown that 71 genes were differentially expressed in all tissues and genotypes (Figure 5.4a). 3090 DEGs were specific to tolerant one with 247 DEGs expressed in both tissues; on the other hand, the susceptible one displayed 1892 genotype-specific DEGs of which only 61 of them shared between tissues (Figure 5.4a). However, intensity difference filtration had lowered the shared number of DEGs between tissues and genotypes dramatically (Figure 5.4b). While the number of DEGs shared by all was three, there were 344 DEGs specific to tolerant with ten shared and 350 DEGs specific to susceptible with seven shared (Figure 5.4b).

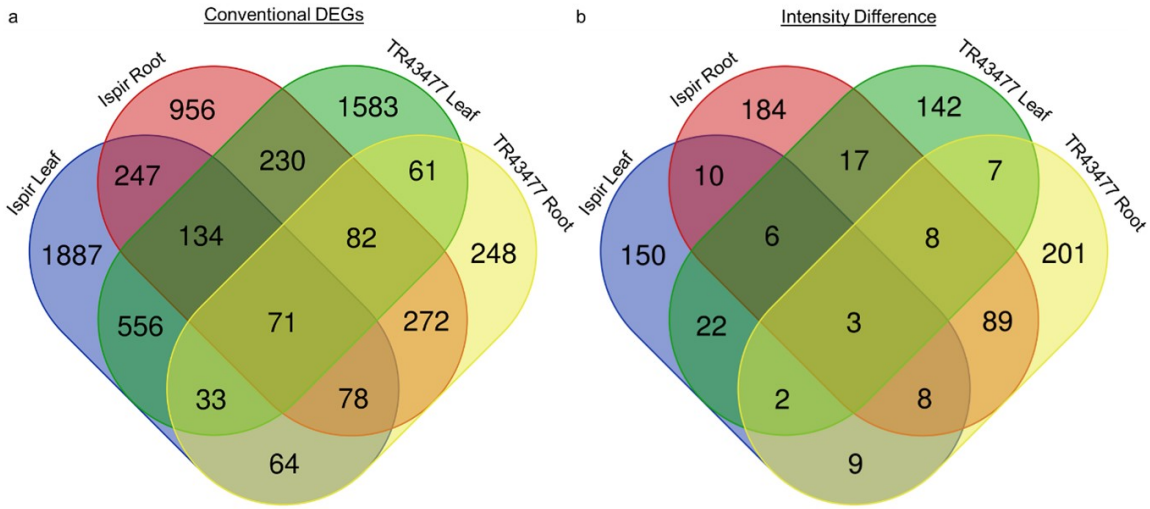

Figure 5.4. Venn diagram comparison of conventional (a) and intensity difference (b) DEG list.

5.1.4. Confirmation of RNA-seq Reliability

To check the reliability of RNA-seq data, expression analysis of randomly selected 10 genes was performed with RT-qPCR for the roots of both genotypes. The results indicated high correlation levels with r values of 0.87 and 0.84 (p¡0.05) for the tolerant (Figure 5.5a) and the susceptible genotype respectively (Figure 5.5b).

5.1.5. Gene Ontology Enrichment and KEGG Pathway Analysis

To gain insight into the role of DEGs of specific tissues, GO enrichment was performed with AgriGO v.2.0 parametric analysis of gene set enrichment (PAGE) tool [95]. The enrichment analysis has displayed the difference in molecular responses of each genotype on leaf or root basis (Figure 5.6) (Full list of GO enriched terms for Ispir Leaf -*IL*-, Ispir Root -*IR*-, TR43477 Leaf -*TL*-, and TR43477 Root -*TR*- can be found in Tables A3, A4, A5 and A6 respectively.). Moreover, KEGG pathway enrichment was performed with PlantGSEA tool [96] to get a broader perspective on the variation (Figure 5.7) (Full list of enriched KEGG pathways for IL, IR, TL and TR can be found in Table A7, Table A8, Table A9 and Table A10 respectively.). Terms associated with photosynthesis were enriched in IL but, according to both databases, depleted in TL.

A similar pattern for porphyrin and chlorophyll metabolism was also suggested by the KEGG results. This outcome was in line with the leaf chlorophyll content of IL and TL (Figure 5.8a): While the chl *b* content of IL demonstrated a substantial increase, the chl *b* content of TL declined and the contrast between the changes was highly significant. Genes of photosystem II and photosynthetic e^- transport modules displayed a strong contrast in salinity-responsive regulation as well (Figure 5.8b). In addition, the *ATP synthase* delta subunit (Phvul.003G211100) was upregulated in IL but it was downregulated in TL along with the *ATP synthase* gamma subunit (Phvul.006G149700) which indicated a disorganized proton conduction system for the susceptible genotype along with a reduced content of chlorophyll (Figure 5.8a).

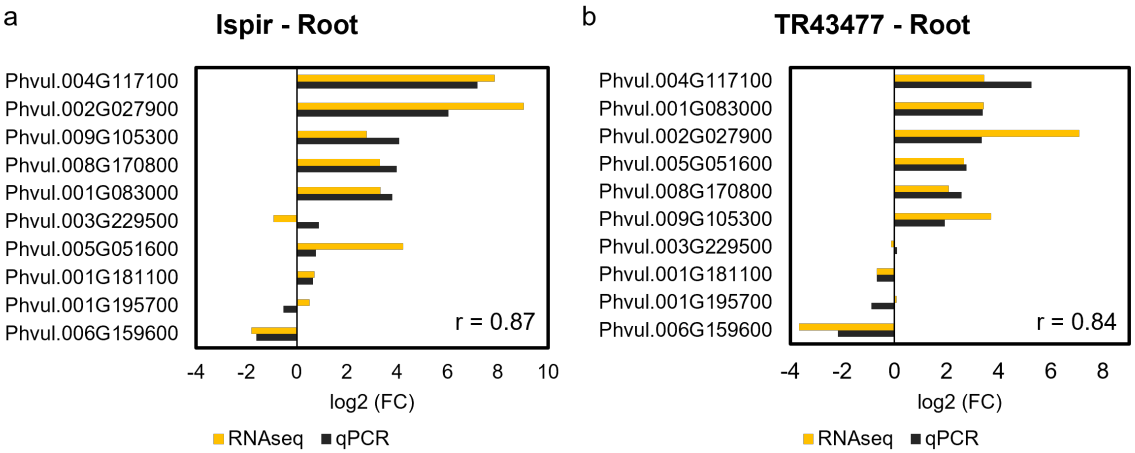

Figure 5.5. RNA-seq confirmation with RT-qPCR. Correlation was performed with 10 genes for the roots of the tolerant (a) and the susceptible (b) genotype.

GO terms for the metabolic process of polysaccharides were depleted in TL together with KEGG terms for carbon fixation, while GO terms and KEGG pathways linked to carbon fixation were enriched in IL (Figure 5.6a; Figure 5.7a). KEGG pathway analysis of sucrose and starch metabolism together with glyoxylate and dicarboxylate metabolism displayed a parallel result: enriched in IL, diminished in TL (Figure 5.7a). Particularly, Phvul.008G210100 (*β-D-glucan exohydrolase*), Phvul.004G029100 (*Starch synthase*), and Phvul.011G107700 (*β-amylase 5*) genes were prominent in IL for sucrose and starch metabolism as indicated by intensity difference analysis.

GO terms related to transcription, translation, and post-translational modification were depleted in IL, while GO terms related to expressional regulation, transcription, and functional modification were enriched in TL. TL showed enrichment and depletion trends for different amino acids concerning this, along with a decrease in terms related to DNA synthesis and ribosome biogenesis.

For IL, cell wall and cytoplasm (cellular components)-based GO terms were enriched, while TL was depleted in GO terms associated with the production of cell wall components. IL demonstrated a complex response for cell-wall modification in GO analysis with decreased cell wall organization but increased pectinesterase activity, while TL displayed decreased cell-wall organization-related terms (Figure 5.6a). Notably, eight different pectinesterase-related genes were upregulated in IL. The KEGG pathway analysis displayed an enrichment pattern in cutin, suberine, and wax biosynthesis, for both IL and TL. IL was also enriched in protein folding activity and cofactor/coenzyme metabolism-related GO terms. On the other hand, TL showed reduced activity of proteolysis and peptidase. Both IL and TL were enriched in KEGG terms for protein synthesis in the endoplasmic reticulum (Figure 5.6a; Figure 5.7a).

Compared to leaves, responses of roots were limited: While TR had enriched GO terms for transcriptional regulation, IR was enriched for functional modification terms in GO and protein processing in endoplasmic reticulum pathway in KEGG. Indeed, five distinct genes of the heat shock protein family (Phvul.004G107700, Phvul.008G112700, Phvul.004G129400, Phvul.009G080200, and Phvul.003G154800) that are part of the endoplasmic reticulum protein processing pathway of KEGG demonstrated significant patterns of upregulation in IR, indicating the activity of unfolded or misfolded protein response. Furthermore, IR displayed decreased GO terms related to helicase activity, probably a sign of halted replication and modification of DNA, along with decreased GO nitrogen compound metabolic process terms, which indicated the diminished translational activity. Though the findings of the KEGG pathway analysis revealed that nitrogen metabolism was depleted both in IR and TL, IR was depleted in amino acid biosynthesis and ribosome biogenesis as well (Figure 5.6b; Figure 5.7b).

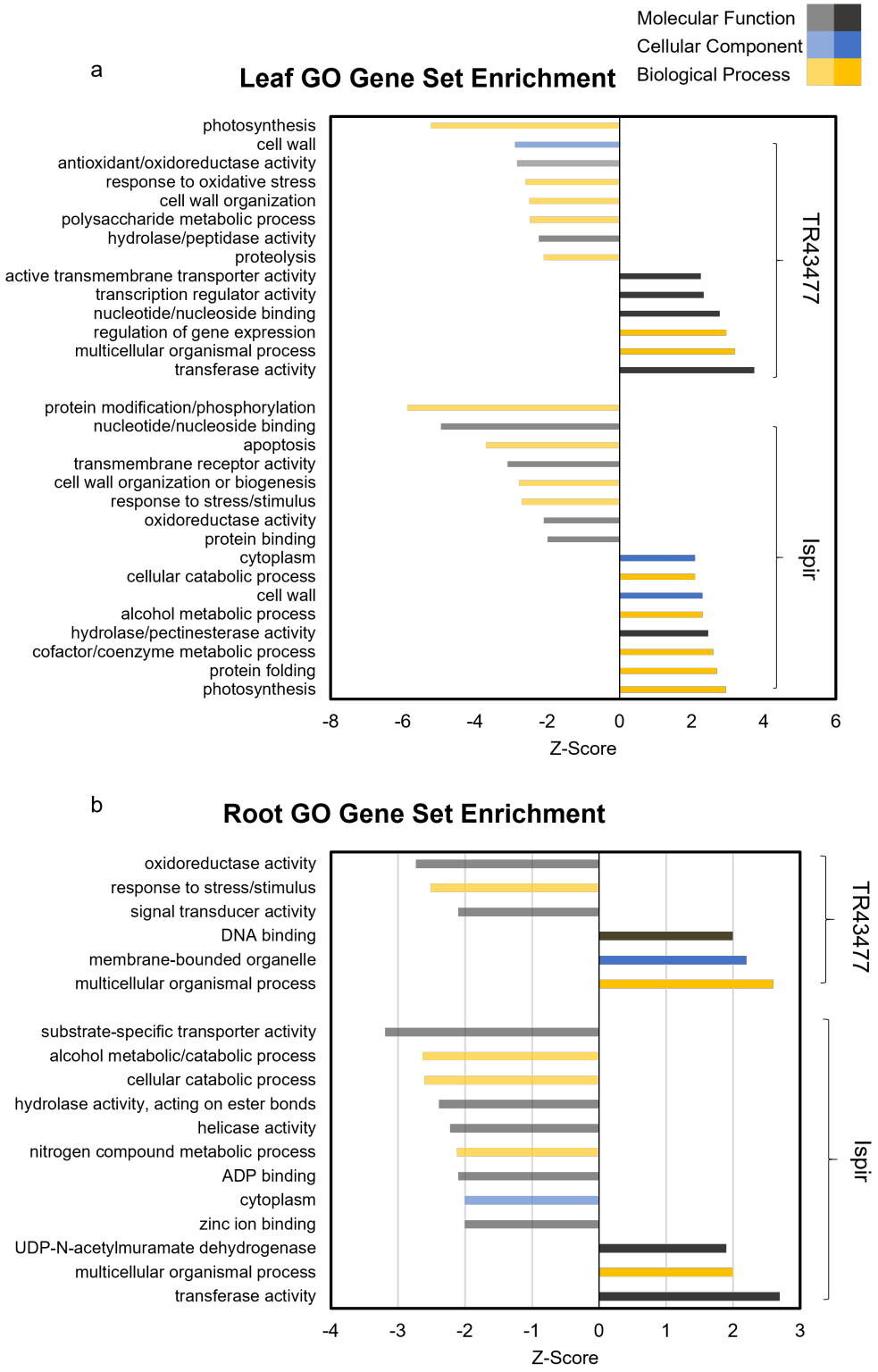

Figure 5.6. GO enrichment analysis of leaf (a) and root (b) tissues. Ontology terms (FDR≤0.05, n≥5) were listed for each tissue. GO terms with the same ontology were combined (with a mean enrichment score) for better data presentation.

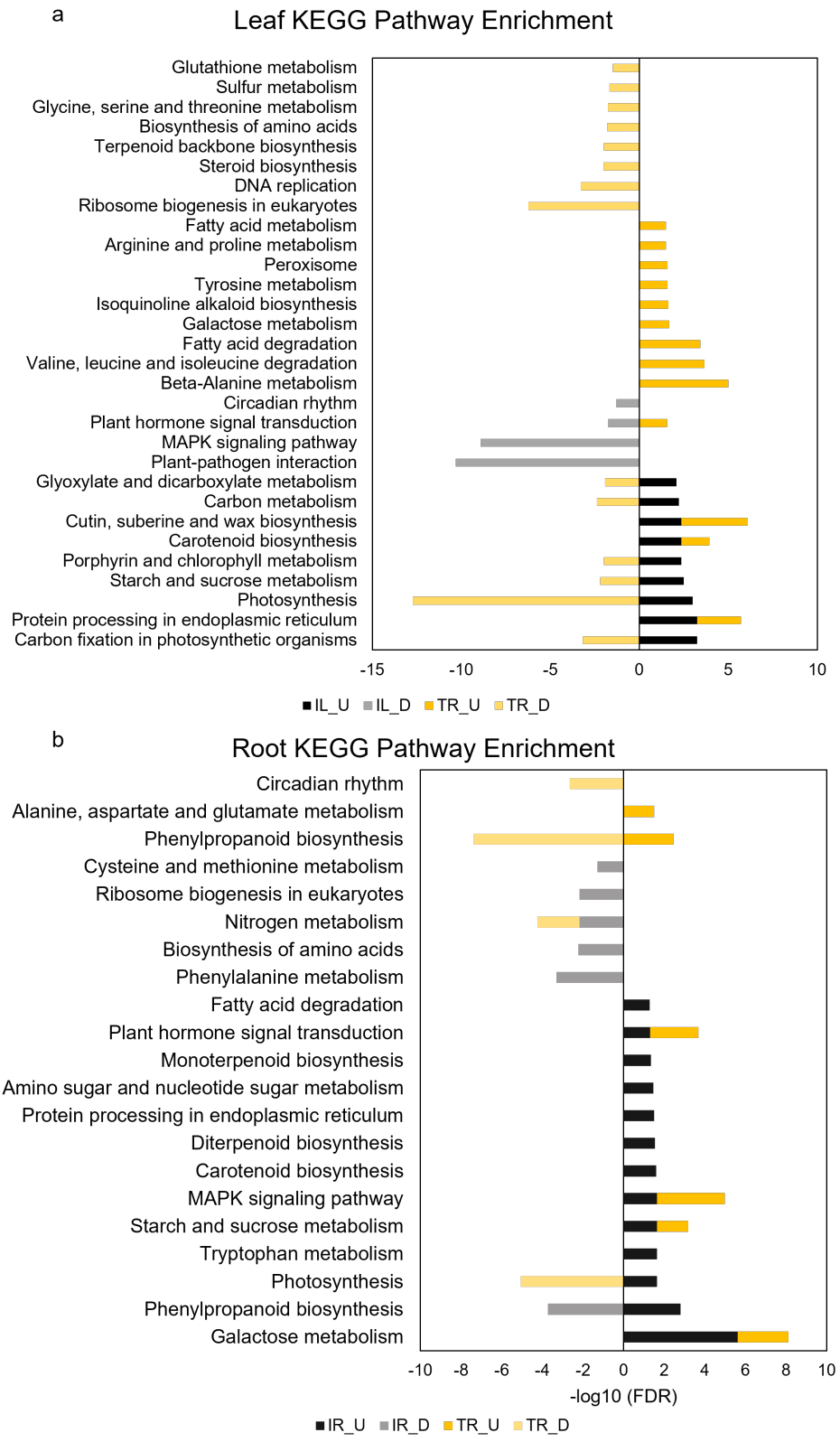

Figure 5.7. KEGG pathway enrichment/depletion analysis of leaf (a) and root (b) tissues. Only terms with FDR≤0.05 were displayed (n≥5) Upregulated and downregulated genes were analyzed separately.

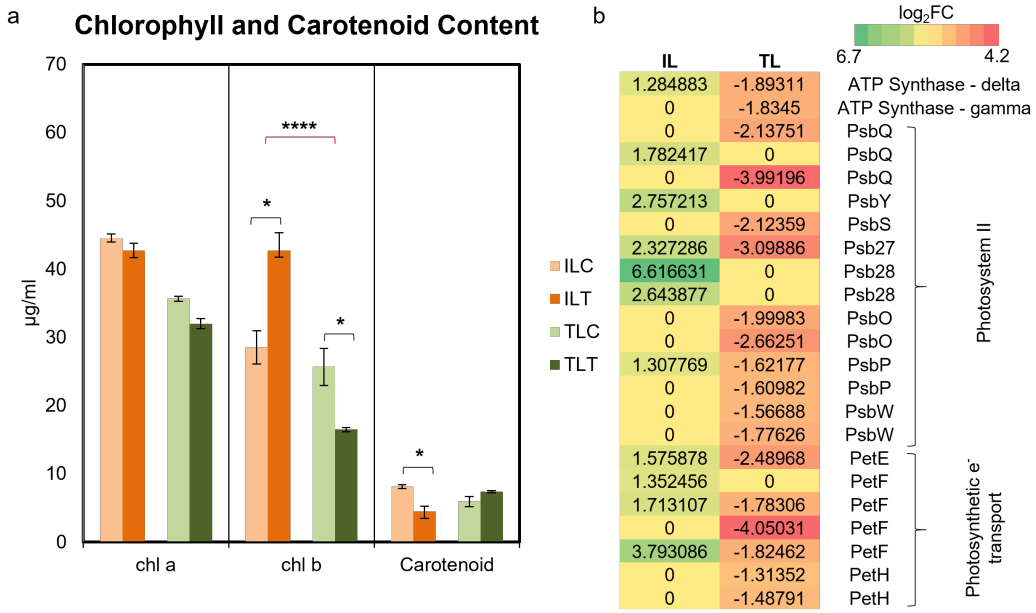

Figure 5.8. Chlorophyll and carotenoid content differences in the leaf tissues (a). "C" – control; "T" - treatment. Values represent mean ± SEM. Heatmap displays the $\log_2$-fold changes of photosynthesis-related transcripts in KEGG pathways (b).

5.2. Metabolomics

Seventy-nine different primary metabolites were detected in untargeted GC-MS analysis. Thirty two metabolites were Ispir-specific, 13 metabolites were TR43477-specific and 34 metabolites were detected in both genotypes (List of metabolites and statistical data for IL, IR, TL and TR can be found in Table A11, Table A12, Table A13 and Table A14 respectively.). Principle component analysis (F1 and F2 represented 50.3% of all data) of genotypes has separated the leaf and root tissue behaviors from each other (Figure 5.9a). The close projection of biological replicates implied a reliable correlation for replicas. Ispir has shown a greater divergence between control and stress-treated components compared to TR43477 for both leaf and root tissues (Figure 5.9a).

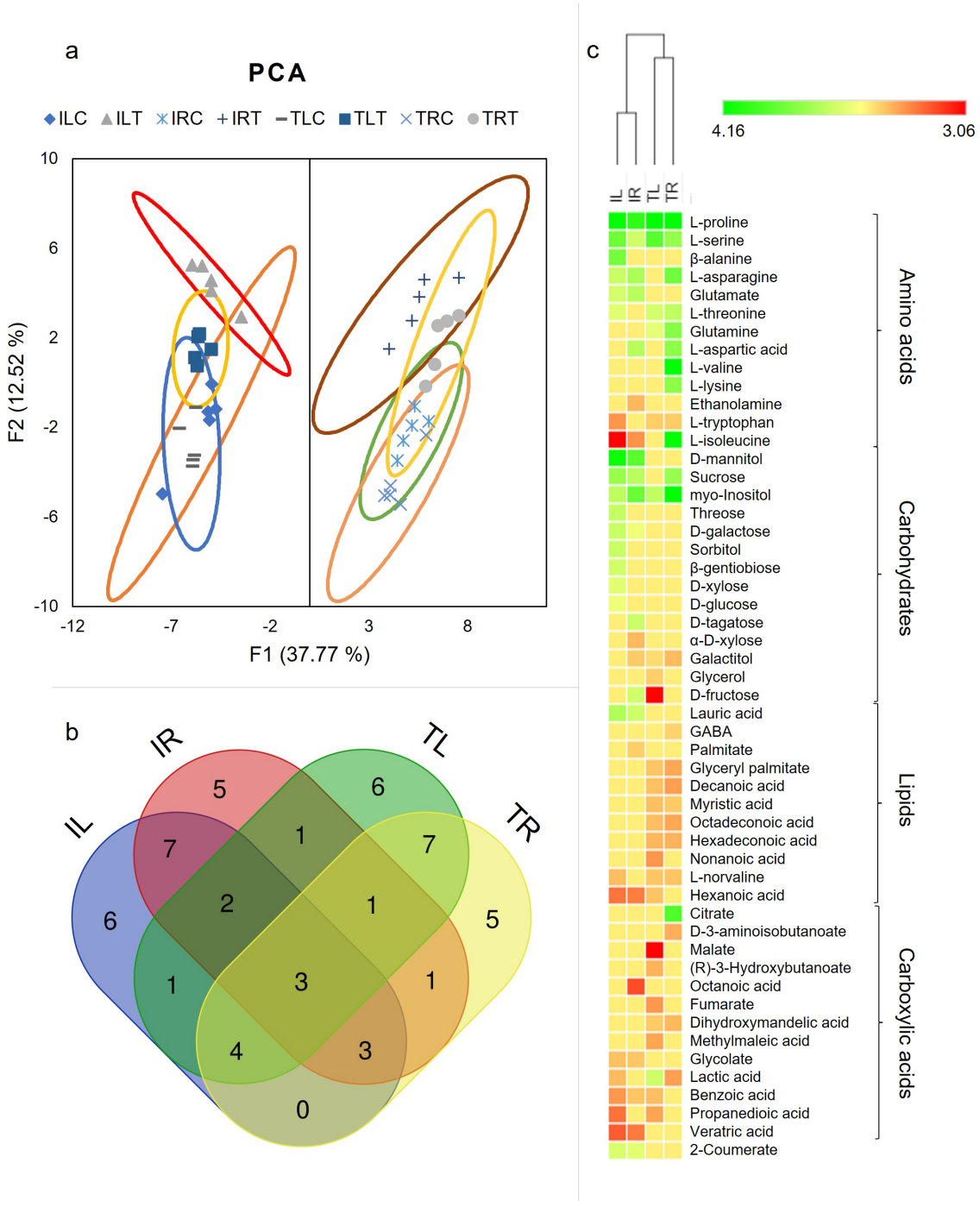

Figure 5.9. PCA displayed the variation of metabolic responses in tissues (a). Venn diagram exhibited the distribution of DADMs among tissues under salt stress (b). Hierarchical clustering demonstrated the differential reaction of the two genotypes (c).

Even though all the tissues had similar numbers of differentially accumulated/ decreased metabolites (DADMs), IL presented the greatest number of accumulated metabolites (17 metabolites) while TL had the greatest number of decreased metabolites (19 metabolites). The quantity of accumulated and decreased metabolites was approximately even for root tissues of both genotypes. Out of a total 52 metabolites that were significantly accumulated/decreased in at least one of the samples, only three (L-proline, L-serine, and myo-Inositol; all were accumulated) were discovered in all tissues and genotypes while 22 were exclusive to specific tissues and genotypes (Figure 5.9b).

Hierarchical clustering analysis of DADMs demonstrated the difference between the responses of separate genotypes to salinity. The procedure positioned the leaf and root tissues of genotypes in the same clade and diverged the tissues of contrasting genotypes (Figure 5.9c). This analysis also displayed the distinction of the tissue metabolic response patterns of genotypes; while IL has accumulated nine separate carbohydrates under salt stress, TL was able to accumulate only one and displayed decreased quantities for another three. A comparable disparity was also apparent in the root tissues, as IR displayed six accumulated and two decreased carbohydrates, while TR only had two accumulated and one decreased metabolite identified as a carbohydrate. (Figure 5.9c; Figure 5.10). Amino acid contents mainly increased in all tissues, but this rise was especially notable for TR as it exhibited nine DADMs for the amino acid class. The lipid contents (primarily structural derivatives of a fatty acid, decanoic acid) of both leaf and root tissues of TR43477 were significantly reduced compared to tissues of Ispir. Carboxylic acid contents have declined in tissues of both genotypes. Additionally, accumulation of 2-coumerate was detected in both tissues of Ispir (Figure 5.9c; Figure 5.10).

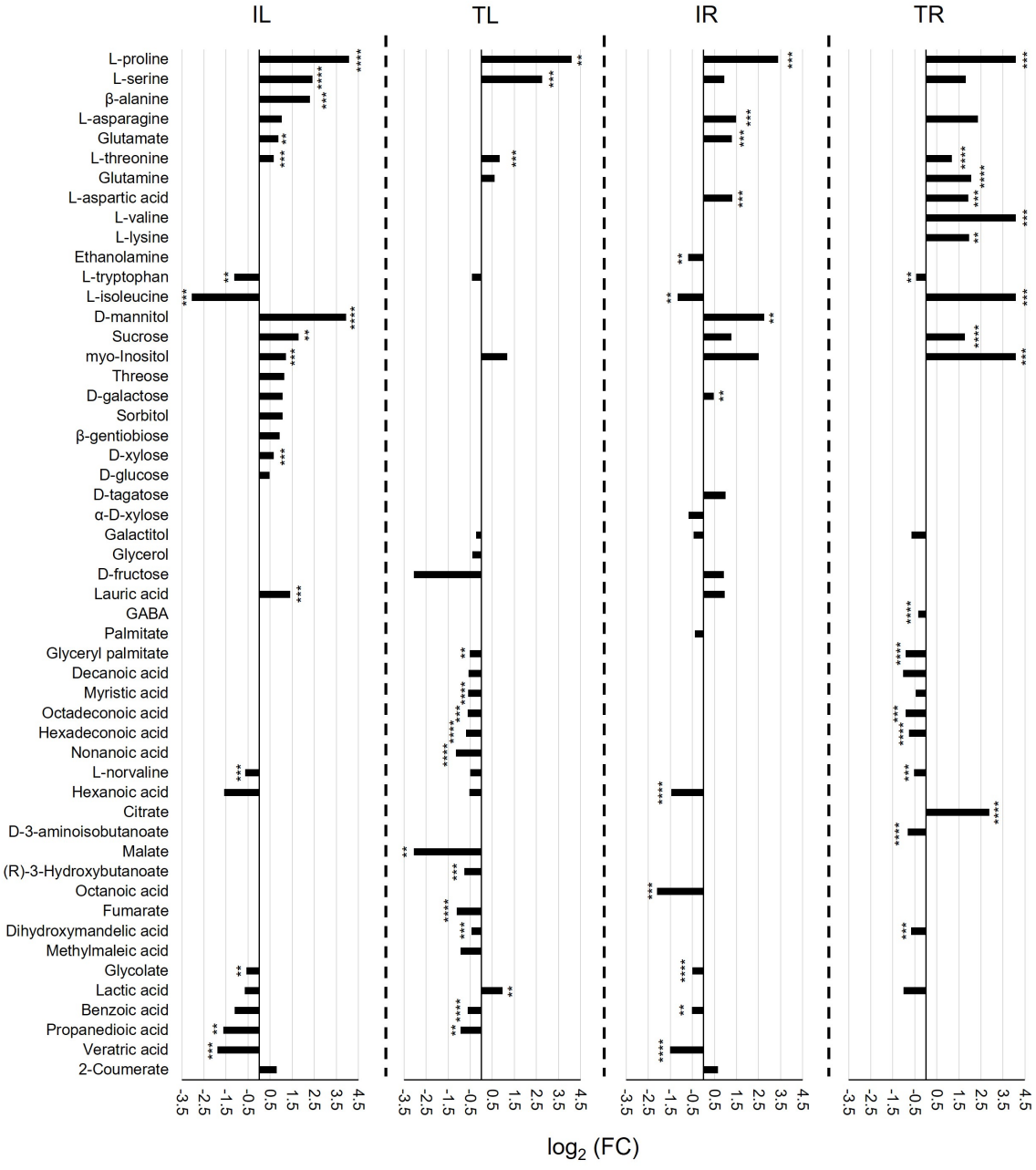

Figure 5.10. Graph representation of significantly accumulated and decreased metabolites in saline conditions. Highly significant ($p<0.01$) changes were denoted with asterisks.

5.3. Transcriptional and Metabolic Patterns of Carbon and Amino Acid Metabolism

The DEGs and DADMs were mapped on the KEGG online database *P.vulgaris* biological pathways. As the untargeted metabolome study mainly uncovered the primary metabolites such as carbohydrates and amino acids, the analysis was focused on the carbon and amino acid metabolism and their relationships to related carbohydrates (Figure 5.11; Table 5.4). Leaf tissue comparison displayed the intensified feeding of citrate cycle in IL through upregulated genes in Fructose-6P – PEP – Oxaloacetate and Fructose-6P – PEP – Pyruvate – Acetyl CoA pathways. Both malate and fumarate amounts were considerably diminished in TL ($p<0.01$; $\log_2 FC>1$). In contrast, their levels were steady in IL. Carbohydrates were mostly accumulated in IL, but there is no significant alteration for many of them in TL (Figure 5.10). Especially, the accumulation of sucrose and glucose in IL signifies the persistent carbon fixation – glycolysis cycle, which is also indicated by the augmented photosynthesis (Figure 5.6a; Figure 5.7a; Figure 5.8).

Leaf tissues of both genotypes displayed an enriched Glutamate - Glutamine/2-Oxogluterate reaction pathway (Figure 5.11; Table 5.4). While IL accumulated glutamate, TL accumulated glutamine; this suggests an imbalance in the direction of reaction among the genotypes. IL presented a boosted asparagine production with accumulated asparagine and an upregulated asparagine biosynthesis-related gene -Phvul.006G069300-, while a homolog of that gene -Phvul.001G252200- was downregulated in TL (Table 5.4).

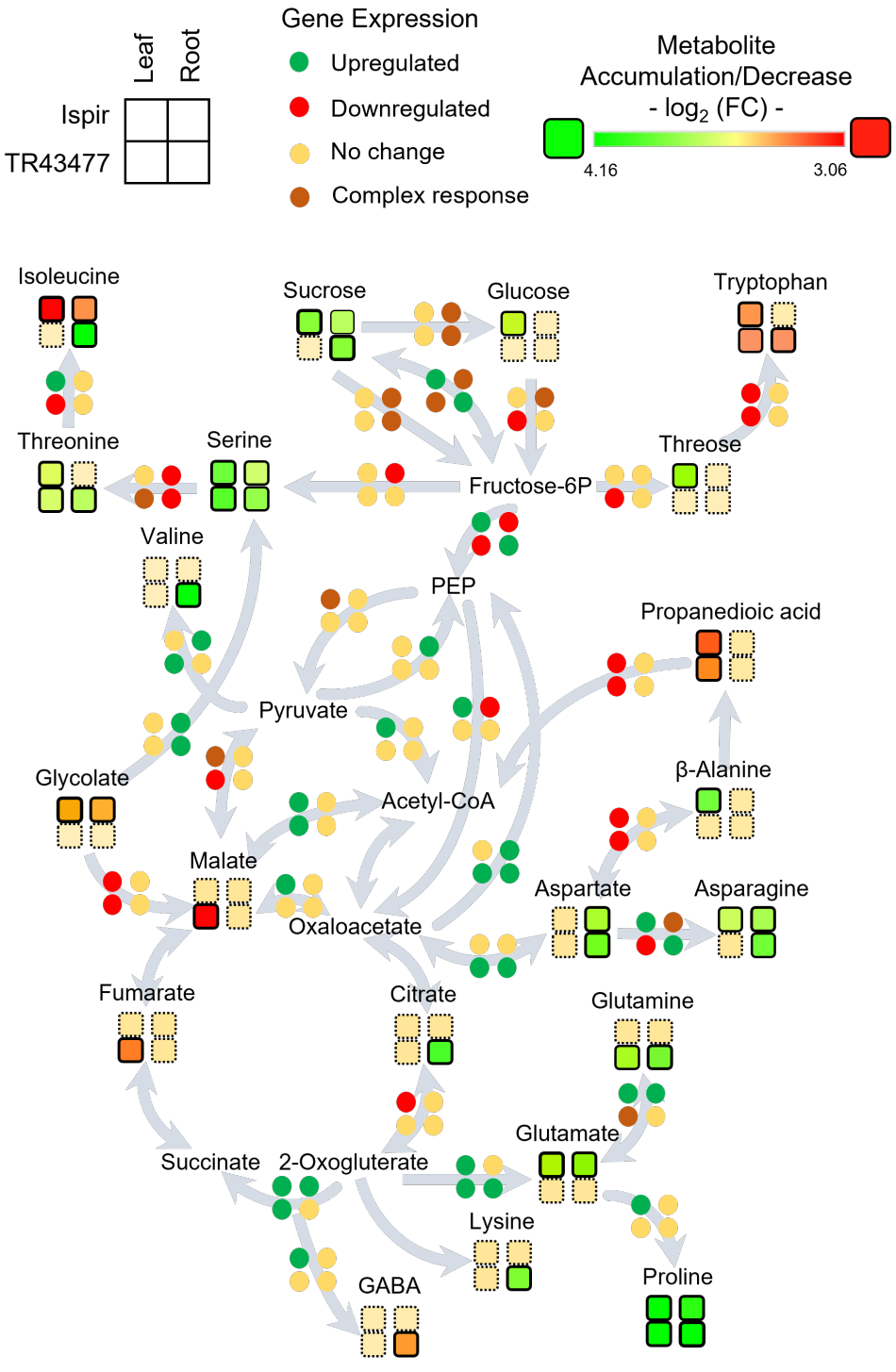

Figure 5.11. Transcript and metabolite changes in primary metabolism. The pathway map was derived from KEGG database. Disc units represent gene expression for one or more genes depending on the pathway. Bold outlines - $p<0.01$.

For the root tissues, genes associated with glycolysis and citric acid cycle displayed a higher inclination to downregulation in the IR compared to TR, which demonstrated a more balanced carbon pathway (Figure 5.11; Table 5.4). Particularly, downregulations of Fructose-6P – PEP – Oxaloacetate pathway genes and upregulations of Oxaloacetate to PEP and Pyruvate to PEP conversions revealed a decelerated energy metabolism in IR compared to TR (Figure 5.11; Table 5.4). Though root tissues of both genotypes accumulated sucrose, IR managed to accumulate fructose, galactose, mannitol, and tagatose as well (Figure 5.10) Moreover, the intensity difference analysis has indicated a sucrose-phosphate synthase homolog Phvul.005G002600, that might have a part in the accumulation of these carbohydrates in IR. Sucrose to glucose/fructose-6P conversions were in complex regulation in the root tissues of both genotypes with different up- and downregulated genes.

IR accumulated glutamate but had reduced isoleucine; TR, in contrast, accumulated isoleucine, valine, glutamine, threonine, and lysine but was depleted in tryptophan content in comparison to IR. Intensity difference analysis has demonstrated IR exclusive upregulation of a putative *2-oxoisovalerate dehydrogenase*, Phvul.009G132900, that is part of 'valine, leucine, and isoleucine degradation pathway in KEGG; the upsurge of this enzyme in IR might have been critical for the content variance for the associated amino acids. Both genotypes accumulated aspartate, asparagine, proline, and serine amino acids; Serine appeared to be accumulated in root tissues of both genotypes, but TR had greater accumulation levels ($\log_2$FC<1.82) compared to IR ($\log_2$FC<0.94). Genes of serine production from fructose-6P and conversion of it to threonine and isoleucine were downregulated in IR simultaneously with a decline in isoleucine amount. On the other hand, this pathway was mainly stable in TR together with the accumulation of isoleucine, serine, and threonine. Then again, serine accumulation in IR might be the consequence of serine biosynthesis via glycolate: Both IR and TR demonstrated an upregulation of '*serine-glyoxylate transaminase*' annotated gene (Phvul.006G029100) that has a role in serine production through glycolate, yet only in IR, glycolate amount was significantly decreased (Figure 5.10; Figure 5.11; Table 5.4).

Table 5.4. Expressional regulation of genes related to primary metabolism. Values represent $\log_2$FC. Arrows indicate the direction of the reaction.

ID	IL	TL	IR	TR	Pathway
Phvul.007G011400	3.33	3.16	3.23	0	2-Oxogluterate → Succinate
Phvul.003G209200	1.57	2.54	0	0	Acetyl-CoA ↔ Malate
Phvul.002G105000	-1.27	0	0	0	Citrate ↔ 2-Oxogluterate
Phvul.004G011200	-1.47	0	0	0	Citrate ↔ 2-Oxogluterate
Phvul.001G045700	0	0	0	1.64	Fructose 6P → PEP
Phvul.001G098100	1.23	-2.45	0	0	Fructose 6P → PEP
Phvul.001G259000	0	0	-1.99	0	Fructose 6P → PEP
Phvul.005G050700	0	-2.01	0	0	Fructose 6P → PEP
Phvul.007G222900	0	0	-3.16	0	Fructose 6P → PEP
Phvul.008G282000	1.75	-4.34	0	0	Fructose 6P → PEP
Phvul.009G006600	1.46	-2.04	0	0	Fructose 6P → PEP
Phvul.011G039100	1.84	-2.47	0	0	Fructose 6P → PEP
Phvul.007G006600	0	-1.67	0	0	Fructose 6P → Therose
Phvul.002G308400	0	0	1.7	0	Glucose → Fructose 6P
Phvul.008G180200	0	-2.01	-1.02	0	Glucose → Fructose 6P
Phvul.001G001000	-1.2	0	0	0	Glycolate → Malate
Phvul.005G051800	0	-1.71	0	0	Glycolate → Malate
Phvul.007G140600	1.3	0	0	0	Oxaloacetate ↔ Malate
Phvul.002G139200	0	2.6	1.81	0	Oxaloacetate → PEP
Phvul.003G285900	0	0	0	1.46	Oxaloacetate → PEP
Phvul.005G066400	2.98	0	-2.85	0	PEP → Oxaloacetate
Phvul.005G095300	1.18	0	0	0	PEP → Oxaloacetate
Phvul.007G047600	-1.53	0	0	0	PEP → Pyruvate
Phvul.007G077700	1.19	0	0	0	PEP → Pyruvate
Phvul.007G110900	1.03	0	0	0	PEP → Pyruvate
Phvul.010G119600	1.11	0	0	0	Pyruvate → Acetyl-CoA
Phvul.003G118800	1.06	0	0	0	Pyruvate → Acetyl-CoA / 2-Oxogluterate → Succinate
Phvul.009G254900	1.37	0	0	0	Pyruvate → Acetyl-CoA / 2-Oxogluterate → Succinate
Phvul.002G309600	-2.16	0	0	0	Pyruvate ↔ Malate
Phvul.005G166400	1.96	0	0	0	Pyruvate ↔ Malate

Table 5.4. Expressional regulation of genes related to primary metabolism. (cont.)

ID	IL	TL	IR	TR	Pathway
Phvul.010G094700	0	-1.74	0	0	Pyruvate ↔ Malate
Phvul.003G098200	0	0	1.68	0	Pyruvate → PEP
Phvul.005G158300	1.31	0	0	0	Succinyl-CoA → GABA
Phvul.006G029100	0	0	3.36	1.82	Glycolate - Serine
Phvul.001G252200	0	-1.49	0	0	Asparagine
Phvul.006G069300	2.09	0	1.92	2.88	Asparagine
Phvul.008G259900	0	0	-2.95	0	Asparagine
Phvul.001G076400	1.16	2.45	0	0	Glutamate
Phvul.009G106800	0	2.17	0	0	Glutamate (via 2-Oxoglutarate) / Aspartate (via Oxaloacetate)
Phvul.010G067200	0	0	0	3.84	Glutamate (via 2-Oxoglutarate) / Aspartate (via Oxaloacetate)
Phvul.004G148300	0	1.57	1.07	0	Glutamine
Phvul.006G155800	0	-1.69	0	0	Glutamine
Phvul.008G237500	8.29	0	3.11	0	Glutamine
Phvul.002G248000	1.22	0	0	0	Isoleucine
Phvul.006G152700	1.12	0	0	0	Isoleucine
Phvul.009G166100	3.57	-3.01	0	0	Isoleucine
Phvul.003G001200	1.67	0	0	0	Proline
Phvul.007G040600	0	0	-1.41	0	Serine
Phvul.004G070100	0	-2.18	0	0	Threonine (via Aspartate)
Phvul.011G012000	0	-1.55	0	0	Threonine (via Aspartate)
Phvul.001G266600	0	2.24	-1.24	0	Threonine (via Serine/Glycine)
Phvul.003G286600	0	-1.42	0	0	Threonine (via Serine/Glycine)
Phvul.006G105400	0	-3.01	0	-1.68	Threonine (via Serine/Glycine)
Phvul.007G014800	-1.45	-1.51	0	0	Tryptophan
Phvul.009G075100	0	3.35	1.6	0	Valine/Isoleucine
Phvul.002G186000	-9.29	0	0	0	Aspartate → Beta-Alanine
Phvul.004G144500	0	-2.1	0	0	Aspartate → Beta-Alanine
Phvul.006G087600	-1.91	-2.23	0	0	Aspartate → Beta-Alanine
Phvul.006G146200	-1.26	-1.41	0	0	Malonate → Acetyl-CoA
Phvul.001G209600	2.33	3.08	5.05	3.99	Sucrose ↔ Fructose

Table 5.4. Expressional regulation of genes related to primary metabolism. (cont.)

ID	IL	TL	IR	TR	Pathway
Phvul.003G127500	0	-1.94	0	0	Sucrose ↔ Fructose
Phvul.009G223800	0	2.06	-1.83	0	Sucrose ↔ Fructose
Phvul.001G191600	0	0	6.12	8.33	Sucrose → Fructose/Glucose
Phvul.002G061200	0	0	-3.21	-4.37	Sucrose → Fructose/Glucose

5.4. Ionomics

Tissue ion content analysis in salt stress has produced valuable results (Full detail of ion content changes for leaf and root tissues can be found in Table A15 and Table A16, respectively.). The most significant changes were observed in Na^+ and K^+ contents, but there were differences in Mg^{+2}, Mn^{+2}, Cu^{+2}, B^{+3}, and Zn^{+2} contents as well (Figure 5.12a; Figure 5.13; Figure 5.14).

Root tissues of both genotypes displayed drastic accumulation of Na^+ ion upon salt-stress as anticipated, but Ispir presented a much better performance: Not only it managed to retain the Na^+ rise at significantly lower levels in the root tissue compared to TR43477 (Figure 5.12d), but also kept the leaf Na^+ content unchanged, in contrast to TR43477. Markedly, levels of Na^+ ion were much higher in IL (3200.56 µg/g) compared to TL (955.9 µg/g) in control conditions; but after salt treatment, Na^+ ion content of TL increased drastically (4536.4 µg/g), while IL Na^+ content did not display a significant variation if not a decrease (2630.8 µg/g) (Figure 5.12c; Figure 5.13). One upregulated and one downregulated Na^+/H^+ antiporter-annotated genes were found as DEG in IR, while no transporter gene related to Na^+ was subjected to differential regulation in TR. Two Na^+ symporter annotated genes were unique to IL as DEGs (Table 5.5) which might signify their potential roles in leaf Na^+ homeostasis in IL during pre-stress and stress conditions.

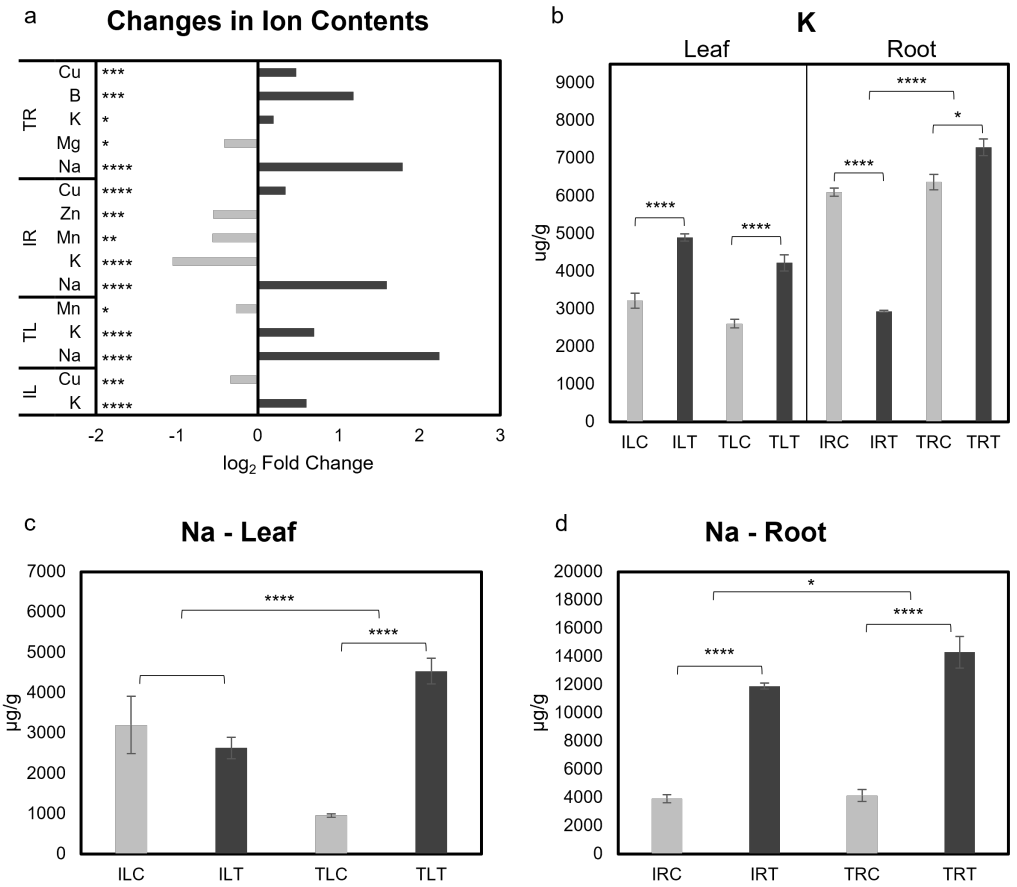

Figure 5.12. Salt responsive ion content differences for tissues and genotypes (a). K^+ (b) and Na^+ (c–d) ion levels were also presented separately to underline the disparity between genotypes (C–control; T–salt treatment). Values represent mean±SEM.

Ispir roots have displayed a significant decrease in K^+ levels under salt stress, yet it increased in TR (Figure 5.12b). There were four separate downregulated $^+$-transport-related DEGs in TR. On the other hand, IR had one unique upregulated and three downregulated K^+-transport-related DEGs. While three K^+-transport-related DEGs were mutual to both IR and TR, leaves of both genotypes regulated entirely diverse sets of genes related to the same term (Table 5.5). Still, K^+ levels were significantly increased in the leaf tissues of both genotypes. Cu^{+2} content has decreased in IL together with five downregulated DEGs related to the transport of Cu^{+2} (Table 5.5). Separately, TL Mn^{+2} levels indicated a significant decrease under treatment. Instead, there was no significant change in IL Mn^{+2} content upon stress, but in both control and treatment conditions, it was roughly 2-fold higher compared to TL (Figure 5.13).

A similar situation was detected for Zn^{+2} ion as well: TL accumulated 3-fold higher than IL in both control and treatment conditions (Figure 5.13).

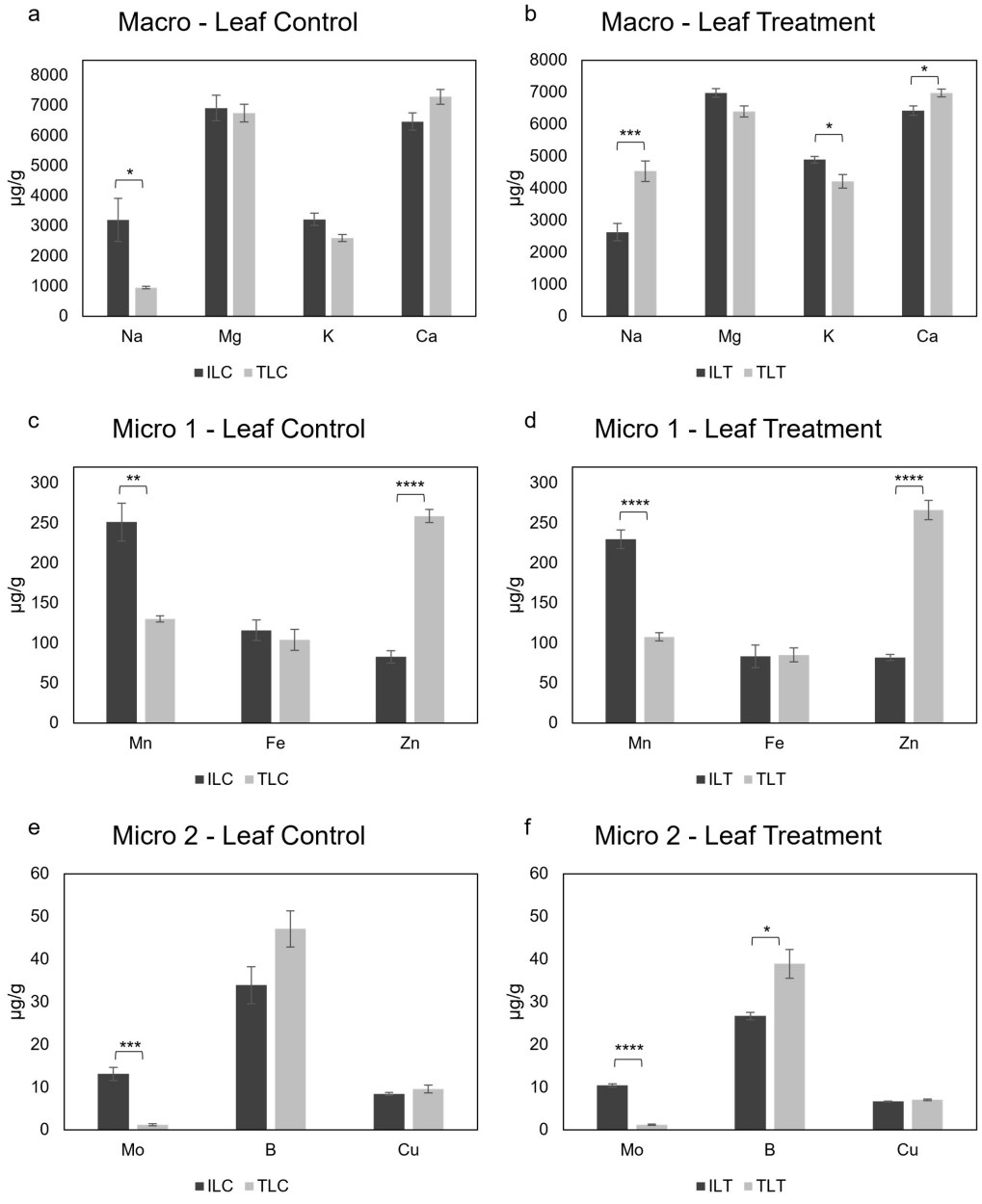

Figure 5.13. Leaf ion content comparisons under control (a, c and e) and salt treatment (b, d, and f) conditions. Values represent mean±SEM.

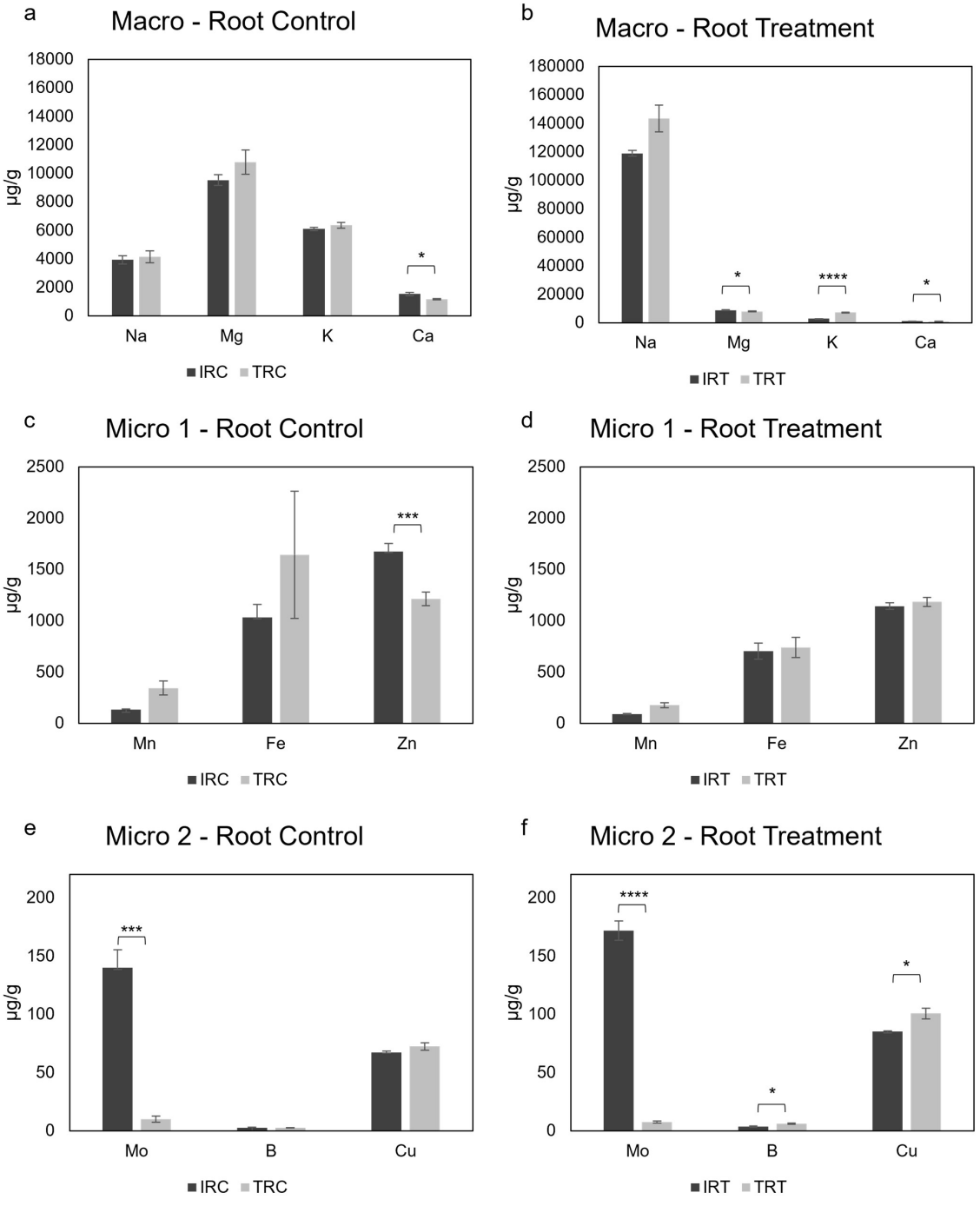

Figure 5.14. Root ion content comparisons under control (a, c and e) and salt treatment (b, d, and f) conditions. Values represent mean±SEM.

Table 5.5. Expressional differences of genes related to ion transport. Values represent $\log_2$FC.

ID	IL	TL	IR	TR	Annotation
Phvul.004G106900	-1.5	0	1.09	0	Cu^{+2} transport family protein-related
Phvul.004G107001	-1.69	-2.33	0	0	Cu^{+2} transport family protein-related
Phvul.004G107100	-2.82	0	0	0	Cu^{+2} transport family protein-related
Phvul.007G075000	-3.06	0	0	0	Cu^{+2} transport family protein-related
Phvul.004G158700	0	3.15	0	0	Cu^{+2} transport protein family
Phvul.007G070001	1.56	0	-1.53	0	Cu^{+2} transport protein family
Phvul.008G282300	-5.21	0	0	0	Cu^{+2} transport protein family
Phvul.004G116400	0	0	1.11	0	Cu^{+2} transport protein family
Phvul.008G282200	0	-3.13	0	0	Cu^{+2} transport protein family
Phvul.011G060400	0	0	-1.93	0	Ctr Cu^{+2} transporter family
Phvul.011G060500	0	-1.7	-2.29	0	Ctr Cu^{+2} transporter family
Phvul.010G095600	-1.58	0	0	0	K^+ efflux antiporter 2
Phvul.002G216200	1.49	0	0	0	K^+ efflux antiporter 3
Phvul.003G160800	0	0	-1.76	-1	K^+ transporter 1
Phvul.009G047300	0	-3.73	0	0	K^+ uptake permease 5
Phvul.002G072300	2.08	0	0	0	K^+ uptake permease 6
Phvul.002G331700	0	0	1.48	0	K^+ uptake permease 6
Phvul.001G246500	0	11.15	0	0	Predicted K^+/H^+ - antiporter
Phvul.008G238100	0	0	-1.94	-2.58	K^+ CHANNEL GORK-RELATED
Phvul.006G164300	0	-5.4	0	0	K^+ channel in Arabidopsis thaliana 1
Phvul.011G181800	-2.51	0	0	0	K^+ channel in Arabidopsis thaliana 1
Phvul.005G040750	-3.22	0	0	0	K^+ channel tetramerization domain-containing
Phvul.002G185300	0	2.44	0	-4.24	K^+ transporter 1
Phvul.008G152200	0	-2.88	-1.5	-1.58	K^+ transporter family protein
Phvul.006G097100	0	0	-2.32	0	Na^+/H^+ exchanger 2
Phvul.001G105500	0	1.73	0	0	Na^+/Ca^{+2} exchanger family protein
Phvul.002G127200	-1.74	0	0	0	solute:Na^+ symporters;urea transmembrane transporter
Phvul.003G089800	0	1.97	1.5	0	Na^+/H^+ antiporter 6
Phvul.006G134033	0	1.74	0	0	Na^+/H^+ antiporter 6
Phvul.006G204300	2.03	0	0	0	divalent anion:Na^+ symporter, DASS family
Phvul.003G042200	0	1.31	0	0	Mg^{+2} transporter 3
Phvul.008G034033	0	1.95	0	0	Mg^{+2} transporter 4
Phvul.007G090901	-6.14	0	0	0	Mg^{+2} transporter 7

Table 5.5. Expressional differences of genes related to ion transport. (cont.)

ID	IL	TL	IR	TR	Annotation
Phvul.003G240100	0	0	-1.06	0	Cd^{+2}/Zn^{+2}-ATPase
Phvul.003G021300	0	0	-2.95	0	Zn^{+2} transporter
Phvul.006G001000	-3.64	0	0	0	Zn^{+2} transporter 1 precursor
Phvul.002G099700	0	0	-1.36	0	Zn^{+2} transporter 10 precursor
Phvul.002G100001	0	0	-1.16	0	Zn^{+2} transporter 10 precursor
Phvul.003G262400	0	0	-6.4	0	Zn^{+2} transporter 10 precursor
Phvul.006G055800	-1.91	-2.97	0	0	Zn^{+2} transporter 11 precursor
Phvul.L007443	0	0	3.42	1.7	Zn^{+2} transporter 11 precursor
Phvul.001G035800	0	0	-1.08	0	Zn^{+2} transporter 4 precursor
Phvul.009G240000	-1.44	0	-1.69	0	Zn^{+2}-exporting ATPase

Cu^{+2} ion contents demonstrated a highly significant increase in root tissues of both Ispir and TR43477 (Figure 5.12a; Figure 5.14), but TR did not display any DEGs linked to the transport of this ion. In contrast, IR presented two up- and three downregulated genes (Table 5.5). TR also accumulated B^{+3} and had a minor drop in Mg^{+2} levels. IR, however, displayed significant decreases in Zn^{+2} and Mn^{+2} ion levels together with mostly downregulated transporter genes linked to both ions (Table 5.5). Nonetheless, Zn^{+2} content was already significantly higher for IR compared to TR in the control (approx. 1.4-fold difference) (Figure 5.14) and salt stress decreased IR Zn^{+2} content similar to the TR Zn^{+2} level. Curiously, Mo^{+2} levels were exceptionally higher (Figure 5.14) in the Ispir tissues for both conditions, though it did not show a significant change under salt-stress conditions.

5.5. Discovery of Novel Salt-Tolerance Gene Relationships

5.5.1. Candidate Gene Selection

Root is the first organ to encounter salinity, and a good tolerance mechanism in the root system can minimize the transmittance of stress to the upper parts of the plant. Thus, priority was given to root transcriptome for selection of candidate genes.

The selection was focused on the upregulated genes in the tolerant genotype: The comparison of the tolerant and the susceptible genotype displayed genes with similar and different regulation in salt stress (Figure 5.4); all genes that were also upregulated in the roots of susceptible genotype were filtered out. Next, the intensity difference filtration displayed the genes with a high regulation difference. This resulted in a 25 gene pre-candidate list (Table 5.6) which contained three transcription factors, three molecular chaperones, five cell wall-structural components, four transmembrane transporters, eight diverse catalytic and two unknown proteins.

Table 5.6. Pre-candidate genes list for functional study.

ID	**Annotation**	**Type**
Phvul.002G318500.2	Pectinesterase/pectinesterase inhibitor 6	Cell Wall Modification
Phvul.003G117100.1	Cell wall / vacuolar inhibitor of fructosidase 1	Cell Wall Modification
Phvul.003G224800.1	Expansin-like b1	Cell Wall Modification
Phvul.005G130900.1	Xyloglucanendohydrolase	Cell Wall Modification
Phvul.009G233200.1	Xyloglucan:xyloglucosyl transferase	Cell Wall Modification
Phvul.004G005400.1	Alkane hydroxylase cyp96a15	Misc. Enzyme
Phvul.005G002600.1	Sucrose-phosphate synthase 4	Misc. Enzyme
Phvul.008G087600.1	Alanine-glyoxylate transaminase	Misc. Enzyme
Phvul.009G131000.1	Naringenin-chalcone synthase	Misc. Enzyme
Phvul.009G199200.1	PHYB activation tagged suppressor 1	Misc. Enzyme
Phvul.010G016000.1	Ribulose bisphosphate carboxylase	Misc. Enzyme
Phvul.011G122900.1	Monothiol glutaredoxin-s13	Misc. Enzyme
Phvul.011G169900.1	Trypsin and protease inhibitor	Misc. Enzyme
Phvul.003G154800.1	Heat shock 70 kda protein 5	Molecular Chaperone
Phvul.004G129400.1	22.0 kda heat shock protein	Molecular Chaperone
Phvul.009G080200.1	17.6 kda class II heat shock protein	Molecular Chaperone

Table 5.6. Pre-candidate genes list for functional study. (cont.)

ID **IR**	**IL** **TR**	**TL** **Annotation**
Phvul.007G061000.1	Ring zinc finger protein	Transcription Factor
Phvul.007G065100.2	Mads box protein	Transcription Factor
Phvul.010G083700.1	Myeloid leukemia factor	Transcription Factor
Phvul.001G180500.1	Nodulin-like protein	Transmembrane Transporter
Phvul.003G164000.1	Protein NRT1/ PTR family 6.2	Transmembrane Transporter
Phvul.011G189900.1	Permease of the major facilitator superfamily	Transmembrane Transporter
Phvul.008G040500.1	Protein NRT1/ PTR family 7.2	Transmembrane Transporter
Phvul.007G225200.1	Late embryogenesis abundant protein	Uncharacterized
Phvul.009G024301.1	Protein of unknown function	Uncharacterized

The remaining batch of genes were investigated for their possible functions in metabolic pathways and stress tolerance, based on their annotations. To narrow down the list, the genes with known/well-defined stress tolerance-related functions such as heat shock proteins and naringenin-chalcone synthase were eliminated together with the uncharacterized ones.

All organisms possess resilience to cope with genetic modifications and disruptions to sustain their fitness through an ability called genetic robustness. This ability can be because of genetic redundancy which represents the compensation for the deficiency of one gene by another with similar function and regulation pattern [109]. To avoid such a compensation mechanism throughout the transgenic knockdown experiments, close in-species homologs were investigated for similarity and expression patterns; genes with highly similar homologs (more than 80% similarity) that have a comparable expression patterns were removed from the list. This filtering in turn lowers the chance of off-site effects of RNAi system as well. The remaining list (Table 5.7) consisted of two transmembrane transporters, two cell wall modifiers and an enzyme.

The cell wall modification activity genes were highly enriched in the roots tissues of the tolerant common bean genotype as can be seen in the GO analysis (Figure 5.6b).

Yet, related candidates were eliminated together with the permease gene as they displayed high number of in-species homologs with greater similarity compared to first two candidates - *Protein NRT1/ PTR family 6.2* (*pvNRT1* thereafter) and *Sucrose-phosphate synthase 4-related* (*pvSPS4* thereafter). While the KEGG enrichment analysis (Figure 5.7b) indicated an enrichment pattern in starch-sucrose metabolism in which the *pvSPS4* gene takes part, the GO enrichment analysis pointed out the mild depletion of transmembrane transportation activity. Nonetheless, most of that depletion is represented by metal-ion transporters, and our selection -*NRT1*- probably functions as a nitrate or peptide transporter.

Table 5.7. Gene list for final selection of candidate genes. Top two genes were selected for further functional studies. (Tol. – tolerant; Sus. – susceptible; Rel. Exp. – relative expression; Max – maximum; reads were represented as control vs treated).

Annotation	**In-species homologs**	**Max. similarity**	**Tol. Rel. Exp.**	**Tol. reads**	**Sus. Rel. Exp.**	**Sus. reads**
Protein NRT1/ PTR family 6.2	2	57%	3.95	10-158	1.9	9-62
Sucrose-phosphate synthase 4-related	2	57%	3.83	74-1094	0.05	61-213
Cell wall / vacuolar inhibitor of fructosidase 1-related	3	69%	3.81	15-219	0.72	22-48
Pectinesterase/pectinesterase inhibitor 6-related	6	61%	2.96	76-606	-0.78	34-28
Permease of the major facilitator superfamily	7	74%	2.71	190-1251	0.89	169-495

5.5.2. RNAi Vector Construction of the Selected Genes

The selected RNAi mechanism – intron-containing hairpin RNA – has proven to be the most effective gene silencing tool in plant systems [110]. This efficient methodology requires a gene-specific region approximately 100 to 850bp long [111].

Relatively unique parts of the selected genes were found via Blast software using the reference RNA sequences of *P.vulgaris* as background. The 280bp and 288bp fragments of *pvSPS4* and *NRT1* genes were selected for RNAi respectively (Figure 5.15a). Moreover, a 268 bp fragment of the human *ferritin* gene (HumFer) with low similarity to *P.vulgaris* L. genes was selected for negative control experiments. For the Gateway cloning (Figure 5.15b-c), these fragments were cloned from the total mRNA of the Ispir root tissues with primers containing *attB* sites via PCR generating 341bp, 349bp, and 329bp products (Figure 5.16).

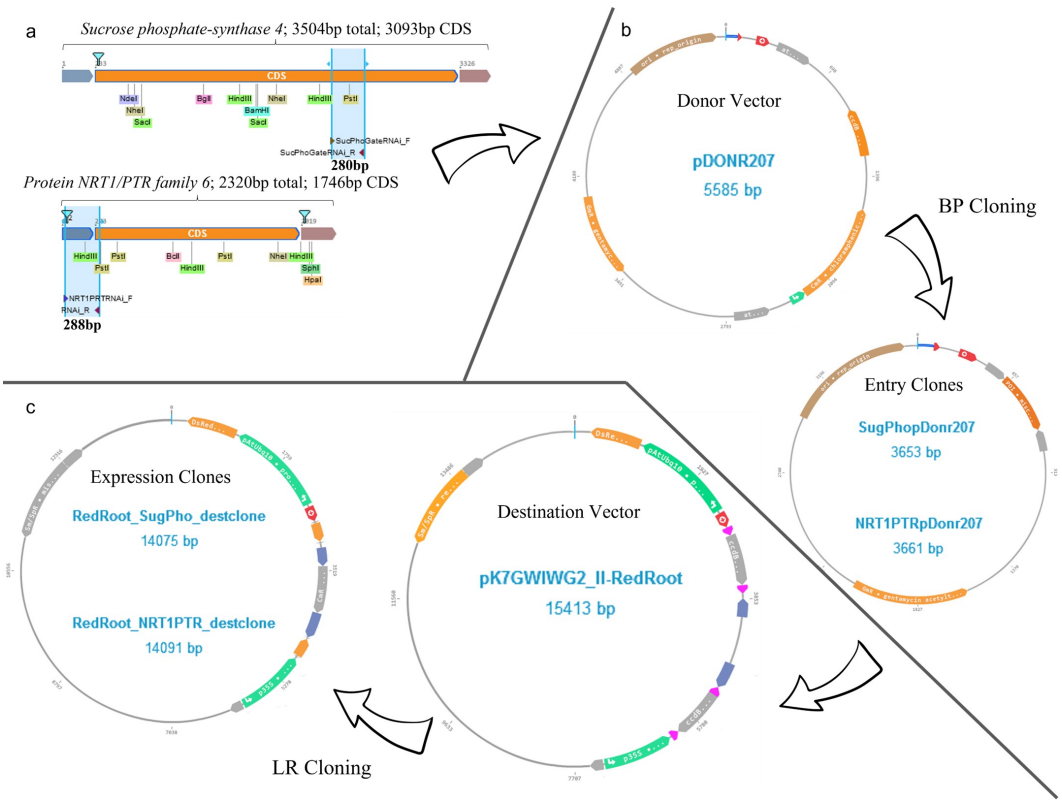

Figure 5.15. Gateway cloning scheme of *pvSPS4* and *pvNRT1* gene parts for ihpRNA based silencing technique.

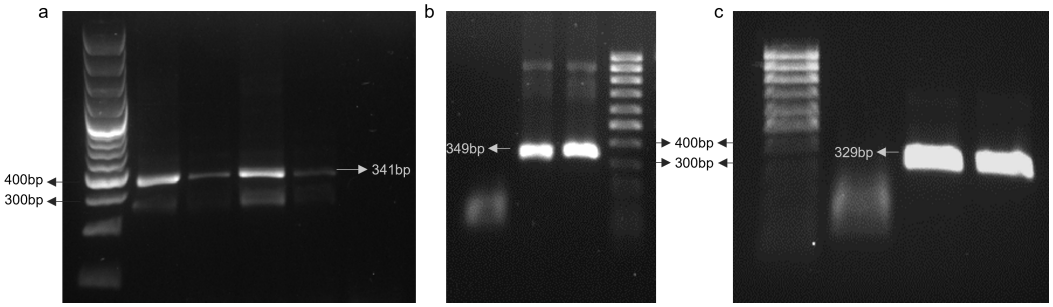

Figure 5.16. Agarose gel images of *attB* site containing parts of (a) *pvSPS4*, (b) *NRT1*, and (c) Human *ferritin* genes.

After purification, products were harnessed in BP cloning reaction to be inserted in the donor vector pDONR207. The results (Figure 5.17a for *pvSPS4*, d for *pvNRT1*, and g for *HumFer*) indicated successful insertion for both gene parts: For both, *ccdB* gene was removed and gene parts were inserted yielding the expected bands with 561bp for *pvSPS4*, 569bp for *pvNRT1* and 549 for HumFer. The resulting entry vectors in turn were used in LR reaction with the destination vector RedRoot to generate expression clones. Both insertions were confirmed through PCR and agarose gel electrophoresis for both gene parts: Figure 5.17b and c show the insertions with 989 and 1065bp bands for *pvSPS4*; e and f show the insertions with 997 and 1073bp bands for *pvNRT1*; and h and i show the insertions with 977 and 1053bp bands for HumFer.

5.5.3. Transformation of *Agrobacterium rhizogenes* K599

Transformation of the *A. rhizogenes* was performed as described by Holsters M. *et al.*, (1978) [112]. $CaCl_2$ was used for the preparation of competent cells and the heat-shock method was employed for transformation of the ihpRNA carrying vectors. The presence of the vectors in the bacterial colonies was verified by both spectinomycin antibiotic selection and colony PCR (Figure 5.18).

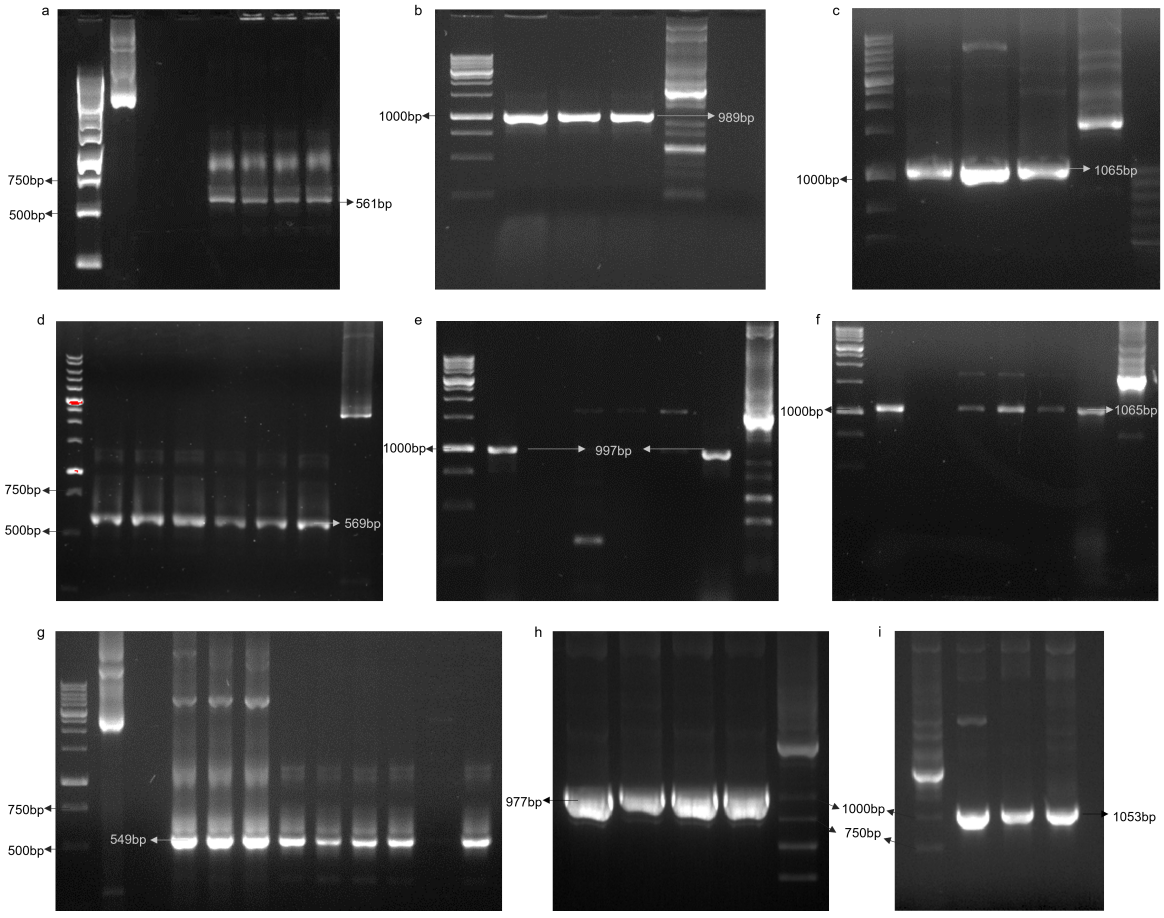

Figure 5.17. Agarose gel images of BP cloning and LR cloning to pDONR207 and RedRoot plasmids, respectively. While (a), (d) and (g) display the BP cloning; (b-c), (e-f) and (h-i) display the double insertion to destination vector.

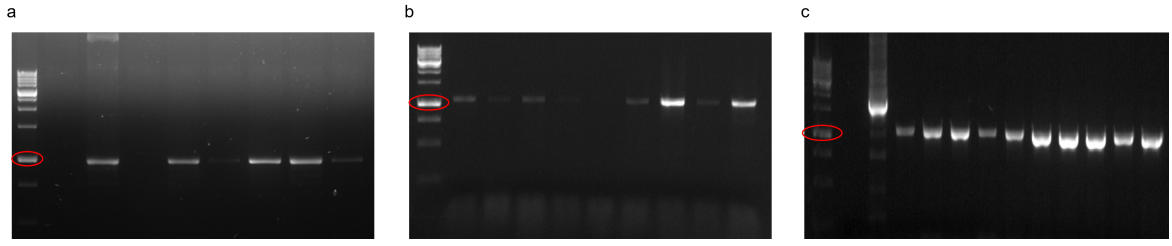

Figure 5.18. Agarose gel images after colony PCR of *A. rhizogenes* colonies carrying (a) *pvSPS4* – 989bp, (b) *pvNRT1* – 1065bp and (c) *HumFer* – 977bp ihpRNA. Red circle indicates the 1000bp on the DNA ladder.

5.5.4. Generation of Composite *P. vulgaris* L. (Ispir) Plants and Verification of knockdown

The generation of composite plants with transgenic roots that carry ihpRNA for *pvSPS4*, *pvNRT1*, and HumFer was performed as described elsewhere [82]. Briefly, following sterilization, Ispir genotype common bean seeds were germinated for two days on sterile wet paper napkins (Figure 5.19a) at 25°C in an incubator. The germinated seeds were transferred to sterile vermiculite and grown until their primary leaves emerged (Figure 5.19b). Plantlets were infected on the shoots with *A. rhizogenes* carrying the RNAi vector using a needle (Figure 5.19c) and incubated in sealed transparent containers (Figure 5.19d) until the hairy roots emerged (Figure 5.19e-f-g) from the infection sites.

Figure 5.19. Hairy-root induction methodology. After germination (a), seedlings were grown in vermiculite (b) and infected at the first leaf stage (c). Plants were grown in high humidity conditions (d) until the emergence of hairy roots (e, f, and g).

After the hairy roots reached 1–3cm in length, the primary roots were cut 1cm below the infection site, leaving the hairy roots as the sole root tissue. Verification of genomic insertion of the vectors was performed by the visualization of dsRed fluorescent protein that is connected to a constitutive promoter (Figure 5.15). The visualization of fluorescence was performed in both non-destructive -through an orange filter and green led light (Figure 5.20a–b–c) –and destructive- through observation of single root tissues under a fluorescent microscope (Figure 5.20d–e).

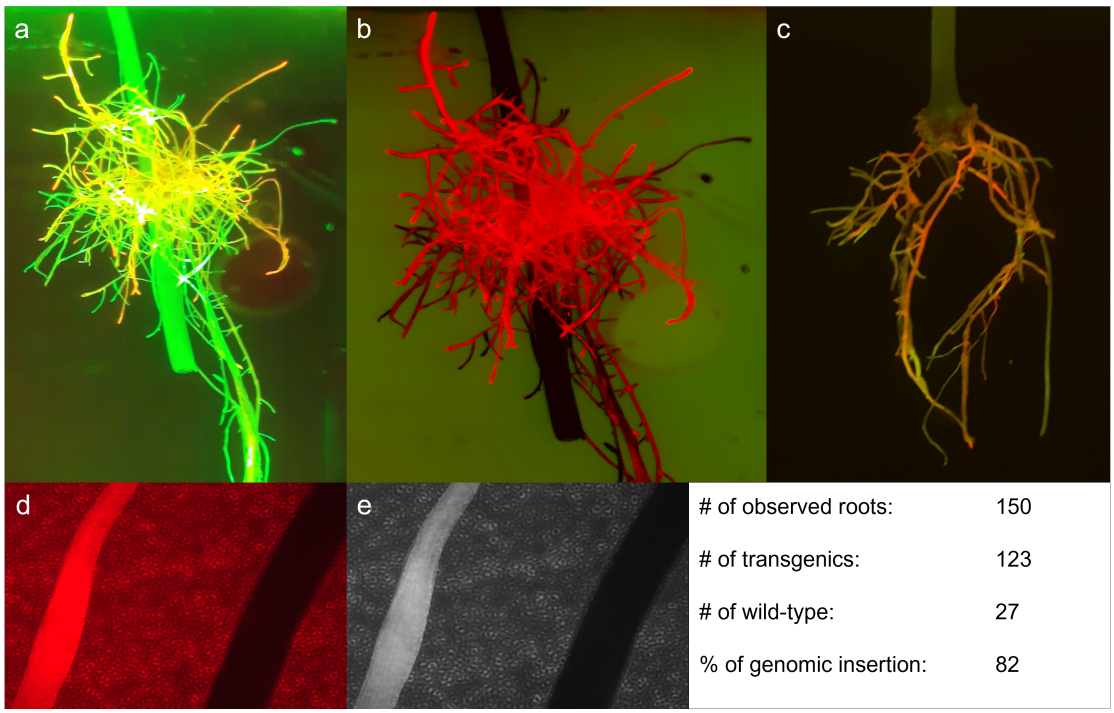

Figure 5.20. Verification of genomic insertion through red fluorescence with a non-destructive (a, b - inverted, and c - background reduced) method. Normal (d) and red-channel inverted (e) fluorescence microscopy also displayed the fluorescence.

After the primary roots were cut, and the fluorescence marker was observed, the plants were sown in vermiculite, and incubated in sealed transparent containers with high humidity for several days, as they are prone to dehydration. When the new roots are enough for nutrient and water uptake (3-4 days after excision), the lid was opened, and the plants were grown for 2-3 more days before salt treatment.

To assess the knockdown pattern, six composite plants carrying *pvSPS4* (SucPho line), *pvNRT1*, and HumFer ihpRNA and six without any vector (Blank) were grown. Three of the plants were used as controls, while the other three were treated with 150mM NaCl for five days. After treatment, root samples were collected for both control and treated plants for RNA extraction. The RNA concentration and purity were determined with spectrophotometry (Table 5.8) and integrity was determined by agarose gel electrophoresis (Figure 5.21).

Table 5.8. Composite root RNA concentrations and spectrophotometric measurements for purity.

Blank	Concentration	260/280	260/230
Control-1	330.13	2.07	2.29
Control-2	135.67	2.14	2.52
Control-3	485.15	2.15	2.34
Treated-1	387.57	2.08	2.43
Treated-2	127.07	2.15	2.96
Treated-3	456.68	2.07	2.44

SucPho	Concentration	260/280	260/230
Control-1	268.71	2.08	2.41
Control-2	130.19	2.19	2.62
Control-3	304.18	2.21	2.62
Treated-1	306.44	2.08	2.45
Treated-2	231.91	2.2	2.38
Treated-3	216.19	2	2.44

NRT1	Concentration	260/280	260/230
Control-1	93.95	2.32	2.93
Control-2	213.65	2.18	2.57
Control-3	370.7	2.22	2.31
Treated-1	230.52	2.19	2.49
Treated-2	304.21	2.26	2.29
Treated-3	106.22	2.22	2.1

HumFer	Concentration	260/280	260/230
Control-1	344.27	1.92	2.14
Control-2	308.16	1.9	2.15
Control-3	373.78	1.93	2.06
Treated-1	350.44	1.91	2.04
Treated-2	343.2	1.9	2.17
Treated-3	487.08	1.92	2.17

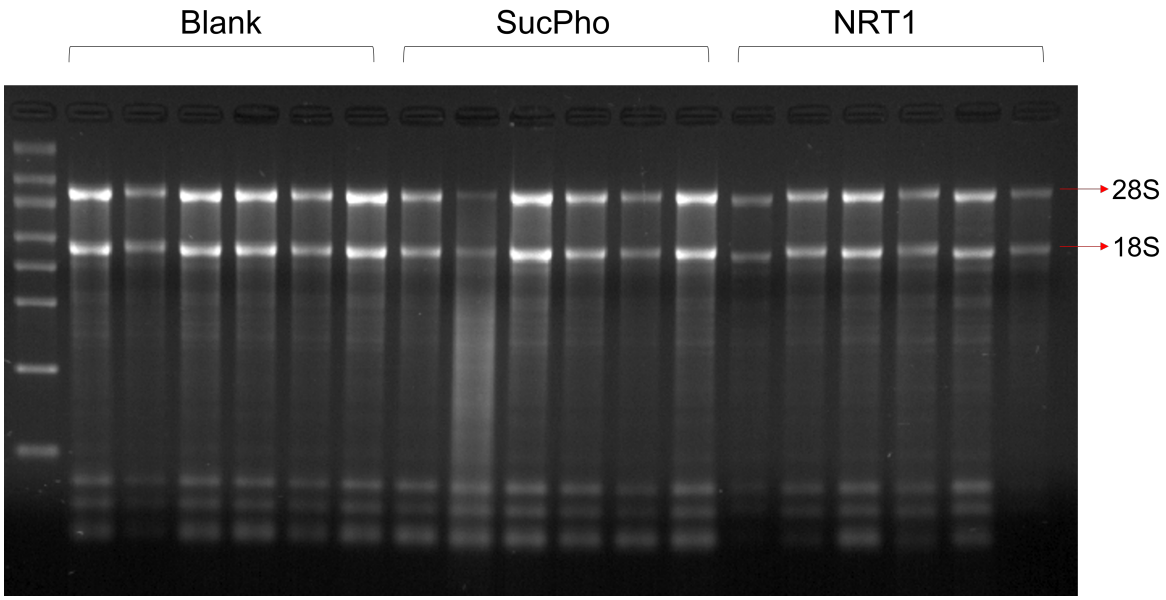

Figure 5.21. RNA samples from Blank, SucPho, and NRT1 hairy roots were determined to be not degraded as their 28S and 18S bands were intact.

RNA samples were used in RT-qPCR experiments to display the knockdown pattern of composite plants under salt treatment conditions (Figure 5.22). Although the knockdown attempts were successful for both genes, *pvSPS4* was selected as the candidate gene for further physiological and molecular evaluation for several reasons: Mock (Humfer) plants did not display a significant upregulation of *pvNRT1* under salt stress. *pvSPS4* presented a much higher read number compared to *NRT1* in RNAseq analysis (Table 5.7) which increases the reliability of the RT-qPCR results. Additionally, it had a higher expression ratio between the tolerant and susceptible genotypes (Table 5.7). Moreover, homologs of *pvSPS4* have been studied more, resulting in more information about its possible function. Therefore, it was more realistic to hypothesize about the roles it takes in salt tolerance pathways, in the case of a positive result.

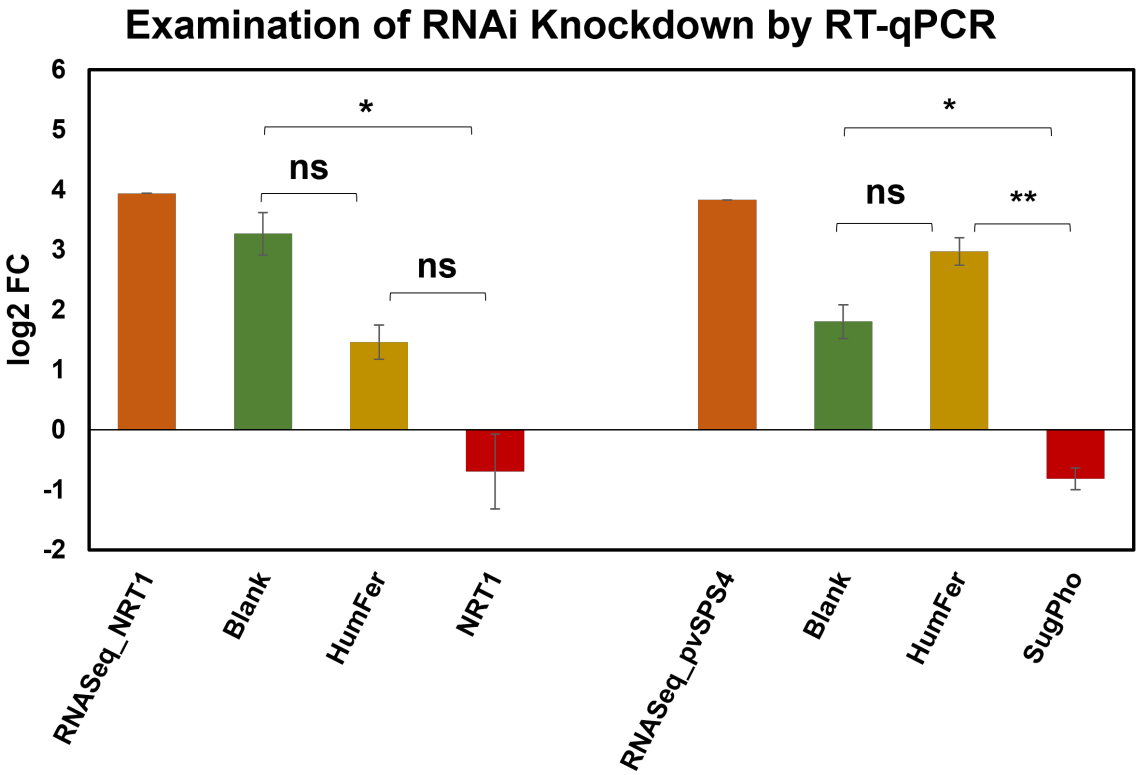

Figure 5.22. RT-qPCR evaluation of RNA knockdown pattern under treatment. SucPho plants displayed significant knockdown for *pvSPS4*. For *pvNRT1*, a variation was absent between the NRT1 and HumFer (n = 3). Values represent mean±SEM.

As the HumFer (negative control) and SucPho plants did not display a significantly different control pvSPS4 expression (Appendix B - Figure B1), the effects of knockdown on protein levels were evaluated with WB as well. The results showed no significant reduction in pvSPS4 levels for lines in control conditions. Under salt treatment, pvSPS4 levels in the SucPho roots dropped nearly by 40%, while there was no reduction for Blank and HumFer roots (Figure 5.23). According to this result, it is safe to presume that the amount of this protein is under strict control, and salt stress increases the turnover rate of the protein. Thus, to keep it steady, an upregulation is necessary under stress conditions, and a lack of it results in amount reduction as happened in SucPho roots.

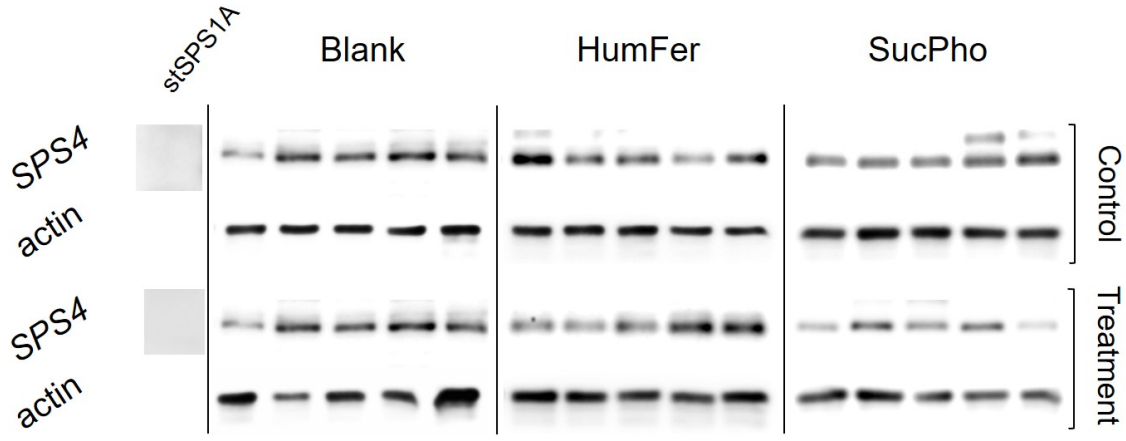

Figure 5.23. WB analysis demonstrated the stress-related pvSPS4 protein decrease (39.24% - $p<0.01$) in SucPho hairy roots (n=5). Solanum tuberosum SPS1A protein was used as a negative control.

5.5.5. Expressional and Translational Analysis of Other SPS Homologs in the Roots

Plants are able to withstand genetic alterations and persist their fitness through genetic vigor. This ability can be because of genetic redundancy which is the compensation for the insufficiency of one gene by a substitute with equivalent function [109]). Though there are several SPS homologs in the genome of *P. vulgaris*, just two, Phvul.006G031700 (*pvSPS3*) and Phvul.003G170100 (*pvSPS1*), share high amino acid sequence similarity (57% and 54% respectively) with *pvSPS4*. This transcriptome study has revealed the root-specific expression of *pvSPS4* and its homolog *pvSPS1* with high transcription rates. Nevertheless, *pvSPS1* demonstrated steady expression under salt stress, unlike *pvSPS4*. The other homolog, *pvSPS3*, had a low transcript level in wild-type root tissues, but an elevated expression with differential regulation pattern in the leaves, which indicated a leaf-specific regulation for this gene.

The impact of *pvSPS4* knockdown on these homologs was examined with RT-qPCR to explore their potential to compensate for the knockdown by an upregulation.

pvSPS4 knockdown did not stimulate differential expression of *pvSPS1* during salt stress. *pvSPS3* did not display an upregulation in response to salinity. It did however display a significant downregulation, yet, with a low transcription level in the roots, this decrease may just show a minor variation in expression (Figure 5.24a).

Since *pvSPS1* is a root-specific homolog, we have also measured the *pvSPS1* protein levels with ELISA. *pvSPS1* protein amount presented a minor but significant rise (approx. 1.3-fold) in SucPho hairy roots in control, but this variation has faded in treatment conditions (Figure 5.24b). Altogether, none of the composite lines have demonstrated a rise in pvSPS1 protein levels in response to salt stress. These findings can be considered as strong indications that the knockdown of *pvSPS4* was not compensated by the action of a homolog under salt-stress conditions.

5.6. Effect of *SPS4* knockdown on Sugar and Ionic Balance

Since SPS enzymes are correlated with the regulation of sugar metabolism and carbon partitioning, we have explored the result of *pvSPS4* knockdown in hairy root tissues was investigated further by quantifying the glucose and sucrose contents (Figure 5.25). Curiously, knockdown had a considerable impact on control glucose content of SucPho roots and no effect on sucrose content. SucPho roots demonstrated a higher glucose content in control conditions compared to Blank and HumFer roots, yet under salt stress conditions it returned to levels seen in the blank (Figure 5.25a).

A more noticeable difference was detected for the glucose/sucrose ratio. Only SucPho glucose/sucrose ratio showed a significant decline in treatment conditions. Moreover, while control glucose/sucrose ratio was significantly higher for SucPho roots compared to others, it was significantly lower in stress conditions which implied an imbalance in sugar partitioning (Figure 5.25b).

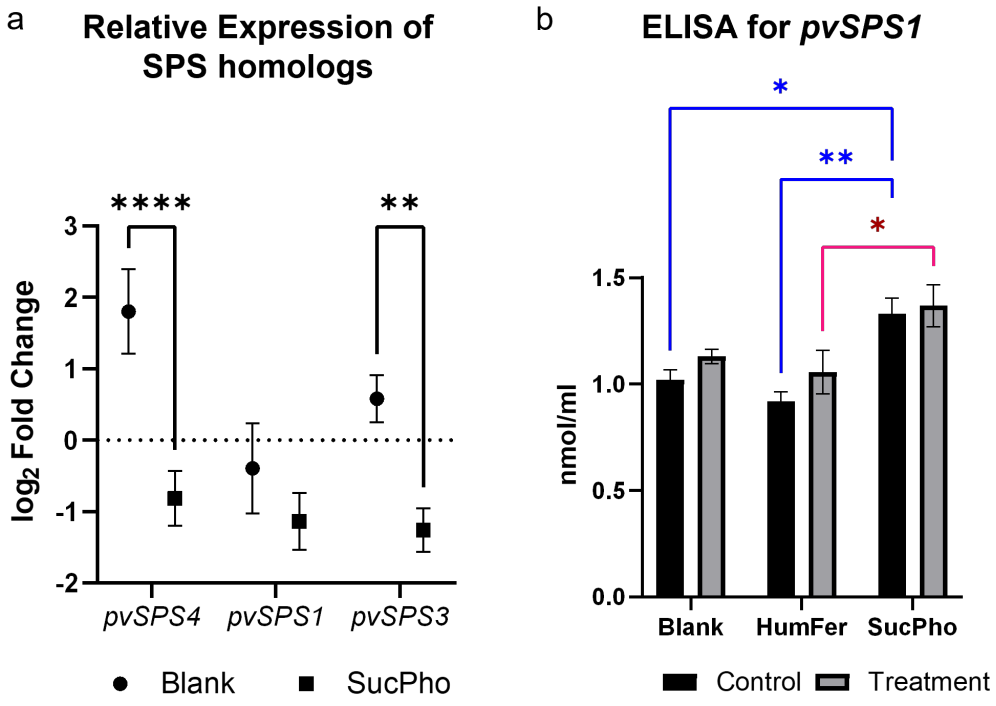

Figure 5.24. Analysis of the SPS homologs in hairy root tissues. *pvSPS3* displayed a significant downregulation under treatment (a) (n=3). Elisa for *pvSPS1* (b) displayed high protein levels in SucPho plants (n=5). Values represent the mean±SEM.

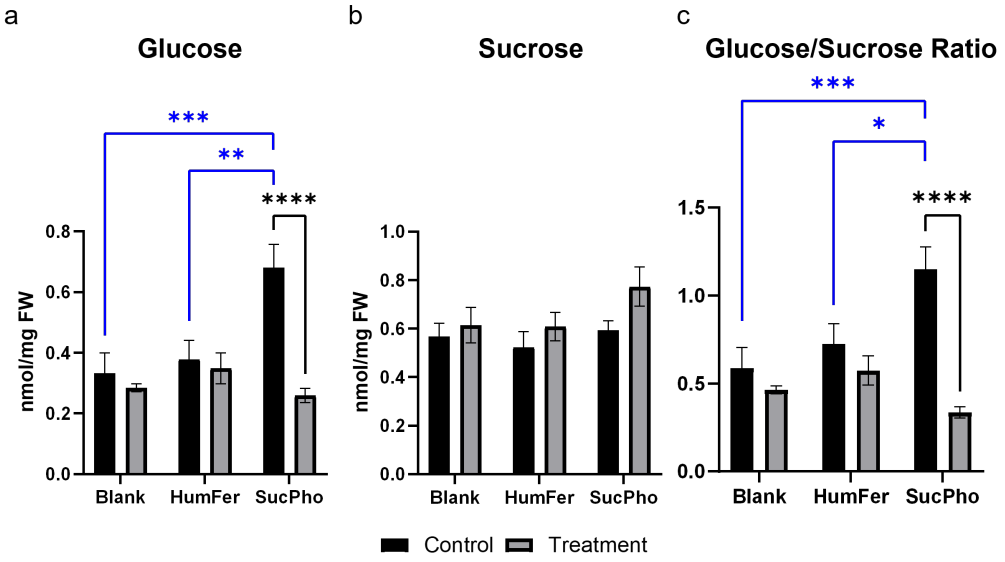

Figure 5.25. Evaluation of glucose (a) and sucrose (b) contents and their ratio (c) in the root tissues. (n=5). Values represent the mean±SEM.

Next, we have investigated the consequences of *pvSPS4* knockdown associated sugar imbalance on the ion uptake and transport together with sodium accumulation by determining, K^+, Ca^{+2}, Mg^{+2}, and Na^+ contents of the root and leaf tissues (Figure 5.26 and Figure 5.27; Full data can be found in Table B1). The *pvSPS4* knockdown had a major impact on both uptake and transport of K^+: Blank and HumFer root K^+ contents displayed similar responses to the omics study (Figure 5.12b) and decreased significantly in response to salt stress whereas SucPho root K^+ levels significantly increased (Figure 5.26a) as observed in the susceptible genotype, TR43477 (Figure 5.12b). The control K^+ level in Blank and HumFer roots was significantly higher than in saline conditions. Although leaves of all composite plants responded in a parallel manner with a significant buildup of K^+ in response to salinity, the amount of variation was different: K^+ content increased by 1.25-fold for Blank and 1.35-fold for HumFer leaves whereas the increase was 1.94-fold for SucPho leaves (Figure 5.27a). The divergence in response of SucPho leaves and roots is interesting as it arises from a significantly lower to higher K^+ level in control and salt treatment conditions respectively (Figure 5.26a and Figure 5.27b).

Overall, the *pvSPS4* knockdown resulted in an imbalance of Ca^{+2} and Mg^{+2} in the tissues. Stressed SucPho plants displayed a significant decline in Ca^{+2} level in both leaf and root tissues but there was no difference between the control and the treatment conditions in other lines (Figure 5.26b and Figure 5.27b). In the SucPho leaf tissues, Ca^{+2} content was much higher than Blank and HumFer leaves (1.81 and 2.16-fold respectively) in control conditions. Salt treatment prompted intense decrease has levelled SucPho leaf Ca^{+2} with HumFer leaf Ca^{+2}, yet Blank leaves had significantly higher Ca^{+2} content in saline conditions compared to other lines (Figure 5.27b). Root tissues have demonstrated a related pattern for Ca^{+2} adjustment: *pvSPS4* knockdown has caused a 1.97-fold decline in the SucPho roots whilst there was no difference in Blank and HumFer roots. Both Blank and HumFer roots demonstrated comparably lower levels of Ca^{+2} in control conditions. In treatment conditions, conversely, roots of Blank plants preserved significantly higher content of Ca^{+2} (1.59-fold) compared to SucPho roots (Figure 5.26b).

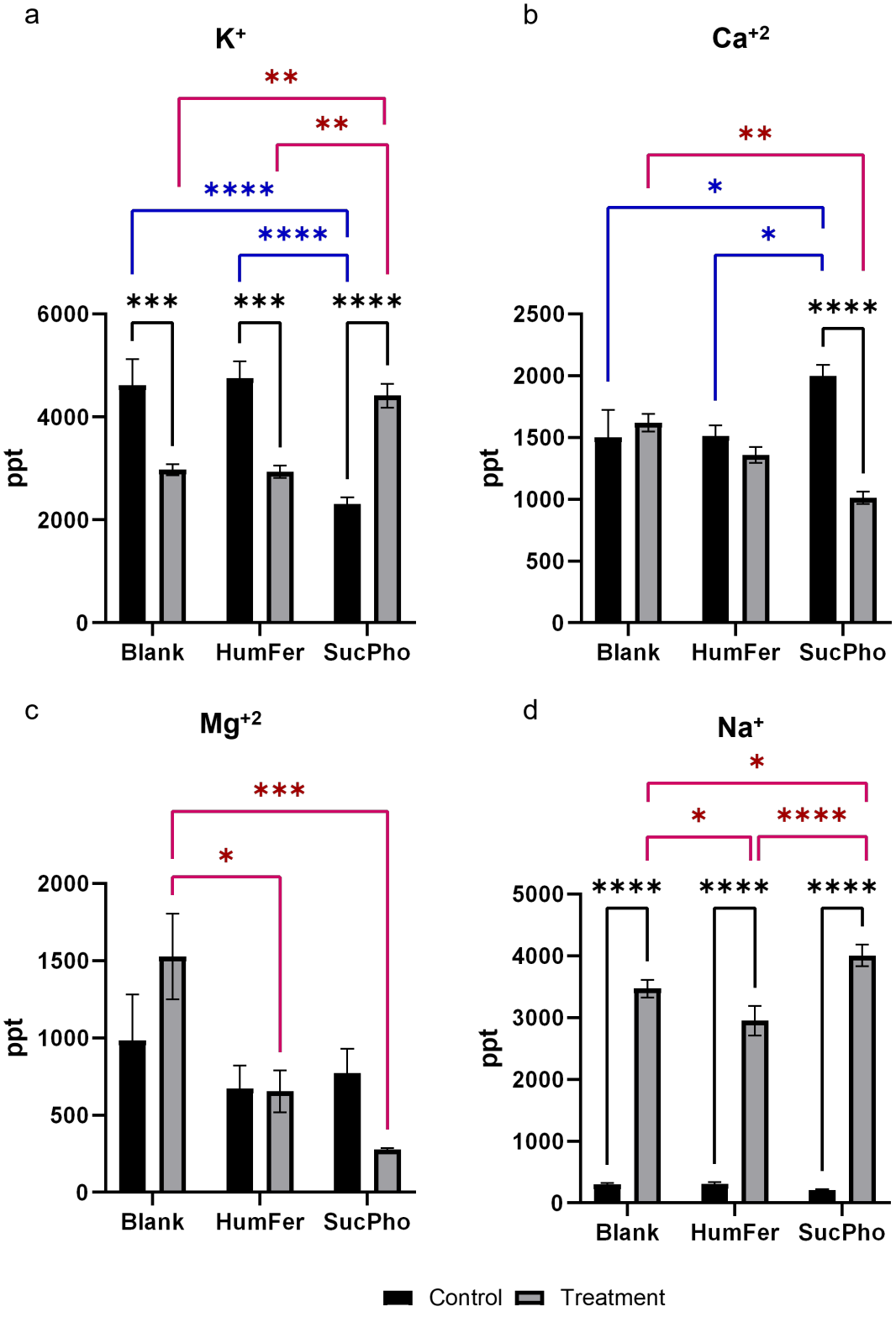

Figure 5.26. Evaluation of K^{+} (a), Ca^{+2} (b), Mg^{+2} (c), and Na^{+} (d) content changes in the root tissues of plants (n=5). Values represent the mean±SEM. ppt: parts per thousand.

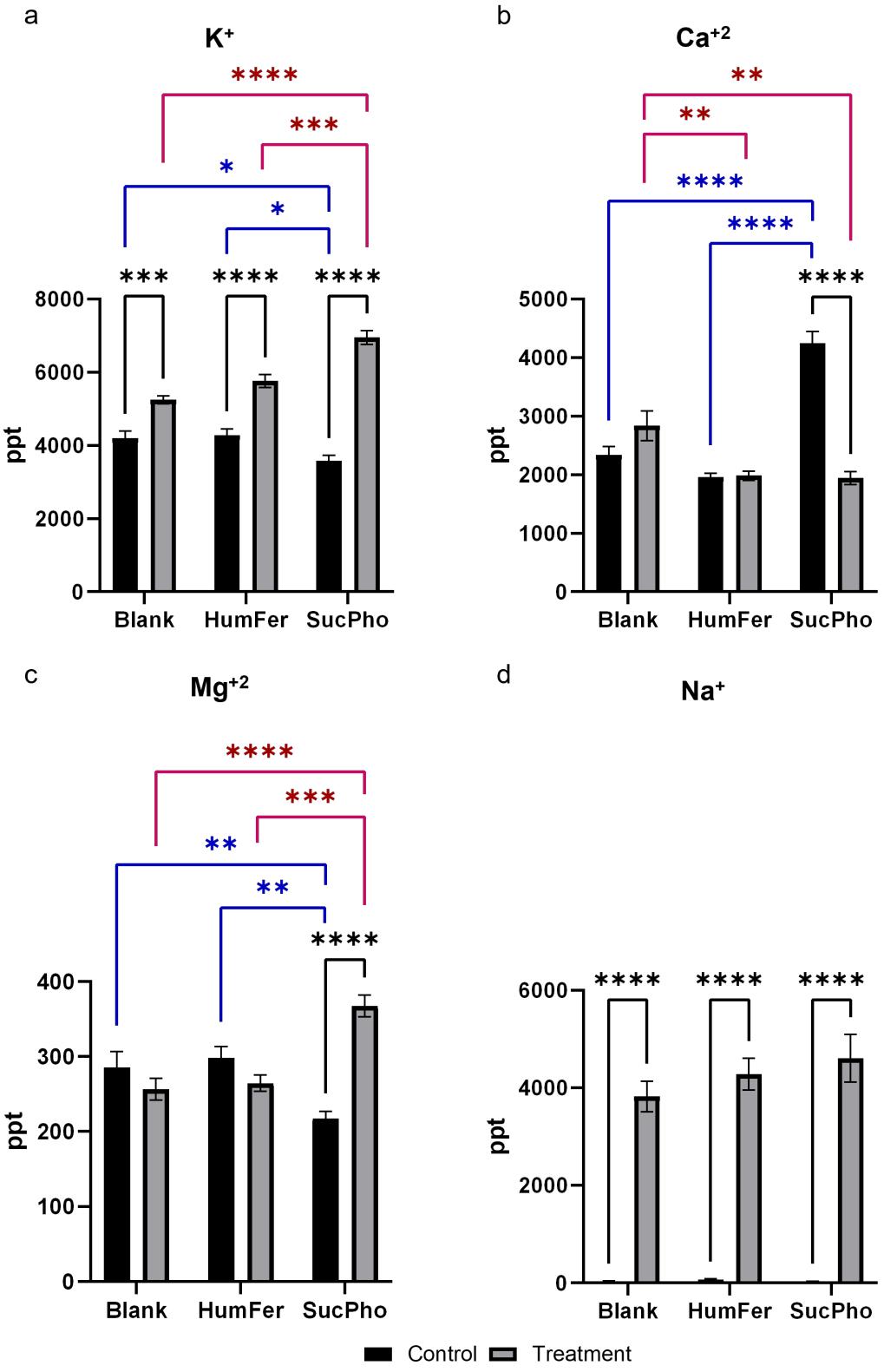

Figure 5.27. Evaluation of K^+ (a), Ca^{+2} (b), Mg^{+2} (c), and Na^+ (d) content changes in the leaf tissues of plants (n=5). Values represent the mean±SEM. ppt: parts per thousand.

Mg^{+2} contents in the leaf tissues exhibited a parallel pattern to Ca^{+2}: Leaf Mg^{+2} levels of Blank and HumFer plants did not display a significant change in response to salt stress, but did have significantly higher levels of leaf Mg^{+2} levels than SucPho in control conditions during salt stress, Mg^{+2} levels increased 1.69-fold upsurge and surpassed the Mg^{+2} levels Blank and HumFer (Figure 5.27c). Comparison of root Mg^{+2} levels showed that Blank and HumFer roots did not significantly change in response to salt treatment, but the roots of SucPho showed a significant decrease (2.77-fold). Although control Mg^{+2} levels for roots were close to each other for all composite lines, roots of Blank plants have accumulated significantly more Mg^{+2} under salt treatment compared to others. (Figure 5.26c).

In the omics part of the study, with another nutrient media (Hoagland's medium) and method, wild-type Ispir (the genotype utilized in the current part of the study) leaves had displayed stable Na^{+} levels upon salt treatment together with high Na^{+} levels in control conditions (Figure 5.12c). None of the composite plant leaves exhibited a similar response; Leaves of all lines presented a significant Na^{+} increase in response to salt treatment and there was no significant difference between the extents of it (Figure 5.27d). In contrast, *pvSPS4* knockdown roots exhibited a profound difference for salt-responsive Na^{+} uptake regulation: They accumulated significantly higher Na^{+} compared to the roots of other lines under saline conditions (Figure 5.26d).

5.7. Physiological and Molecular Analysis of *SPS4* Knockdown Under Salt Stress

Physiological analyses to understand the effects of the *SPS4* knockdown consisted of the measurements of the changes in RWC, electrolyte leakage and leaf area upon salinity treatment (Figure 5.28). The Blank, HumFer, and SucPho knockdown composite plant lines had quite similar shoot and leaf phenotypes to each other in control conditions, yet a minor reduction in growth was observed for the SucPho plants (Figure 5.28a).

Nevertheless, the distinction was much more evident under saline conditions. While the Blank leaves appeared resilient, even though smaller compared to control case, SucPho leaves were wilted and exhibited signs of necrosis. On the other hand, performance of HumFer plants in response to salt stress were in between the Blank and SucPho with visible signs of stress (Figure 5.28a). The diminished growth of SucPho was evident with 45% reduction in leaf area upon salt treatment. Conversely, in Blank and HumFer plants leaf area losses were not significant (Figure 5.28b-c). Furthermore, SucPho leaves have shown an 11%, loss in RWC in response to salt stress while the decrease was roughly 4% for both Blank and HumFer leaves (Figure 5.28d).

That the *pvSPS4* knockdown caused leaf area and RWC reductions under salt stress indicated high cellular damage for the leaf tissues. Indeed, leaf sections from salt stressed SucPho leaves lost significantly more electrolytes in the 4 hour compared to others. The difference was still significant between SucPho and Blank leaves after 8 hours (Figure 5.28e). In contrast, *pvSPS4* knockdown did not generate a significant electrolyte leakage in control conditions (Figure B2).

The effect of salt stress on the photosynthetic machinery of composite plants was evaluated with photosynthetic pigment content measurement (Figure 5.29). While none of the pigments displayed a significant change under stress conditions for blank and Humfer plants (Figure 5.29a-b), both chl *a* and chl *b* contents showed significant reductions in SucPho plants under salt stress. On the other hand, chl *a* and chl *b* contents did not show a significant difference in transformed and non-transformed plants in control conditions.

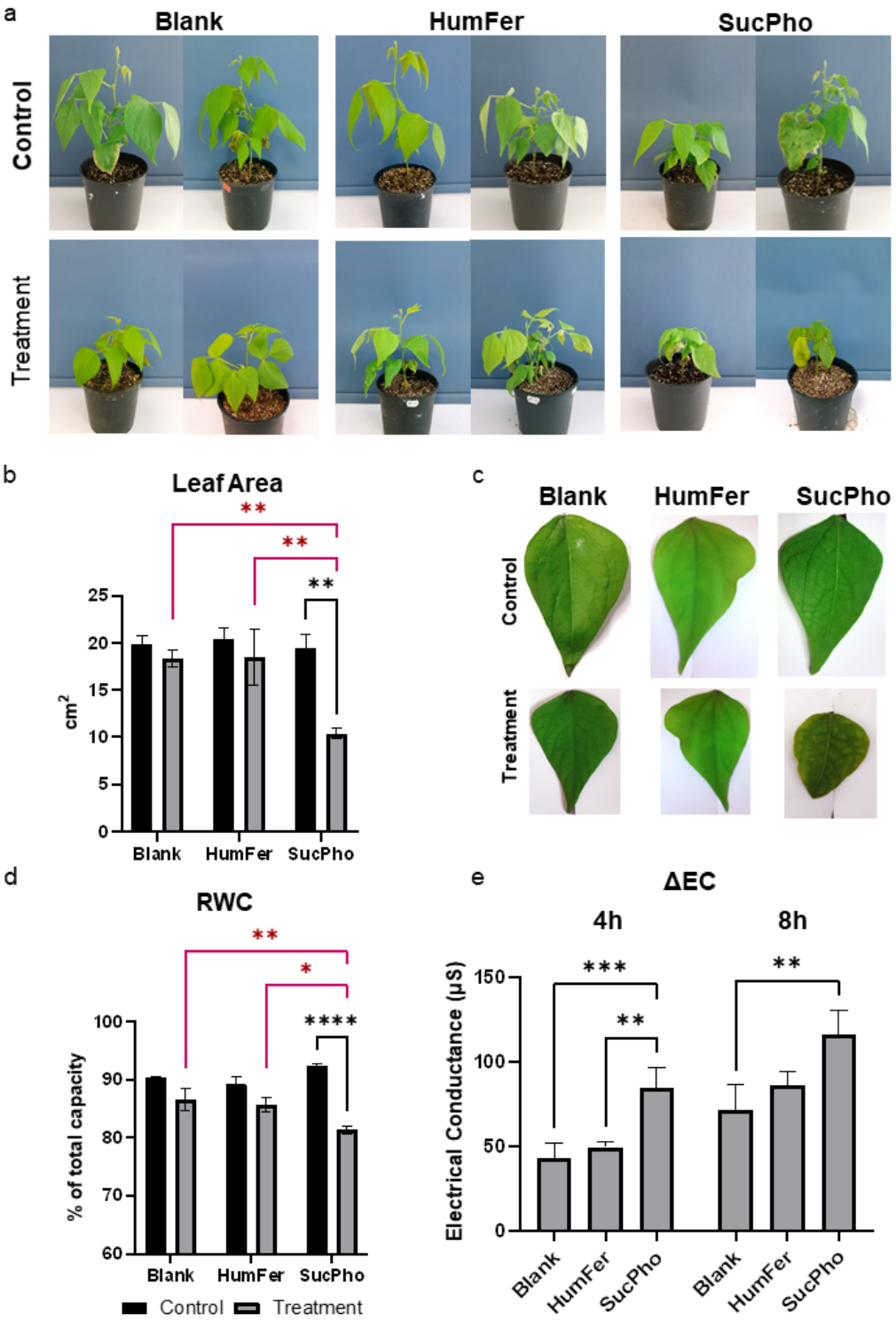

Figure 5.28. Phenotype (a) and physiological comparisons of composite lines with leaf area measurements (b, c) RWC (d) and electrolyte leakage (e) (n=5). Values represent the mean±SEM.

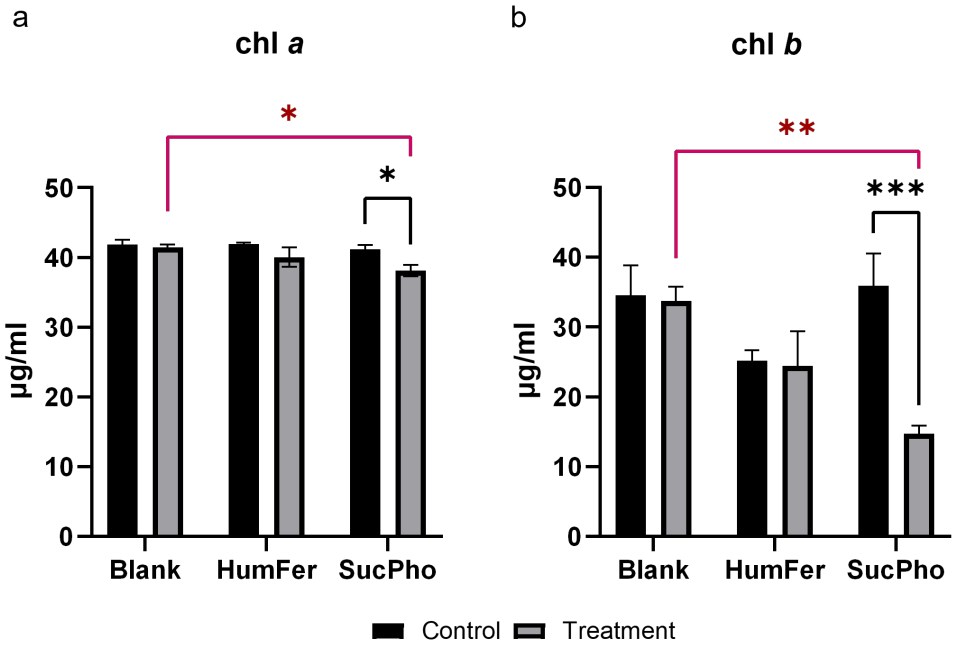

Figure 5.29. Chlorophyll content analysis of the leaves. SucPho leaves displayed reductions in chl *a* (a) and chl *b* (b) levels upon salt treatment (n=5). Values represent the mean±SEM.

5.8. Evaluation of Osmoprotection and Antioxidant Capacity

To understand the physiological outcomes of root *pvSPS4* knockdown, we investigated the variations in osmoprotection and antioxidant capabilities of the composite lines (Figure 5.30). Both mechanisms are proven to be salt stress responsive, and a decline in capacity implies the intensified sensitivity to stress (reviewed in [113]). To infer the osmoprotection capability of the composite lines in response to salt stress, we have performed a content analysis of the key osmoprotectant proline [114] in tissues (Figure 5.30a, b). Intriguingly, leaf tissues of all lines accumulated significantly different levels of proline from each other. Blank leaf proline levels have increased by 17.95-fold, HumFer leaf proline levels have displayed a 3.51-fold upsurge, while the change was only 1.63-fold for SucPho leaves (Figure 30a).

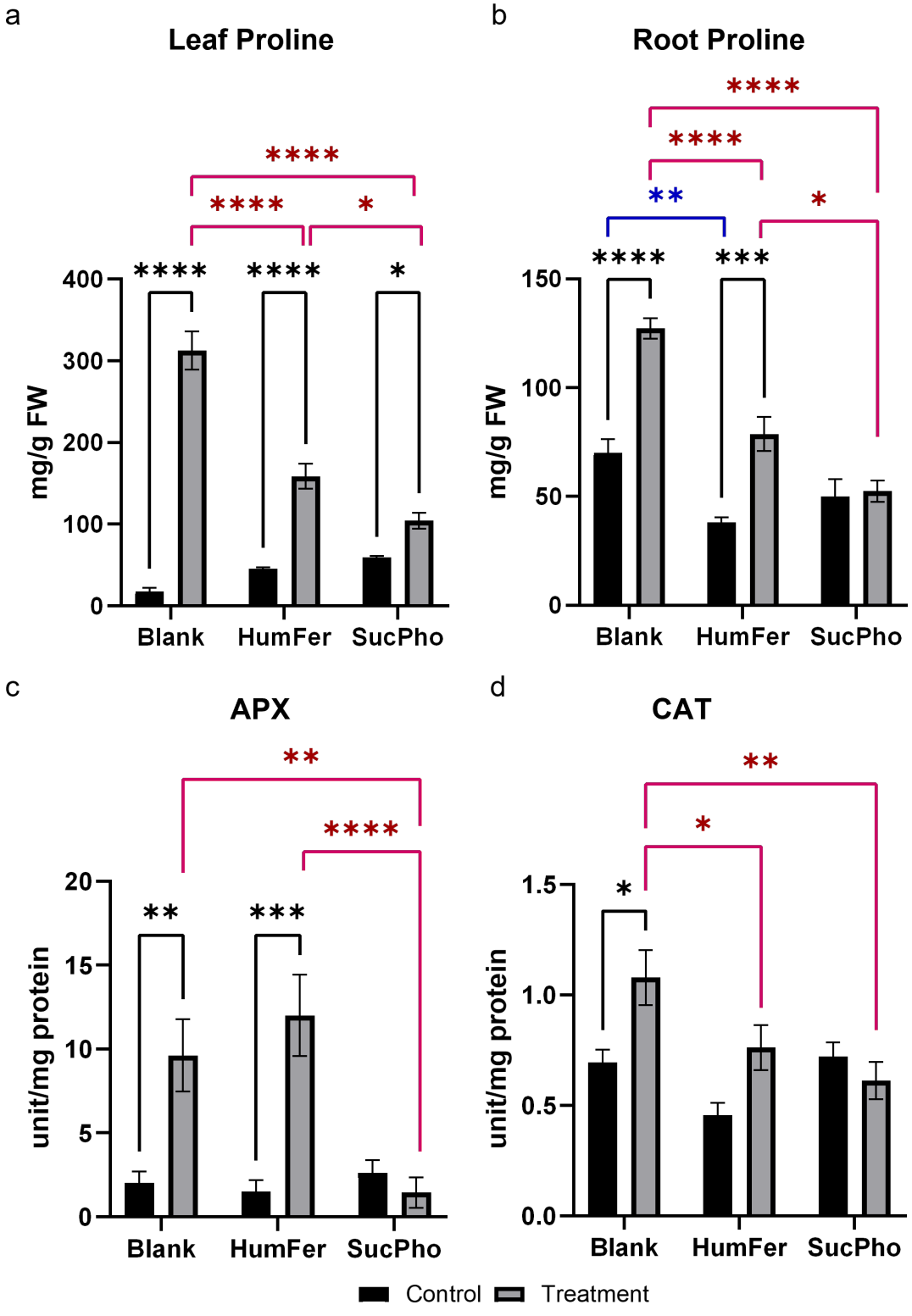

Figure 5.30. Examination of osmoprotection -proline content (a, b)- and antioxidant removal -APX (c) and CAT (d) activity - capabilities of plants (n=5). Values represent the mean±SEM.

Under salt stress the root proline contents of Blank and HumFer lines demonstrated a significant increase (1.91 and 2.01-fold respectively), but such response was not present in SucPho roots (Figure 30b).

To measure the enzymatic antioxidant capacities of the composite plant leaves, first protein concentrations of leaf crude extracts were determined (Table 10). Equal amounts of protein were used for enzymatic measurements. APX and CAT activity measurements displayed the inability of SucPho for oxidative stress alleviation through these enzymes.

Table 5.9. Composite root RNA concentrations and spectrophotometric measurements for purity.

Sample	Concentration (mg/ml)		Sample	Concentration (mg/ml)
BC1	0.97821		BT1	1.6288
BC2	1.38673		BT2	1.35116
BC3	1.21296		BT3	1.57506
BC4	1.22952		BT4	1.27128
BC5	1.22431		BT5	1.09086
HC1	1.32599		HT1	1.49959
HC2	1.67282		HT2	0.96242
HC3	1.58498		HT3	1.48845
HC4	1.19499		HT4	1.27576
HC5	1.49222		HT5	1.31379
SC1	1.40153		ST1	1.2457
SC2	1.2368		ST2	1.16593
SC3	1.36787		ST3	0.98156
SC4	1.23524		ST4	1.15855
SC5	1.24459		ST5	1.01726

Under salt stress, a reduced antioxidant capacity was observed in the SucPho leaves (Figure 5.30c-d). The *pvSPS4* knockdown did not result in a significant difference in leaf APX activity in control conditions but leaves of the SucPho plants did not display an increase of APX activity under salt stress. In contrast, APX activity in the Blank and HumFer leaves rose by 4.77 and 7.95-fold respectively (Figure 30c). Likewise, leaves of the SucPho plants did not display any increase in CAT activity under saline conditions in contrast to Blank leaves that demonstrated more than a 1.5-fold increase, yet although an increase was seen in HumFer leaves it was not significant (Figure 30d).

5.9. The Correlation of Responses

Even though the majority of the responses of Blank and HumFer plants to salt stress were highly similar to each other and diverged from the responses of SucPho, there were notable distinctions between them. The implemented methodology created an additional variable, distinct from the application of salt stress, with the initiation of RNAi mechanism. Hence, all the data for the stress response of the composite lines collectively was plotted on the $\log_2$ scale to visualize the disparities between them (Figure 5.31a). Responses of the Blank (black) and HumFer (yellow) lines displayed a vastly overlapping pattern in comparison to SucPho (red) in the graph. Furthermore, to calculate the similarity of the response patterns of the lines, we performed a correlation analysis (Figure 5.31b). Blank and HumFer lines demonstrated a very high correlation level with r-value of 0.95 for stress response. On the other hand, root *pvSPS4* knockdown resulted in a major decline in correlation. These results validated the scope of the *pvSPS4* knockdown over the impact of RNAi machinery on the stress response.

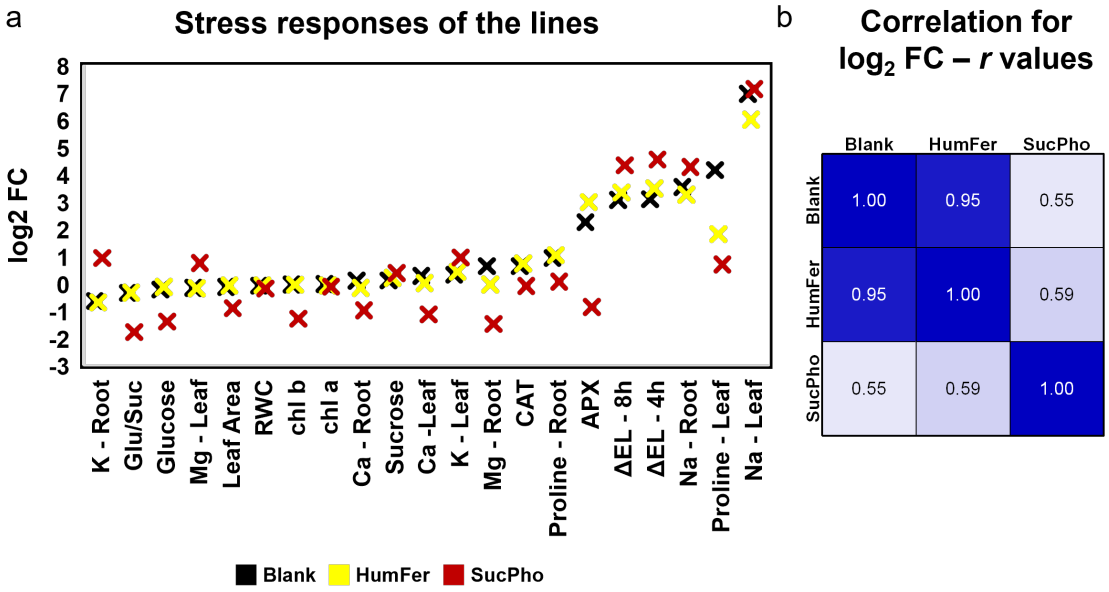

Figure 5.31. Evaluation and comparison of the responses Blank, HumFer, and SucPho gave to salt-stress (a). Spearman-r correlation of $\log_2$ fold-changes (b) has shown the distinctions of the responses.

6. DISCUSSION

Salinity in agricultural soil coupled with yield drop in salt-sensitive crops is one of the most critical emergencies in the world. Though numerous effects of salinity-generated dehydration and ionic imbalance on plant growth and development are identified, many parts of this process remain to be clarified. Therefore, it is crucial to understand molecular mechanisms of salt-stress response and tolerance for the production of tolerant crops. The first part of our study has focused on the transcriptomic, metabolomic, and ion content distinctions of two contrasting common bean genotypes under salt stress to find new tolerance-related genes, metabolites, ions, and the pathways that link them to each other. And the second part of the study was performed to understand the role of a sucrose metabolism gene, *pvSPS4*, that was selected using the results of the first part of the study, in salt tolerance.

6.1. Comparative Omics Study of Common Bean Genotypes Under Salt Stress

The contact of root tissues with high salt concentration promotes signaling cascades that primarily adjust the ionic balance with Na^+ influx constraint and root-to-shoot Na^+ translocation. Then, mechanisms that scavenge toxic ions to vacuoles are activated to protect the cellular activities. The robustness of this systemic reaction, rather than a qualitative difference, constitutes the key factor for the variation in tolerance between glycophytes and halophytes [115–117]. Furthermore, too much salt in the environment results in an impasse as it both produces water stress and delivers the cheap osmolytes to sustain the water capacity. As this situation continues, with the buildup of ions, the intensifying imbalance disturbs the molecular mechanisms in salt-susceptible species. Differential success in lessening this tension is observed among different genotypes, which might help us identify the molecular basis and characterize better tolerance mechanisms.

6.1.1. Carbon Fixation with Osmotic and Ionic Balance

The ion study showed that both genotypes accumulated high Na^+ levels in root tissues upon salt stress, but IR managed to maintain it at significantly lower amounts than TR (Figure 5.12a and d). A more remarkable variation was detected for the leaf tissues: IL preserved the level of Na^+ following salt treatment whilst there was a large-scale Na^+ buildup in TL. This suggests a better Na^+ exclusion capability for IR that was not due to root-to-leaf translocation of the surplus of Na^+ as indicated by the steady IL Na^+ levels. The much greater Na^+ level of IL in the control contrasted to TL (3.3-fold, p-value<0.05) (Figure 5.13a) might also be an efficient approach against stress-driven Na^+ influx to the leaves. In either case, this difference might be one of the crucial factors explaining the superior durability of Ispir genotype.

On the other hand, the situation is different with K^+ levels: The K^+ decline in roots of Ispir can be anticipated as common bean is a glycophyte, even though Ispir is a fairly salt-tolerant genotype. The reduction in cellular K^+ levels was detected previously both in glycophytes [118,119] and in halophytes [119–121]. Nonetheless, K^+ levels in the roots of the susceptible TR43477 have increased upon treatment (Figure 5.12a and b). Since much of the Na^+ entrance to the root cells is through K^+ channels [122–125], Ispir roots probably avoid the excessive Na^+ influx via shutting down the K^+ channels, which as a trade-off, may cause lower K^+ content in the roots. A less effective approach adopted by TR43477 permits for high Na^+ buildup both in leaf and in root tissues together with K^+. Possibly better vacuole sequestration in roots on top of better exclusion ability might alleviate the negative effect of a slightly lower K^+/Na^+ ratio in the Ispir roots. Another crucial feature of this difference might be the capacity to achieve a much favorable K^+/Na^+ proportion in the leaves of the Ispir genotype. IL has managed to improve its K^+/Na^+ ratio by 1.8-fold while this ratio decreased by 2.9-fold in TL under salt stress. This asymmetry, on the other hand, could be a critical component for the examined contrast in the photosynthetic capabilities of these genotypes.

Salt stress develops a major limitation on the photosynthetic function [126]. Na^+ accumulation in chloroplasts disturbs growth mainly by interrupting the photosynthetic electron transport [127, 128] and restraining the PSII activity [129–132]. Furthermore, it reduces chlorophyll content in susceptible plants such as potato [133], tomato [134], pea [135], as well as common bean [136]. Nevertheless, Ispir, unlike TR43477, demonstrated an enhanced carbon fixation metabolism with enriched GO terms and KEGG pathways (Figure 5.6a; Figure 5.7a) and an active chlorophyll content regulation (Figure 5.8a). Photosynthesis function is tightly connected to stomata, which control water loss/photosynthesis equilibrium [137]. As a major stomatal guard cell osmoregulator [138, 139], K^+ synchronizes the gas exchange and transpiration rates [140], which can be severely disturbed by salt stress [141]. Accumulated Na^+ competes with K^+ for the regulation of stomata, which triggers substantial side effects such as obstruction of regulation through ABA and CO_2 [142, 143]. As salt-tolerant plants are recognized to have more effective stomatal regulation compared to sensitive ones [144], better stomatal regulation through a higher K^+/Na^+ ratio for Ispir leaves may be the core of its higher photosynthetic capacity. This link is further implied by the reduced glycolate production in Ispir leaf tissues, which is an indication of decreased photorespiration. Photorespiration consumes ATP together with the reducing power of the photosynthetic electron transport system and reduces the efficiency of CO_2 fixation [145]. Since photosynthesis/photorespiration rate depends primarily on the CO_2/O_2 levels which on the other hand depends on stomatal density and conductance [41, 146, 147], Ispir possibly is a better stomatal regulator compared to TR43477 under salt stress. An enrichment of pectinesterase-related terms and genes in Ispir leaves (Figure 5.6a, Table A3) further supports this hypothesis: Amsbury *et al.* (2016) [148] have shown that the guard cells in Arabidopsis have a high content of un-esterified pectins. The guard-cell pectins were displayed to be esterified in an Arabidopsis mutant deficient for a potent *pectinesterase* (*PME6*). The absence of this enzyme caused a decreased guard cell dynamic motility and, in turn, crippled the stomatal function resulting in susceptibility to low-water conditions. Indeed, one of the pectinesterase genes (Phvul.001G209400) that demonstrated upregulation in IL is a somewhat close homolog (with 43% similarity) of Arabidopsis *PME6*; thus, might be performing a comparable role in common bean.

Declined glycolate content and enriched pectinesterase-related terms together with the enriched photosynthesis pathway genes, increased chlorophyll content, and highly up-regulated genes that were annotated as *Rubisco*, are good indicators of an augmented photosynthesis/lower photorespiration rate and a better stomatal regulatory system in Ispir genotype.

The enhanced photosynthetic capability and enriched carbon fixation (Figure 5.6a, Figure 5.7a, and Figure 5.8) in IL have plausibly resulted in buildup of various carbohydrates (nine types including sucrose and glucose- Figure 5.9c and Figure 5.10) and enrichment in sucrose and starch metabolism (Figure 5.11). Particularly, intense upregulation of a *starch synthase* (Phvul.004G029100) together with a *β-amylase* (Phvul.011G107700), which is involved in the starch breakdown [149], in IL also suggested an enriched starch metabolism (Table 5.4). In turn, TL was depleted in such metabolites and displayed a reduction in polysaccharide metabolic processes (Figure 5.6a). The enhanced carbohydrate metabolism and soluble sugar contents in Ispir indicate a superior tolerance mechanism in this genotype as carbohydrates provide osmoprotection, membrane stability, and turgor maintenance under osmotic stress [150]. Soluble carbohydrates are also metabolic sources of energy, act as signaling molecules in plant growth regulation [151,152] and have functions in plant-stress response regulation [153,154]. The variation in the carbohydrate quantity might also explain the high contrast between the carbohydrate levels of the root systems of the genotypes (Figure 5.9c; Figure 5.10). In particular, buildup of mannitol ($\log_2$FC–2.76; p-value$<$0.01), a well-known osmoprotectant [155–158] and hydroxyl radical quencher [156, 159], may be crucial for the tolerance of Ispir roots to the excessive ion uptake [160] and better osmoregulation [161].

Another implication of the distinction of ionic regulation between the root tissues of these two genotypes is the significant decreases in IR Mn^{+2} and Zn^{+2} ion levels (Figure 5.12a). Particularly Zn^{+2} ion was shown to have positive effects on the abiotic stress tolerance [162, 163]. In the present study, salt treatment has resulted in a significant decline of Zn^{+2} content in IR (changed from 1674.8 μg/g to 1143.4μg/g).

In TR, though, the control-condition amount was already low (1.3-fold compared to IR, p-value<0.005) and stayed nearly unaffected after exposure to salt (a decline from 1214.12 μg/g to 1184.2μg/g) (Figure 5.14c-d). It is intriguing to further investigate this divergence to figure out if the higher preliminary Zn^{+2} content contributes to the salt tolerance. One possibility is that Zn^{+2} accumulated in IR in control conditions was incorporated into Zn-containing metalloproteins [164] required for an efficient stress response such as *alcohol dehydrogenase* [165], *carbonic anhydrase* [166], and *superoxide dismutase* [167]. As TR roots did not have such a pool of Zn^{+2} they might have failed to respond to the stress as effectively as IR due to the lower activity/availability of such metalloproteins. On the other hand, salt-treatment caused Mn^{+2} reduction in IR may be due to allocation of the ion to the leaf tissues for the maintenance of relatively high leaf Mn^{+2} content in Ispir (1.9-fold higher in control conditions compared to TL – Figure 5.13c-d) while already low TL Mn^{+2} levels demonstrated a significant decline after salt treatment. As Mn^{+2} is an important element for photosystem II to operate and its shortage interrupts the photosynthetic productivity and permanence [168–170], this allocation pattern might be a key aspect of tolerance as well.

6.1.2. Protein and Amino Acid Metabolism

Natural variation in salinity tolerance is incredibly high in the plant kingdom, even within the same species, which is manifested in separate growth responses of distinct genotypes [4]. Under salt stress, IL exhibited reduced protein production and modification but enriched protein protection-related terms (Figure 5.6a). It is plausible that holding translation in minimum is an effective way to keep the proteome from oxidative stress coupled with salinity conditions. On the other hand, the reaction of TL was less cautious: Terms for transcription were boosted but translation and proteolysis terms were reduced (Figure 5.6a). The distribution of energy and important components to transcription under conditions where ordinary levels of translation is not feasible may be one of the weak points of the salt-sensitive genotype. Root tissues were dissimilar in their response too: IR displayed a decrease in growth and production-related terms, while TR was only diminished in nitrogen metabolism (Figure 5.7b).

Keeping the root smaller under saline conditions may be one of the ways to restrict the contact of the nutrient-uptake interface to saline environment.

Curiously, TR accumulated the maximum number of amino acids amongst tissues and genotypes (valine, isoleucine, and lysine were exclusive to TR). Even though the accumulation of amino acids is commonly assumed as representation of tolerance (see review [171]), catabolism of lysine, valine, isoleucine, and leucine were identified as critical pathways for osmotic stress tolerance in Arabidopsis [172]. Pointedly, IR did not accumulate valine and had reduced amount of isoleucine in response to salt stress (Figure 5.10; Figure 5.11) and this might be due to upregulation of a 2-oxoisovalerate dehydrogenase homolog, Phvul.009G132900, which was demonstrated to have a key role in branched-chain amino acid catabolism [173]. The rise in lysine content in TR deserves special consideration, since, as mentioned, it may be considered as a tolerance mechanism as lysine accumulates in some drought-tolerant plant ecotypes [174, 175]. But lysine catabolism, especially saccharopine (SACPATH) pathway, a very stress-responsive protective system [174–181], appeared to be dormant in the TR43477 compared to Ispir: The latter genotype has two upregulated SACPATH pathway genes in the genome including the only gene annotated as *lysine-ketoglutarate reductase/saccharopine dehydrogenase*. SACPATH pathway can lead to the production of proline via glutamate or α-aminoadipate [182–184]. Even though the proline levels were increased in both tissues and genotypes, glutamate was only accumulated in Ispir tissues (Figure 5.10; Figure 5.11). Thus the higher lysine levels in TR may be merely the result of more intensive proteolysis coupled with stress (for a review, see [185]).

The disparity in glutamate/glutamine biosynthesis also deserves interest as glutamate -glutamine/ 2-oxoglutarate reaction is enriched in both genotypes yet glutamate/glutamine conversion pathway is mostly activated in Ispir tissues (Figure 5.11). While both tissues of Ispir accumulated glutamate, TR43477 tissues accumulated glutamine, which suggests a disparity in the reaction direction for these genotypes. Glutamate is vital for stress tolerance as it was shown to sustain amino-acid synthesis under osmotic stress [186] and initiate stress tolerance pathways via H_2O_2 burst [187].

It also acts as a signaling molecule for stress response pathways [188] and regulates the stomatal aperture under low-water conditions [189, 190]. Glutamate is also necessary for the biosynthesis of glutathione, an active compound of the antioxidant defense system [191]. Glutamine has also been implicated in stress responses, acting as a regulator of a transcription factor [192]. Overexpression of the enzyme necessary for its production, glutamine synthase, yields improved abiotic stress tolerance in several species [193, 194]. Still, glutamate appears to be a hub for stress response patterns.

Furthermore, the imbalance of regulation in glutamate/glutamine cycle genes (Figure 5.11; Table 5.4) may be an additional clue of the distinction in stress-responsive nitrogen metabolism for these genotypes [195,196] as suggested by the KEGG pathway analysis (Figure 5.7a-b). Regarding that, asparagine biosynthesis and content were also regulated differently among genotypes and tissues. Asp was mainly accumulated in the root tissues of both genotypes, but also exhibited low but significant accumulation in the leaves of Ispir (Figure 5.10; Figure 5.11). An "*asparagine synthase-1*" annotated gene (Phvul.006G069300) was upregulated in all tissues except for TL, where a different member of this gene family annotated as "*asparagine synthase-3*" (Phvul.001G252200) was downregulated. If the elevated Asp levels in TR were primarily due to risen proteolysis as considered above, the buildup of this amino acid in both tissues of Ispir may suggest the better nitrogen storage capacity of this genotype, since Asp is recognized to be a good nitrogen reserve molecule [197,198]. Since salinity decreases nitrogen assimilation and acquisition capability of plants [199, 200], and nitrogen is a vital building block for amino acids, hormones such as auxin and other important amine-compounds, nitrogen withholding may be an additional crucial characteristic of Ispir's salt tolerance.

6.1.3. Other Aspects of Tolerance

Undoubtedly, plant salinity tolerance mechanisms are intricate and complex features that cannot be attributed to the changes in only a few biological processes such as carbon fixation and amino acid biosynthesis of the primary metabolism [4, 201].

Secondary metabolism is also known to be highly responsive to environmental factors including salt stress [201, 202]. Our previous study on Ispir in salt stress has demonstrated the enrichment of secondary metabolism genes in reply to salt in both leaf and root tissues [17]. The current comparative study exhibited that the roots of Ispir were differentially enriched in KEGG terms related to terpenoid metabolism (Figure 5.7b), a type of metabolism that contains volatile unsaturated hydrocarbon compounds with high structural diversity [203]. Other studies have reported terpenoids to increase in response to salinity and to be engaged in tolerance responses [202, 204, 205]. A recent study in *Zea mays* displayed the accumulation of phytoalexin terpenoids in root tissues as a key characteristic of an abiotic stress response and hormonal regulation under stress conditions [206]. Terpenoid biosynthesis has been associated with photosynthetic machinery, especially chloroplasts, in non-stressed plants before [207,208] and the impairment of terpenoid production in drought stress conditions was related to a decrease in levels of available substrates due to disturbed photosynthesis [209–212]. The photosynthetic machinery in Ispir, compared to TR43477, displayed a rather improved response under salt-stress conditions, thus allowing the production of new terpenoids in the roots. Furthermore, IR was diminished in esterase and alcohol catabolism-related GO terms (Figure 5.6b), which implies superior preservation of secondary metabolites such as terpenoids [213].

The avoidance of salinity-induced decline of photosynthetic activity in Ispir might also have a positive consequence for respiratory metabolism. As salt stress does not shown to affect cellular O_2 levels, the respiration rate mainly depends on the resource of substrate and biochemical regulation. Thus, the adverse effects of salt stress on the respiratory machinery can be mostly credited to lower carbon fixation [136, 214] and interruption of the electron transport chain due to accumulation of ions [215]. Though there is no definite data for the effect of increased or decreased respiration rates on the efficiency of salt stress tolerance [216], respiratory homeostasis was associated with superior tolerance responses in a few species [216, 217]. In this respect, the elevated levels of lactic acid in TL under saline conditions ($\log_2$FC–0.97; p-value$<$0.01) (Figure 5.10) might be a sign of perturbed mitochondrial and boosted anaerobic respiration.

In contrast, lactic acid levels in IL have slightly reduced in response to salt stress ($\log_2$FC– -0.64; p-value<0.05), which might also be linked to higher intensity of alcohol metabolism in IL. Out of five homologs of *alcohol dehydrogenase 1* (*ADH1*), one (Phvul.001G067300) was significantly upregulated in IL, while the others were not regulated in either genotype. The activity of this gene might have been enough for the reduction of toxic acetaldehyde [218, 219] to ethanol, thus avoiding the accumulation of lactic acid in IL. Additionally, *ADH1* upregulation might have had other positive effects since this gene is known to respond to abiotic stresses and is crucial for tolerance to osmotic and salt stresses [165, 220, 221].

Like other cellular activities, lipid metabolism is also affected by salt stress [113]. Indeed, in our study, the lipid content was low in TR43477 tissues (Figure 5c), which may be a sign of susceptibility, as described before in drought stress conditions [222, 223].

Lastly, in addition to the salt-caused differences, the constitutive 55- to 177-fold variation in Mo content between Ispir and TR43477 tissues under both conditions (Figure 5.13e-f; Figure 5.14e-f) can be essential for salt tolerance in Ispir. Mo has been reported in several studies to enhance abiotic stress tolerance in drought, salinity, and low-temperature conditions [224–227]. In saline conditions, Mo was shown to adjust the antioxidant machinery and osmotic balance in Chinese cabbage [227]. Moreover, it was reported to increase chlorophyll and carotene contents together with photosynthesis rate and have a positive effect on ionic balance regulation in the same species [228]. Thus, it is plausible that the higher Mo in Ispir contributes to its superior salt tolerance.

6.2. Functional Analysis of *pvSPS4* Knockdown

Soluble sugar metabolism under stress conditions is composed of complex processes involving synchronized synthesis and catabolic reactions. It is linked to variations in carbon fixation, changes in source-sink partitioning, and transcription [47, 229, 230]. In the sink tissues such as root, soluble sugars are subjected to rapid conversion.

Sucrose is catabolized into glucose and fructose, as these hexoses can commence resynthesis of sucrose [47]. Sucrose and glucose are versatile metabolites involved in the adjustment of various biochemical and molecular functions such as development, energy partition, metabolite production, signaling, and osmoregulation under stress conditions [231, 232]. That is why deciphering their regulation is key to pinpoint the connections among these salt stress-responsive networks.

Sucrose resynthesis in the roots by the action of sucrose metabolism enzymes such as SPS is considered to be crucial for its storage or intercellular transport. Sink SPS metabolism has been associated with protein storage [233], starch accumulation [234], cellulose production [235], and it can be vital for regulation of carbohydrate partitioning [234]. Nevertheless, evidence concerning sucrose resynthesis and the role of SPS activity in sinks, especially under stress conditions, is still inadequate. To focus on this issue, in this part of the study, we have studied the effect of the knockdown of root-specific, salt-responsive common bean SPS homolog, *pvSPS4*, under salt stress.

We have used *A. rhizogenes* mediated hairy root induction to produce composite plants with *pvSPS4* knockdown roots through RNAi. Two experimental control lines were constructed to assess the effects of *pvSPS4* knockdown: Blank line with no vector insertion to use as the main background, and HumFer line with RNAi prompted to serve as a background solely to evaluate the effects of RNAi activity. RNAi off-target effects can arise when short interfering RNAs (siRNAs) modify the expression of genes separate from their target [236,237]. There is accumulating evidence that some of these off-target effects are result of siRNAs functioning as microRNAs (miRNAs), targeting mRNAs that contain partial sequence matches to the siRNAs [236, 238, 239]. In this respect, the observed phenotype distinctions between HumFer and Blank lines are reasonable as in HumFer plants, the RNAi apparatus is active. Nevertheless, SucPho line was displayed to have significant impediments on the salt tolerance mechanism, compared to both HumFer and Blank, by correlation analysis (Figure 5.31).

6.2.1. *pvSPS4* May Regulate Ionic Balance Through the Adjustment of Sugar Balance in the Roots

Although *pvSPS4* was upregulated under stress conditions for Blank and HumFer roots, the protein levels were stable. But SucPho roots displayed a nearly 40% decrease in pvSPS4 protein content under salt treatment implying a high turnover rate for this enzyme in such conditions. *pvSPS4* knockdown caused *pvSPS3* downregulation under treatment conditions in the roots and an upsurge in *pvSPS1* protein content in both conditions. Though we did not detect a significant decrease in transcription or protein content of *pvSPS4* in control conditions, we might conclude that knockdown resulted in a problem in SPS enzyme balance in the root tissues which might be the main source of differences observed in SucPho plants in control conditions.

pvSPS4 knockdown triggered a 1.92-fold higher glucose accumulation in control conditions in the roots, yet the sucrose levels did not change. On the other hand, there was no considerable difference in glucose or sucrose levels between the lines in treatment conditions. Nevertheless, the distinctions between the glucose contents have altered the glucose/sucrose ratio of the lines. The imbalance was apparent in SucPho lines with a significant disparity in the control condition (Fig 5.25c). The difference in this ratio for SucPho roots was overall 2.71 times higher than the roots of other lines upon salt treatment. Curiously, in the first part of the study, a similar difference was observed between the roots of the salt-tolerant Ispir and salt-susceptible TR43477 genotypes, with the latter displaying a 2.35 times greater decrease under salt stress. The resemblance of this difference indicates that glucose/sucrose ratio can be a crucial subject for the salt tolerance response. Given that these sugars have major and independent roles in regulatory signaling [240–246], changes in the sucrose-hexose ratio can have adverse effects on various signal transduction relays. In turn, these sugar-sensing pathways can disturb the sucrose metabolism [247–249], creating a feedback loop. Therefore, it is fair to assume that balance regulation of these sugars is vital for a proper stress response.

The *pvSPS4* knockdown also caused an ionic imbalance in leaf and root tissues under control conditions, which was deepened under treatment when compared to the other two lines. The imbalance was evident for K^+ in SucPho roots (Figure 5.26a), there was a sharp distinction in Ca^{+2} content for both conditions in both tissues (Fig 5.26b and Fig 5.27b) and SucPho plants could not manage to balance Mg^{+2} levels in the leaves (Fig 5.27c). Yet, this imbalance did not produce a major difference in Na^+ accumulation for SucPho plants. Although SucPho roots accumulated significantly higher Na^+, this did not affect the leaf Na^+ levels (Fig 5.26d and Fig 5.27d).

There are several means that a glucose/sucrose imbalance can be associated with ionic imbalance: Both sucrose and glucose act as osmolytes and sustain homeostasis in the cell [46], yet sucrose is much more common and important in osmoregulation than glucose [250]. Moreover, both sugars were displayed to regulate membrane potential in different extents [251], and both K^+ and Ca^{+2} uptake are strongly associated with membrane polarization status of the cell [252–254]. Notably, K^+ ions have to move against their concentration gradient to enter the root. To make this movement energetically favorable, the activity of H^+-ATPases, which are demonstrated to be stimulated by sucrose [255] are needed [256]. Therefore, a lack of balance between glucose and sucrose in the root tissues might have interrupted the maintenance of cellular osmolarity, membrane potential, and H^+ gradient, particularly in the case of salt stress, and resulted in dysregulation of ion uptake mechanisms in common bean.

Another potential way for glucose/sucrose imbalance to result in the ionic imbalance is the disturbance of the expressional regulation of circadian clock genes. Research has demonstrated the relationships between the circadian clock, immunity, and the sugars in plants [257, 258]. The clock genes were observed to be in strong interaction with sucrose levels and invertases – enzymes that catalyze sucrose to hexose – which suggests that the fine regulation of hexose/sucrose ratio is imperative for an appropriate stress-response [259]. Additionally, a properly operational clock is required for the regulation of cellular auxin levels and response to it in the root tissues [260]. The hormone auxin is a potent inducer of the K^+ uptake through regulation of the H^+pumps [261, 262].

It holds a crucial role in the intercellular Ca^{+2} and K^{+} transport and Ca^{+2} signaling through cation channel stimulation [263–265]. Hence, the disproportion in SucPho root K^{+} and Ca^{+2} contents in both control and salt treatment conditions can be due to interruption of auxin regulation through the circadian clock. Furthermore, Ca^{+2} content and signaling were shown to be vital in modifying the selectivity and absorption of other ions, including magnesium [266], for proper salt tolerance in several plants [267–269] which might explain the significant changes in Mg^{+2} levels for SucPho plants upon treatment.

6.2.2. Transmission and Effect of Ionic Imbalance to the Leaves

The plant circadian clock of different organs has been shown to be dependent [270] so, any interruption of the clock through the glucose/sucrose imbalance in one part of the plant can be expected to influence other parts as well. Likewise, any disruption in Ca^{+2} signaling possesses prospective to have major adverse effects on K^{+} levels and transport [271–274] which is tightly coupled with the regulation of source to sink nutrient transportation including sucrose [252]. Thus, a disruption in the root circadian clock concurrently with Ca^{+2} signaling may have been the leading reason for the transmission of subsequent complications to the upper parts of the plant.

The interruption of the ionic regulation and possibly shoot-to-root nutrient transport had caused a weakened salt stress response for the leaf tissues in SucPho plants. Their leaves exhibited diminished chlorophyll content (Figure 5.29) and compromised physiology (Figure 5.28). As the comparative omics part of the study indicated, conservation of chlorophyll levels is very critical for an effective salt tolerance response, so identifying the mechanism that triggered chlorophyll content reduction in SucPho leaves upon salt stress is essential to understand related physiological outcomes. Leaf Ca^{+2} and Mg^{+2} levels presented both conditional and directional contrasts for SucPho plants (Figure 5.27b-c). Mg^{+2} is a major element in chlorophyll metabolism [275] and takes role in Rubisco activation [276]. An unbalanced rise in the Mg^{+2} content might have been responsible for the distractions in the chlorophyll synthesis in SucPho.

Moreover, it might have had adverse effects on the TCA cycle and amino acid synthesis as well [277]. Ca^{+2} also possesses key roles in photosynthesis [278], energy production [279], and regulation of salt stress responses in plants [40]. Consequently, the joint impact of Mg^{+2} and Ca^{+2} imbalance in the leaves have the potential to result in growth reduction as indicated by leaf area measurements (Figure 5.28a, b, and c) and interfere with the salt stress response in SucPho plants.

Furthermore, leaf and root tissues of SucPho plants, in contrast to Blank and HumFer, could not manage to accumulate the key osmoprotectant proline [114] in response to salt stress (Figure 5.30a-b) which indicated an instability in osmoregulation ability for SucPho. Indeed, the leaves of SucPho plants lost significantly more water compared to other lines (Figure 5.28.d). This setback might be caused by the above-mentioned interruptions in photosynthesis and energy metabolism together with the impact of Mg^{+2} accumulation on amino-acid synthesis. Another suspect for the insufficiency in proline production can be the interruption of Ca^{+2} signaling which plays a main role in the control of proline accumulation upon ionic stress conditions [280].

Salt stress, generates oxidative stress with a rise in reactive oxygen species (ROS) [281]. A decrease in water content leads to stomatal closure and a related drop in CO_2 content, a vital electron acceptor, and results in the overproduction of ROS [282, 283]. As SucPho leaves faced a higher rate of RWC loss in stress conditions (Figure 5.28d), it is safe to assume that they also generated more ROS as well. Yet, oxidative stress did not evoke a strong APX (Figure 5.30c) activity in the SucPho as it did in Blank and HumFer leaves. The lack of an adequate quantity of proline, which was shown to have antioxidant enzyme regulatory role [284] as well as $OH\cdot$ scavenging roles [285] may have worsened the harmful consequences of oxidative stress in SucPho. Availability and balance of Ca^{+2} are also essential for a proper antioxidant response [286, 287] so the observed imbalance in Ca^{+2} is an additional potential actor in this disturbance. As the cellular membranes are highly prone to damage by ROS [288], the significantly elevated electrolyte leakage for the SucPho leaves under stress conditions (Figure 5.28e) can be linked with the inadequate antioxidant exclusion capacity of SucPho.

6.3. Conclusion

To understand the molecular basis of differential response to salt stress in two common bean genotypes, we performed comparative analyses of transcriptome, metabolome and ionic content in the root and leaf tissues of these genotypes. The data implied that the maintenance of photosynthetic machinery via the control of Na^+ accumulation in leaves and the effective sequestration of K^+ in roots may be crucial for the stability of carbohydrate and energy metabolisms under saline conditions. Together with the subsequent osmoprotection and higher substrate availability, a superior regulation of amino acid metabolism, the notable shift in the ratio between glutamine and glutamate, the conservation of ionic balance, and the higher accumulation capability for certain ions, such as Mo and Mn in roots and leaves and Zn in roots, might be the essentials of salt-tolerance in Ispir genotype of common bean. The results of this part of the study have assisted us to select a high potential stress-response gene, *pvSPS4* for a functional study.

pvSPS4 knockdown in the roots of common bean has disrupted the glucose/ sucrose balance in the root tissues which in turn obstructed the constitution of ionic balance under salt stress. K^+ and Ca^{+2} imbalances in the root system possibly had negative outcomes in the root-to-shoot nutrient transport system and invoked a Ca^{+2} and Mg^{+2} imbalance in the leaf tissues. The adverse effects of ionic disproportion together with declined water availability in the leaves, distorted the photosynthesis and possibly energy production metabolism; reduced the growth, and resulted in increased cellular damage due to interruption of osmoprotection and antioxidant removal machinery. Considering the extent of salt susceptibility which the knockdown of the *pvSPS4* caused, it is safe to say that this sugar metabolism gene holds a critical role in salt-tolerance pathways and deserves attention in the future development of salt-tolerant varieties.

REFERENCES

1. Shrivastava, P. and R. Kumar, "Soil salinity: A serious environmental issue and plant growth promoting bacteria as one of the tools for its alleviation", *Saudi Journal of Biological Sciences*, Vol. 22, No. 2, pp. 123–131, Mar. 2015.

2. Jamil, A., S. Riaz, M. Ashraf and M. R. Foolad, *Gene expression profiling of plants under salt stress*, Vol. 30, Taylor & Francis Group, Sep. 2011.

3. Munns, R., "Genes and salt tolerance: bringing them together", *New Phytologist*, Vol. 167, No. 3, pp. 645–663, Jul. 2005.

4. Munns, R. and M. Tester, "Mechanisms of salinity tolerance", *Annual Review of Plant Biology*, Vol. 59, No. 1, pp. 651–681, Jun. 2008.

5. Muchate, N. S., G. C. Nikalje, N. S. Rajurkar, P. Suprasanna and T. D. Nikam, "Plant salt stress: Adaptive responses, tolerance mechanism and bioengineering for salt tolerance", *The Botanical Review*, Vol. 82, No. 4, pp. 371–406, Dec. 2016.

6. Davies, F. and J. Bowman, "Horticulture, food security, and the challenge of feeding the world", *Acta Horticulturae*, , No. 1128, pp. 1–6, Nov. 2016.

7. Shahzad, M., C. Zörb, C.-M. Geilfus and K. H. Mühling, "Apoplastic Na+ in Vicia faba leaves rises after short-term salt stress and is remedied by silicon", *Journal of Agronomy and Crop Science*, Vol. 199, No. 3, pp. 161–170, Jun. 2013.

8. Munns, R., "Comparative physiology of salt and water stress", *Plant, Cell and Environment*, Vol. 25, No. 2, pp. 239–250, Feb. 2002.

9. Tester, M. and R. Davenport, "Na+ tolerance and Na+ transport in higher plants.", *Annals of Botany*, Vol. 91, No. 5, pp. 503–27, Apr. 2003.

10. Shabala, S. and T. A. Cuin, "Potassium transport and plant salt tolerance.", *Physiologia Plantarum*, Vol. 133, No. 4, pp. 651–69, Aug. 2008.

11. Foolad, M. R., "Recent advances in genetics of salt tolerance in tomato", *Plant Cell, Tissue and Organ Culture*, Vol. 76, pp. 101–119, 2004.

12. Monforte, A. J., M. J. Asíns and E. A. Carbonell, "Salt tolerance in Lycopersicon species VI. Genotype-by-salinity interaction in quantitative trait loci detection: constitutive and response QTLs", *TAG Theoretical and Applied Genetics*, Vol. 95, No. 4, pp. 706–713, Sep. 1997.

13. Nilsen, E. T., D. M. Orcutt and M. G. Hale, *The physiology of plants under stress*, Wiley, 1996.

14. Broughton, W. J., G. Hernández, M. Blair, S. Beebe, P. Gepts and J. Vanderleyden, "Beans (Phaseolus spp.) – model food legumes", *Plant and Soil*, Vol. 252, No. 1, pp. 55–128, May 2003.

15. Chinnusamy, V., A. Jagendorf and J.-K. Zhu, "Understanding and improving salt tolerance in plants", *Crop Science*, Vol. 45, No. 2, p. 437, 2005.

16. Dasgan, Y. and S. Koc, "Evaluation of salt tolerance in common bean genotypes by ion regulation and searching for screening parameters", *Journal of Food Agriculture & Environment*, pp. 363–372, 2009.

17. Hiz, M. C., B. Canher, H. Niron and M. Turet, "Transcriptome analysis of salt tolerant common bean (Phaseolus vulgaris L.) under saline conditions", *PLOS One*, Vol. 9, No. 3, p. e92598, Mar. 2014.

18. Arbona, V., M. Manzi, C. Ollas and A. Gómez-Cadenas, "Metabolomics as a Tool to Investigate Abiotic Stress Tolerance in Plants", *International Journal of Molecular Sciences*, Vol. 14, No. 3, pp. 4885–4911, Mar. 2013.

19. Arbona, V., D. J. Iglesias, M. Talón and A. Gómez-Cadenas, "Plant phenotype demarcation using nontargeted LC-MS and GC-MS metabolite profiling", *Journal of Agricultural and Food Chemistry*, Vol. 57, No. 16, pp. 7338–7347, Aug. 2009.

20. Kim, H. K. and R. Verpoorte, "Sample preparation for plant metabolomics", *Phytochemical Analysis*, Vol. 21, No. 1, pp. 4–13, Jan. 2010.

21. Desbrosses, G., D. Steinhauser, J. Kopka and M. Udvardi, "Metabolome analysis using GC-MS", *Lotus japonicus Handbook*, pp. 165–174, Springer-Verlag, Berlin/Heidelberg, 2005.

22. Luedemann, A., K. Strassburg, A. Erban and J. Kopka, "TagFinder for the quantitative analysis of gas chromatography—mass spectrometry (GC-MS)-based metabolite profiling experiments", *Bioinformatics*, Vol. 24, No. 5, pp. 732–737, Mar. 2008.

23. Matsuda, F., K. Yonekura-Sakakibara, R. Niida, T. Kuromori, K. Shinozaki and K. Saito, "MS/MS spectral tag-based annotation of non-targeted profile of plant secondary metabolites", *The Plant Journal*, Vol. 57, No. 3, pp. 555–577, Feb. 2009.

24. Burton, L., G. Ivosev, S. Tate, G. Impey, J. Wingate and R. Bonner, "Instrumental and experimental effects in LC–MS-based metabolomics", *Journal of Chromatography B*, Vol. 871, No. 2, pp. 227–235, Aug. 2008.

25. Fiehn, O., G. Wohlgemuth, M. Scholz, T. Kind, D. Y. Lee, Y. Lu, S. Moon and B. Nikolau, "Quality control for plant metabolomics: reporting MSI-compliant studies", *The Plant Journal*, Vol. 53, No. 4, pp. 691–704, Feb. 2008.

26. Kerchev, P. I., B. Fenton, C. H. Foyer and R. D. Hancock, "Plant responses to insect herbivory: interactions between photosynthesis, reactive oxygen species and hormonal signalling pathways", *Plant, Cell & Environment*, Vol. 35, No. 2,

pp. 441–453, Feb. 2012.

27. Kim, J. K., T. Bamba, K. Harada, E. Fukusaki and A. Kobayashi, "Time-course metabolic profiling in Arabidopsis thaliana cell cultures after salt stress treatment", *Journal of Experimental Botany*, Vol. 58, No. 3, pp. 415–424, Feb. 2007.

28. Wang, Y., L. Xu, H. Shen, J. Wang, W. Liu, X. Zhu, R. Wang, X. Sun and L. Liu, "Metabolomic analysis with GC-MS to reveal potential metabolites and biological pathways involved in Pb &Cd stress response of radish roots.", *Scientific Reports*, Vol. 5, p. 18296, Dec. 2015.

29. Kusano, M., T. Tohge, A. Fukushima, M. Kobayashi, N. Hayashi, H. Otsuki, Y. Kondou, H. Goto, M. Kawashima, F. Matsuda, R. Niida, M. Matsui, K. Saito and A. R. Fernie, "Metabolomics reveals comprehensive reprogramming involving two independent metabolic responses of Arabidopsis to UV-B light", *The Plant Journal*, Vol. 67, No. 2, pp. 354–369, Jul. 2011.

30. Ullah, N., M. Yüce, Z. Neslihan Öztürk Gökçe and H. Budak, "Comparative metabolite profiling of drought stress in roots and leaves of seven Triticeae species", *BMC Genomics*, Vol. 18, No. 1, p. 969, Dec. 2017.

31. Guo, R., Z. Yang, F. Li, C. Yan, X. Zhong, Q. Liu, X. Xia, H. Li and L. Zhao, "Comparative metabolic responses and adaptive strategies of wheat (Triticum aestivum) to salt and alkali stress", *BMC Plant Biology*, Vol. 15, No. 1, p. 170, 2015.

32. Sanchez, D. H., F. L. Pieckenstain, F. Escaray, A. Erban, U. Kraemer, M. K. Udvardi and J. Kopka, "Comparative ionomics and metabolomics in extremophile and glycophytic Lotus species under salt stress challenge the metabolic preadaptation hypothesis: Ionomic and metabolomic phenotypes of L. creticus under salt stress", *Plant, Cell & Environment*, Vol. 34, No. 4, pp. 605–617, Apr. 2011.

33. Scalabrin, E., M. Radaelli, G. Rizzato, P. Bogani, M. Buiatti, A. Gambaro and G. Capodaglio, "Metabolomic analysis of wild and transgenic Nicotiana langsdorffii plants exposed to abiotic stresses: unraveling metabolic responses", *Analytical and Bioanalytical Chemistry*, Vol. 407, No. 21, pp. 6357–6368, Aug. 2015.

34. Ward, J. L., S. Forcat, M. Beckmann, M. Bennett, S. J. Miller, J. M. Baker, N. D. Hawkins, C. P. Vermeer, C. Lu, W. Lin, W. M. Truman, M. H. Beale, J. Draper, J. W. Mansfield and M. Grant, "The metabolic transition during disease following infection of Arabidopsis thaliana by Pseudomonas syringae pv. tomato", *The Plant Journal*, Vol. 63, No. 3, pp. 443–457, Aug. 2010.

35. Leiss, K. A., F. Maltese, Y. H. Choi, R. Verpoorte and P. G. L. Klinkhamer, "Identification of chlorogenic acid as a resistance factor for thrips in chrysanthemum.", *Plant Physiology*, Vol. 150, No. 3, pp. 1567–75, Jul. 2009.

36. Baker, J. M., N. D. Hawkins, J. L. Ward, A. Lovegrove, J. A. Napier, P. R. Shewry and M. H. Beale, "A metabolomic study of substantial equivalence of field-grown genetically modified wheat", *Plant Biotechnology Journal*, Vol. 4, No. 4, pp. 381–392, Jul. 2006.

37. Kusano, M., H. Redestig, T. Hirai, A. Oikawa, F. Matsuda, A. Fukushima, M. Arita, S. Watanabe, M. Yano, K. Hiwasa-Tanase, H. Ezura and K. Saito, "Covering Chemical Diversity of Genetically-Modified Tomatoes Using Metabolomics for Objective Substantial Equivalence Assessment", *PLoS ONE*, Vol. 6, No. 2, p. e16989, Feb. 2011.

38. Salt, D. E., I. Baxter and B. Lahner, "Ionomics and the study of the plant ionome", *Annual Review of Plant Biology*, 2008.

39. Almeida, D. M., M. Margarida Oliveira and N. J. Saibo, *Regulation of Na+and K+homeostasis in plants: Towards improved salt stress tolerance in crop plants*, 2017.

40. Manishankar, P., N. Wang, P. Köster, A. A. Alatar and J. Kudla, "Calcium signaling during salt stress and in the regulation of ion homeostasis", *Journal of Experimental Botany*, Vol. 69, No. 17, pp. 4215–4226, Jul. 2018.

41. Chen, Z.-H., G. Chen, F. Dai, Y. Wang, A. Hills, Y.-L. Ruan, G. Zhang, P. J. Franks, E. Nevo and M. R. Blatt, "Molecular evolution of grass stomata", *Trends in Plant Science*, Vol. 22, No. 2, pp. 124–139, Feb. 2017, publisher: Elsevier.

42. Abbas, G., M. Saqib, J. Akhtar and M. A. ul Haq, "Interactive effects of salinity and iron deficiency on different rice genotypes", *Journal of Plant Nutrition and Soil Science*, 2015.

43. Krasensky, J. and C. Jonak, "Drought, salt, and temperature stress-induced metabolic rearrangements and regulatory networks", *Journal of Experimental Botany*, Vol. 63, No. 4, pp. 1593–1608, Feb. 2012.

44. Journet, E. P., R. Bligny and R. Douce, "Biochemical changes during sucrose deprivation in higher plant cells.", *Journal of Biological Chemistry*, Vol. 261, No. 7, pp. 3193–3199, Mar. 1986.

45. Yu, S.-M., "Cellular and Genetic Responses of Plants to Sugar Starvation", *Plant Physiology*, Vol. 121, No. 3, pp. 687–693, Nov. 1999.

46. Gupta, A. K. and N. Kaur, "Sugar signalling and gene expression in relation to carbohydrate metabolism under abiotic stresses in plants", *Journal of Biosciences*, Vol. 30, No. 5, pp. 761–776, Dec. 2005.

47. Roitsch, T., "Source-sink regulation by sugar and stress", *Current Opinion in Plant Biology*, Vol. 2, No. 3, pp. 198–206, Jun. 1999.

48. Ho, L. C., "Metabolism and compartmentation of imported sugars in sink organs in relation to sink strength", *Annual Review of Plant Physiology and Plant Molecular Biology*, Vol. 39, No. 1, pp. 355–378, Jun. 1988.

49. Krapp, A. and M. Stitt, "An evaluation of direct and indirect mechanisms for the sink-regulation of photosynthesis in spinach: Changes in gas exchange, carbohydrates, metabolites, enzyme activities and steady-state transcript levels after cold-girdling source leaves", *Planta*, Vol. 195, No. 3, Jan. 1995.

50. Chen, J.-G., "Sweet sensor, surprising partners", *Science's STKE*, Vol. 2007, No. 373, pp. pe7–pe7, Feb. 2007.

51. Coruzzi, G. and D. R. Bush, "Nitrogen and Carbon Nutrient and Metabolite Signaling in Plants", *Plant Physiology*, Vol. 125, No. 1, pp. 61–64, Jan. 2001.

52. Rolland, F., E. Baena-Gonzalez and J. Sheen, "Sugar sensing and signalling in plants: conserved and novel mechanisms", *Annual Review of Plant Biology*, Vol. 57, No. 1, pp. 675–709, Jun. 2006.

53. Koch, K. E., "Carbohydrate-modulated gene expression in plants", *Annual Review of Plant Physiology and Plant Molecular Biology*, Vol. 47, No. 1, pp. 509–540, Jun. 1996.

54. Koch, K., "Sucrose metabolism: regulatory mechanisms and pivotal roles in sugar sensing and plant development", *Current Opinion in Plant Biology*, Vol. 7, No. 3, pp. 235–246, Jun. 2004.

55. Kutschera, U. and A. Heiderich, "Sucrose metabolism and cellulose biosynthesis in sunflower hypocotyls", *Physiologia Plantarum*, Vol. 114, No. 3, pp. 372–379, 2002.

56. Sturm, A., "Invertases: Primary structures, functions, and roles in plant development and sucrose partitioning", *Plant Physiology*, Vol. 121, No. 1, pp. 1–8, Sep. 1999.

57. Lemoine, R., S. La Camera, R. Atanassova, F. Dédaldéchamp, T. Allario, N. Pourtau, J.-L. Bonnemain, M. Laloi, P. Coutos-Thévenot, L. Maurousset, M. Faucher,

C. Girousse, P. Lemonnier, J. Parrilla and M. Durand, "Source-to-sink transport of sugar and regulation by environmental factors", *Frontiers in Plant Science*, Vol. 4, 2013.

58. Durand, M., B. Porcheron, N. Hennion, L. Maurousset, R. Lemoine and N. Pourtau, "Water deficit enhances C export to the roots in Arabidopsis thaliana plants with contribution of sucrose transporters in both shoot and roots", *Plant Physiology*, Vol. 170, No. 3, pp. 1460–1479, Mar. 2016.

59. Mewis, I., M. A. M. Khan, E. Glawischnig, M. Schreiner and C. Ulrichs, "Water stress and aphid feeding differentially influence metabolite composition in Arabidopsis thaliana (L.)", *PLOS One*, Vol. 7, No. 11, p. e48661, Nov. 2012.

60. Verslues, P. E., M. Agarwal, S. Katiyar[U+2010]Agarwal, J. Zhu and J.-K. Zhu, "Methods and concepts in quantifying resistance to drought, salt and freezing, abiotic stresses that affect plant water status", *The Plant Journal*, Vol. 45, No. 4, pp. 523–539, 2006.

61. DaCosta, M. and B. Huang, "Changes in Carbon Partitioning and Accumulation Patterns during Drought and Recovery for Colonial Bentgrass, Creeping Bentgrass, and Velvet Bentgrass", *Journal of the American Society for Horticultural Science*, Vol. 131, No. 4, pp. 484–490, Jul. 2006.

62. Chua, T. K., J. M. Bujnicki, T.-C. Tan, F. Huynh, B. K. Patel and J. Sivaraman, "The structure of sucrose phosphate synthase from Halothermothrix orenii reveals its mechanism of action and binding mode", *The Plant Cell*, Vol. 20, No. 4, pp. 1059–1072, Apr. 2008.

63. Huber, S. C. and J. L. Huber, "Role and regulation of sucrose-phosphate synthase in higher plants", *Annual Review of Plant Physiology and Plant Molecular Biology*, Vol. 47, No. 1, pp. 431–444, Jun. 1996.

64. Stitt, M., I. Wilke, R. Feil and H. W. Heldt, "Coarse control of sucrose-phosphate synthase in leaves: Alterations of the kinetic properties in response to the rate of photosynthesis and the accumulation of sucrose", *Planta*, Vol. 174, No. 2, pp. 217–230, May 1988.

65. Baxter, C. J., C. H. Foyer, J. Turner, S. A. Rolfe and W. P. Quick, "Elevated sucrose-phosphate synthase activity in transgenic tobacco sustains photosynthesis in older leaves and alters development", *Journal of Experimental Botany*, Vol. 54, No. 389, pp. 1813–1820, Aug. 2003.

66. Chen, S., M. Hajirezaei and F. Börnke, "Differential expression of sucrose-phosphate synthase isoenzymes in tobacco reflects their functional specialization during dark-governed starch mobilization in source Lleaves", *Plant Physiology*, Vol. 139, No. 3, pp. 1163–1174, Nov. 2005.

67. Geigenberger, P., R. Reimholz, U. Deiting, U. Sonnewald and M. Stitt, "Decreased expression of sucrose phosphate synthase strongly inhibits the water stress-induced synthesis of sucrose in growing potato tubers", *The Plant Journal*, Vol. 19, No. 2, pp. 119–129, 1999.

68. Lunn, J. E. and E. MacRae, "New complexities in the synthesis of sucrose", *Current Opinion in Plant Biology*, Vol. 6, No. 3, pp. 208–214, Jun. 2003.

69. Huber, S. C. and J. L. Huber, "Role of sucrose-phosphate synthase in sucrose metabolism in leaves", *Plant Physiology*, Vol. 99, No. 4, pp. 1275–1278, Aug. 1992.

70. Lutfiyya, L. L., N. Xu, R. L. D'Ordine, J. A. Morrell, P. W. Miller and S. M. Duff, "Phylogenetic and expression analysis of sucrose phosphate synthase isozymes in plants", *Journal of Plant Physiology*, Vol. 164, No. 7, pp. 923–933, Jul. 2007.

71. Reimholz, R., M. Geiger, V. Haake, U. Deiting, K.-P. Krause, U. Sonnewald and

M. Stitt, "Potato plants contain multiple forms of sucrose phosphate synthase, which differ in their tissue distributions, their levels during development, and their responses to low temperature", *Plant, Cell & Environment*, Vol. 20, No. 3, pp. 291–305, 1997.

72. Amirjani, M. R., "Effect of salinity stress on growth, sugar content, pigments and enzyme activity of rice", *International Journal of Botany*, Vol. 7, No. 1, pp. 73–81, Dec. 2010.

73. Peng, J., J. Liu, L. Zhang, J. Luo, H. Dong, Y. Ma, X. Zhao, B. Chen, N. Sui, Z. Zhou and Y. Meng, "Effects of soil salinity on sucrose metabolism in cotton leaves", *PLOS One*, Vol. 11, No. 5, p. e0156241, May 2016.

74. Fresneau, C., J. Ghashghaie and G. Cornic, "Drought effect on nitrate reductase and sucrose-phosphate synthase activities in wheat (Triticum durum L.): role of leaf internal CO2", *Journal of Experimental Botany*, Vol. 58, No. 11, pp. 2983–2992, Aug. 2007.

75. Xu, W., K. Cui, A. Xu, L. Nie, J. Huang and S. Peng, "Drought stress condition increases root to shoot ratio via alteration of carbohydrate partitioning and enzymatic activity in rice seedlings", *Acta Physiologiae Plantarum*, Vol. 37, No. 2, p. 9, Jan. 2015.

76. Du, Y., Q. Zhao, L. Chen, X. Yao, H. Zhang, J. Wu and F. Xie, "Effect of drought stress during soybean R2–R6 growth stages on sucrose metabolism in leaf and seed", *International Journal of Molecular Sciences*, Vol. 21, No. 2, p. 618, Jan. 2020.

77. Bilska-Kos, A., J. Mytych, S. Suski, J. Magoń, P. Ochodzki and J. Zebrowski, "Sucrose phosphate synthase (SPS), sucrose synthase (SUS) and their products in the leaves of Miscanthus × giganteus and Zea mays at low temperature", *Planta*, Vol. 252, No. 2, p. 23, Jul. 2020.

78. Christey, M. C. and R. H. Braun, "Production of hairy root cultures and transgenic plants by Agrobacterium rhizogenes-mediated transformation", *Transgenic Plants*, Vol. 286, pp. 047–060, Humana Press, New Jersey, Aug. 2004.

79. Chilton, M.-D., D. A. Tepfer, A. Petit, C. David, F. Casse-Delbart and J. Tempé, "Agrobacterium rhizogenes inserts T-DNA into the genomes of the host plant root cells", *Nature*, Vol. 295, No. 5848, pp. 432–434, Feb. 1982.

80. Collier, R., B. Fuchs, N. Walter, W. Kevin Lutke and C. G. Taylor, "Ex vitro composite plants: an inexpensive, rapid method for root biology: Ex vitro composite plants", *The Plant Journal*, Vol. 43, No. 3, pp. 449–457, Jul. 2005.

81. Costantino, P., L. Spanò, M. Pomponi, E. Benvenuto and G. Ancora, "The T-DNA of Agrobacterium rhizogenes is transmitted through meiosis to the progeny of hairy root plants", *Journal of Molecular and Applied Genetics*, Vol. 2, No. 5, pp. 465–470, 1984.

82. Estrada-Navarrete, G., X. Alvarado-Affantranger, J.-E. Olivares, G. Guillén, C. Díaz-Camino, F. Campos, C. Quinto, P. M. Gresshoff and F. Sanchez, "Fast, efficient and reproducible genetic transformation of Phaseolus spp. by Agrobacterium rhizogenes", *Nature Protocols*, Vol. 2, No. 7, pp. 1819–1824, Jul. 2007.

83. Kereszt, A., D. Li, A. Indrasumunar, C. D. Nguyen, S. Nontachaiyapoom, M. Kinkema and P. M. Gresshoff, "Agrobacterium rhizogenes -mediated transformation of soybean to study root biology", *Nature Protocols*, Vol. 2, No. 4, pp. 948–952, Apr. 2007.

84. Hoagland, D., D. Arnon, D. R. Hoagland, D. I. Arnon and C. B. Hutchison, "The water-culture method for growing plants without soil", pp. 1884–1949, 1938.

85. Sanchez, D. H., F. Lippold, H. Redestig, M. A. Hannah, A. Erban, U. Krämer, J. Kopka and M. K. Udvardi, "Integrative functional genomics of salt acclimati-

zation in the model legume Lotus japonicus", *Plant Journal*, Vol. 53, No. 6, pp. 973–987, Nov. 2008.

86. Barbas, C. F., D. R. Burton, J. K. Scott and G. J. Silverman, "Quantitation of DNA and RNA.", *CSH Protocols*, Vol. 2007, No. 11, p. pdb.ip47, Nov. 2007.

87. Andrews, S. and Babraham Bioinformatics, *FastQC: A quality control tool for high throughput sequence data*, 2010.

88. Bolger, A. M., M. Lohse and B. Usadel, "Trimmomatic: A flexible trimmer for Illumina sequence data", *Bioinformatics*, 2014.

89. Kim, D., B. Langmead and S. L. Salzberg, "HISAT: A fast spliced aligner with low memory requirements", *Nature Methods*, 2015.

90. Li, H., B. Handsaker, A. Wysoker, T. Fennell, J. Ruan, N. Homer, G. Marth, G. Abecasis and R. Durbin, "The sequence alignment/map format and SAMtools", *Bioinformatics*, 2009.

91. McCarthy, D. J., Y. Chen and G. K. Smyth, "Differential expression analysis of multifactor RNA-Seq experiments with respect to biological variation", *Nucleic Acids Research*, 2012.

92. Borges, A., S. M. Tsai and D. G. G. Caldas, "Validation of reference genes for RT-qPCR normalization in common bean during biotic and abiotic stresses", *Plant Cell Reports*, Vol. 31, No. 5, pp. 827–838, May 2012.

93. Livak, K. J. and T. D. Schmittgen, "Analysis of relative gene expression data using real-time quantitative PCR and the 2-$\Delta\Delta$CT method", *Methods*, 2001.

94. Smedley, D., S. Haider, S. Durinck, L. Pandini, P. Provero, J. Allen, O. Arnaiz, M. H. Awedh, R. Baldock, G. Barbiera, P. Bardou, T. Beck, A. Blake, M. Bonierbale, A. J. Brookes, G. Bucci, I. Buetti, S. Burge, C. Cabau, J. W.

Carlson, C. Chelala, C. Chrysostomou, D. Cittaro, O. Collin, R. Cordova, R. J. Cutts, E. Dassi, A. Di Genova, A. Djari, A. Esposito, H. Estrella, E. Eyras, J. Fernandez-Banet, S. Forbes, R. C. Free, T. Fujisawa, E. Gadaleta, J. M. Garcia-Manteiga, D. Goodstein, K. Gray, J. A. Guerra-Assunção, B. Haggarty, D. J. Han, B. W. Han, T. Harris, J. Harshbarger, R. K. Hastings, R. D. Hayes, C. Hoede, S. Hu, Z. L. Hu, L. Hutchins, Z. Kan, H. Kawaji, A. Keliet, A. Kerhornou, S. Kim, R. Kinsella, C. Klopp, L. Kong, D. Lawson, D. Lazarevic, J. H. Lee, T. Letellier, C. Y. Li, P. Lio, C. J. Liu, J. Luo, A. Maass, J. Mariette, T. Maurel, S. Merella, A. M. Mohamed, F. Moreews, I. Nabihoudine, N. Ndegwa, C. Noirot, C. Perez-Llamas, M. Primig, A. Quattrone, H. Quesneville, D. Rambaldi, J. Reecy, M. Riba, S. Rosanoff, A. A. Saddiq, E. Salas, O. Sallou, R. Shepherd, R. Simon, L. Sperling, W. Spooner, D. M. Staines, D. Steinbach, K. Stone, E. Stupka, J. W. Teague, A. Z. Dayem Ullah, J. Wang, D. Ware, M. Wong-Erasmus, K. Youens-Clark, A. Zadissa, S. J. Zhang and A. Kasprzyk, "The BioMart community portal: An innovative alternative to large, centralized data repositories", *Nucleic Acids Research*, 2015.

95. Tian, T., Y. Liu, H. Yan, Q. You, X. Yi, Z. Du, W. Xu and Z. Su, "AgriGO v2.0: A GO analysis toolkit for the agricultural community, 2017 update", *Nucleic Acids Research*, 2017.

96. Yi, X., Z. Du and Z. Su, "PlantGSEA: a gene set enrichment analysis toolkit for plant community.", *Nucleic acids research*, 2013.

97. Benjamini, Y. and Y. Hochberg, "Controlling the False Discovery Rate: a Practical and Powerful Approach to Multiple Testing", *Journal of the Royal Statistical Society*, 1995.

98. Lisec, J., N. Schauer, J. Kopka, L. Willmitzer and A. R. Fernie, "Gas chromatography mass spectrometry–based metabolite profiling in plants", *Nature Protocols*, Vol. 1, No. 1, pp. 387–396, Jun. 2006.

99. Mihaylova, V., V. Lyubomirova and R. Djingova, "Optimization of sample preparation and ICP-MS analysis for determination of 60 elements for characterization of the plant ionome", *International Journal of Environmental Analytical Chemistry*, Vol. 93, No. 13, pp. 1441–1456, Nov. 2013.

100. Kanehisa, M. and S. Goto, "KEGG: Kyoto encyclopedia of genes and genomes", *Nucleic Acids Research*, Vol. 28, No. 1, pp. 27–30, Jan. 2000.

101. Kanehisa, M. and Y. Sato, "KEGG Mapper for inferring cellular functions from protein sequences", *Protein Science*, Vol. 29, No. 1, pp. 28–35, 2020.

102. Warren, C. R., "Rapid Measurement of Chlorophylls with a Microplate Reader", *Journal of Plant Nutrition*, Vol. 31, No. 7, pp. 1321–1332, Jun. 2008.

103. Schneider, C. A., W. S. Rasband and K. W. Eliceiri, *NIH Image to ImageJ: 25 years of image analysis*, 2012.

104. Bates, L. S., R. P. Waldren and I. D. Teare, "Rapid determination of free proline for water-stress studies", *Plant and Soil*, Vol. 39, No. 1, pp. 205–207, Aug. 1973.

105. Simonian, M. H. and J. A. Smith, "Spectrophotometric and colorimetric determination of protein concentration", *Current Protocols in Toxicology*, Vol. 10, No. 1, Nov. 2001.

106. Maness, N., "Extraction and analysis of soluble carbohydrates", R. Sunkar (Editor), *Plant Stress Tolerance*, Vol. 639, pp. 341–370, Humana Press, Totowa, NJ, 2010.

107. Maeda, H., S. Matsu-Ura, T. Senba, S. Yamasaki, H. Takai, Y. Yamauchi and H. Ohmori, "Resorufin as an electron acceptor in glucose oxidase-catalyzed oxidation of glucose.", *Chemical & Pharmaceutical Bulletin*, Vol. 48, No. 7, pp. 897–902, 2000.

108. Kulshrestha, S., P. Tyagi, V. Sindhi and K. S. Yadavilli, "Invertase and its applications – A brief review", *Journal of Pharmacy Research*, Vol. 7, No. 9, pp. 792–797, Sep. 2013.

109. Tautz, D., "Redundancies, development and the flow of information", *BioEssays*, 1992.

110. Wesley, S. V., C. A. Helliwell, N. A. Smith, M. Wang, D. T. Rouse, Q. Liu, P. S. Gooding, S. P. Singh, D. Abbott, P. A. Stoutjesdijk, S. P. Robinson, A. P. Gleave, A. G. Green and P. M. Waterhouse, "Construct design for efficient, effective and high-throughput gene silencing in plants", *The Plant Journal*, Vol. 27, No. 6, pp. 581–590, 2001.

111. Yan, P., W. Shen, X. Gao, X. Li, P. Zhou and J. Duan, "High-throughput construction of intron-containing hairpin RNA vectors for RNAi in plants", *PLOS One*, Vol. 7, No. 5, p. e38186, May 2012.

112. Holsters, M., D. de Waele, A. Depicker, E. Messens, M. van Montagu and J. Schell, "Transfection and transformation of Agrobacterium tumefaciens", *Molecular and General Genetics MGG*, Vol. 163, No. 2, pp. 181–187, Jan. 1978.

113. Parida, A. K. and A. B. Das, "Salt tolerance and salinity effects on plants: a review", *Ecotoxicology and Environmental Safety*, Vol. 60, No. 3, pp. 324–349, Mar. 2005.

114. Hayat, S., Q. Hayat, M. N. Alyemeni, A. S. Wani, J. Pichtel and A. Ahmad, "Role of proline under changing environments: A review", *Plant Signaling & Behavior*, Vol. 7, No. 11, pp. 1456–1466, Nov. 2012.

115. Flowers, T. J. and T. D. Colmer, "Salinity tolerance in halophytes", *New Phytologist*, Vol. 179, No. 4, pp. 945–963, Sep. 2008.

116. Flowers, T. J. and T. D. Colmer, "Plant salt tolerance: adaptations in halo-

phytes", *Annals of Botany*, Vol. 115, No. 3, pp. 327–331, Feb. 2015.

117. Maathuis, F. J. M., I. Ahmad and J. Patishtan, "Regulation of Na+ fluxes in plants", *Frontiers in Plant Science*, Vol. 5, 2014.

118. Kronzucker, H. J., M. W. Szczerba, M. Moazami[U+2010]Goudarzi and D. T. Britto, "The cytosolic Na+ : K+ ratio does not explain salinity-induced growth impairment in barley: a dual-tracer study using 42K+ and 24Na+", *Plant, Cell & Environment*, Vol. 29, No. 12, pp. 2228–2237, 2006.

119. Wang, C.-M., J.-L. Zhang, X.-S. Liu, Z. Li, G.-Q. Wu, J.-Y. Cai, T. J. Flowers and S.-M. Wang, "Puccinellia tenuiflora maintains a low Na+ level under salinity by limiting unidirectional Na+ influx resulting in a high selectivity for K+ over Na+", *Plant, Cell & Environment*, Vol. 32, No. 5, pp. 486–496, 2009.

120. Wang, S., G. Zhao, Y. Gao, Z. Tang and C. Zhang, "Puccinellia tenuiflora exhibits stronger selectivity for K+ over Na+ than wheat", *Journal of Plant Nutrition*, Vol. 27, No. 10, pp. 1841–1857, Jan. 2005.

121. Wang, S.-M., J.-L. Zhang and T. J. Flowers, "Low-affinity Na+ uptake in the halophyte Suaeda maritima", *Plant Physiology*, Vol. 145, No. 2, pp. 559–571, Oct. 2007.

122. Amtmann, A. and D. Sanders, "Mechanisms of Na+ uptake by plant cells", J. A. Callow (Editor), *Advances in Botanical Research*, Vol. 29, pp. 75–112, Academic Press, Jan. 1998.

123. Garciadeblás, B., M. E. Senn, M. A. Bañuelos and A. Rodríguez[U+2010]Navarro, "Sodium transport and HKT transporters: the rice model", *The Plant Journal*, Vol. 34, No. 6, pp. 788–801, 2003.

124. James, R. A., C. Blake, C. S. Byrt and R. Munns, "Major genes for Na+ exclusion, Nax1 and Nax2 (wheat HKT1;4 and HKT1;5), decrease Na+ accumulation

in bread wheat leaves under saline and waterlogged conditions", *Journal of Experimental Botany*, Vol. 62, No. 8, pp. 2939–2947, May 2011.

125. Laurie, S., K. A. Feeney, F. J. M. Maathuis, P. J. Heard, S. J. Brown and R. A. Leigh, "A role for HKT1 in sodium uptake by wheat roots", *The Plant Journal*, Vol. 32, No. 2, pp. 139–149, 2002.

126. Munns, R., R. A. James and A. Läuchli, "Approaches to increasing the salt tolerance of wheat and other cereals", *Journal of Experimental Botany*, Vol. 57, No. 5, pp. 1025–1043, Mar. 2006.

127. Boyer, J. S., "Water deficits and photosynthesis", T. T. Kozlowski (Editor), *Soil Water Measurement, Plant Responses, and Breeding for Drought Resistance*, pp. 153–190, Academic Press, Jan. 1976.

128. Kirst, G. O., "Salinity tolerance of eukaryotic marine algae", *Annual Review of Plant Physiology and Plant Molecular Biology*, Vol. 41, No. 1, pp. 21–53, 1990.

129. Everard, J. D., R. Gucci, S. C. Kann, J. A. Flore and W. H. Loescher, "Gas exchange and carbon partitioning in the leaves of celery (Apium graveolens L.) at various levels of root zone salinity", *Plant Physiology*, Vol. 106, No. 1, pp. 281–292, Sep. 1994.

130. Kao, W.-Y., T.-T. Tsai and C.-N. Shih, "Photosynthetic gas exchange and chlorophyll a fluorescence of three wild soybean species in response to NaCl treatments", *Photosynthetica*, Vol. 41, No. 3, pp. 415–419, Sep. 2003.

131. Mishra, S. K., D. Subrahmanyam and G. S. Singhal, "Interrelationship between salt and light stress on primary processes of photosynthesis", *Journal of Plant Physiology*, Vol. 138, No. 1, pp. 92–96, May 1991.

132. Parida, A., A. Das and B. Mittra, "Effects of NaCl stress on the structure, pigment complex composition, and photosynthetic activity of mangrove Bruguiera

parviflora chloroplasts", *Photosynthetica*, Vol. 41, No. 2, p. 191, Jun. 2003.

133. Abdullah, Z. and R. Ahmad, "Effect of pre- and post-kinetin treatments on salt tolerance of different potato cultivars growing on saline soils", *Journal of Agronomy and Crop Science*, Vol. 165, No. 2-3, pp. 94–102, 1990.

134. Moghaieb, R. E. A., H. Saneoka, J. Ito and K. Fujita, "Characterization of salt tolerance in tomato plant in terms of photosynthesis and water relations", *Soil Science and Plant Nutrition*, Vol. 47, No. 2, pp. 377–385, Jun. 2001.

135. Hamada, A. M. and A. E. El-Enany, "Effect of NaCl salinity on growth, pigment and mineral element contents, and gas exchange of broad bean and pea plants", *Biologia Plantarum*, Vol. 36, No. 1, pp. 75–81, Jan. 1994.

136. Seemann, J. R. and C. Critchley, "Effects of salt stress on the growth, ion content, stomatal behaviour and photosynthetic capacity of a salt-sensitive species, Phaseolus vulgaris L", *Planta*, Vol. 164, No. 2, pp. 151–162, May 1985.

137. Jones, H. G., "Stomatal control of photosynthesis and transpiration", *Journal of Experimental Botany*, Vol. 49, No. Special_Issue, pp. 387–398, Mar. 1998.

138. Hedrich, R., "Ion channels in plants", *Physiological Reviews*, Vol. 92, No. 4, pp. 1777–1811, Oct. 2012.

139. Talbott, L. D. and E. Zeiger, "Central roles for potassium and sucrose in guard-cell osmoregulation", *Plant Physiology*, Vol. 111, No. 4, pp. 1051–1057, Aug. 1996.

140. Kim, T.-H., M. Böhmer, H. Hu, N. Nishimura and J. I. Schroeder, "Guard cell signal transduction network: Advances in understanding abscisic acid, CO2, and Ca2+ signaling", *Annual Review of Plant Biology*, Vol. 61, No. 1, pp. 561–591, May 2010.

141. Liu, X., Y. Fan, M. Mak, M. Babla, P. Holford, F. Wang, G. Chen, G. Scott,

G. Wang, S. Shabala, M. Zhou and Z.-H. Chen, "QTLs for stomatal and photosynthetic traits related to salinity tolerance in barley", *BMC Genomics*, Vol. 18, No. 1, p. 9, Jan. 2017.

142. Fricke, W., G. Akhiyarova, D. Veselov and G. Kudoyarova, "Rapid and tissue[U+2010]specific changes in ABA and in growth rate in response to salinity in barley leaves", *Journal of Experimental Botany*, Vol. 55, No. 399, pp. 1115–1123, May 2004.

143. Jaschke, W. D., A. D. Peuke, J. S. Pate and W. Hartung, "Transport, synthesis and catabolism of abscisic acid (ABA) in intact plants of castor bean (Ricinus communis L.) under phosphate deficiency and moderate salinity", *Journal of Experimental Botany*, Vol. 48, No. 9, pp. 1737–1747, Sep. 1997.

144. Hedrich, R. and S. Shabala, "Stomata in a saline world", *Current Opinion in Plant Biology*, Vol. 46, pp. 87–95, Dec. 2018.

145. Keys, A. J., R. J. Ellis and J. C. Gray, "Rubisco: Its role in photorespiration", *Philosophical Transactions of the Royal Society of London. B, Biological Sciences*, Vol. 313, No. 1162, pp. 325–336, Oct. 1986.

146. Hetherington, A. M. and F. I. Woodward, "The role of stomata in sensing and driving environmental change", *Nature*, Vol. 424, No. 6951, pp. 901–908, Aug. 2003.

147. Zhao, C., Y. Wang, K. X. Chan, D. B. Marchant, P. J. Franks, D. Randall, E. E. Tee, G. Chen, S. Ramesh, S. Y. Phua, B. Zhang, A. Hills, F. Dai, D. Xue, M. Gilliham, S. Tyerman, E. Nevo, F. Wu, G. Zhang, G. K.-S. Wong, J. H. Leebens-Mack, M. Melkonian, M. R. Blatt, P. S. Soltis, D. E. Soltis, B. J. Pogson and Z.-H. Chen, "Evolution of chloroplast retrograde signaling facilitates green plant adaptation to land", *Proceedings of the National Academy of Sciences*, Vol. 116, No. 11, pp. 5015–5020, Mar. 2019.

148. Amsbury, S., L. Hunt, N. Elhaddad, A. Baillie, M. Lundgren, Y. Verhertbruggen, H. V. Scheller, J. P. Knox, A. J. Fleming and J. E. Gray, "Stomatal function requires pectin de-methyl-esterification of the guard cell wall", *Current Biology*, Vol. 26, No. 21, pp. 2899–2906, Nov. 2016.

149. Scheidig, A., A. Fröhlich, S. Schulze, J. R. Lloyd and J. Kossmann, "Downregulation of a chloroplast-targeted β-amylase leads to a starch-excess phenotype in leaves", *The Plant Journal*, Vol. 30, No. 5, pp. 581–591, 2002.

150. Ende, W. V. d. and D. Peshev, "Sugars as antioxidants in plants", N. Tuteja and S. S. Gill (Editors), *Crop Improvement Under Adverse Conditions*, pp. 285–307, Springer New York, New York, NY, 2013.

151. Jang, J. C. and J. Sheen, "Sugar sensing in higher plants.", *The Plant Cell*, Vol. 6, No. 11, Nov. 1994.

152. Pego, J. V., A. J. Kortstee, C. Huijser and S. C. M. Smeekens, "Photosynthesis, sugars and the regulation of gene expression", *Journal of Experimental Botany*, Vol. 51, No. suppl_1, pp. 407–416, Feb. 2000.

153. Chinnusamy, V., K. Schumaker and J.-K. Zhu, "Molecular genetic perspectives on cross[U+2010]talk and specificity in abiotic stress signalling in plants", *Journal of Experimental Botany*, Vol. 55, No. 395, pp. 225–236, Jan. 2004.

154. Ho, S.-L., Y.-C. Chao, W.-F. Tong and S.-M. Yu, "Sugar coordinately and differentially regulates growth- and stress-related gene expression via a complex signal transduction network and multiple control mechanisms", *Plant Physiology*, Vol. 125, No. 2, pp. 877–890, Feb. 2001.

155. Abebe, T., A. C. Guenzi, B. Martin and J. C. Cushman, "Tolerance of mannitol-accumulating transgenic wheat to water stress and salinity", *Plant Physiology*, Vol. 131, No. 4, pp. 1748–1755, Apr. 2003.

156. Shen, B., R. G. Jensen and H. J. Bohnert, "Increased resistance to oxidative stress in transgenic plants by targeting mannitol biosynthesis to chloroplasts", *Plant Physiology*, Vol. 113, No. 4, pp. 1177–1183, Apr. 1997.

157. Tarczynski, M. C., R. G. Jensen and H. J. Bohnert, "Stress protection of transgenic tobacco by production of the osmolyte mannitol", *Science*, Vol. 259, No. 5094, pp. 508–510, Jan. 1993.

158. Thomas, J. C., M. Sepahi, B. Arendall and H. J. Bohnert, "Enhancement of seed germination in high salinity by engineering mannitol expression in Arabidopsis thaliana", *Plant, Cell & Environment*, Vol. 18, No. 7, pp. 801–806, 1995.

159. Smirnoff, N. and Q. J. Cumbes, "Hydroxyl radical scavenging activity of compatible solutes", *Phytochemistry*, Vol. 28, No. 4, pp. 1057–1060, Jan. 1989.

160. Stoop, J. M. H., J. D. Williamson and D. Mason Pharr, "Mannitol metabolism in plants: a method for coping with stress", *Trends in Plant Science*, Vol. 1, No. 5, pp. 139–144, May 1996.

161. Hellebusi, J. A., "Osmoregulation", *Annual Review of Plant Physiology*, Vol. 27, No. 1, pp. 485–505, Jun. 1976.

162. Ahmad, P., M. A. Ahanger, M. N. Alyemeni, L. Wijaya, D. Egamberdieva, R. Bhardwaj and M. Ashraf, "Zinc application mitigates the adverse effects of NaCl stress on mustard [Brassica juncea (L.) Czern & Coss] through modulating compatible organic solutes, antioxidant enzymes, and flavonoid content", *Journal of Plant Interactions*, Vol. 12, No. 1, pp. 429–437, Jan. 2017.

163. Bagci, S. A., H. Ekiz, A. Yilmaz and I. Cakmak, "Effects of zinc deficiency and drought on grain yield of field-grown wheat cultivars in central Anatolia", *Journal of Agronomy and Crop Science*, Vol. 193, No. 3, pp. 198–206, 2007.

164. McCall, K. A., C.-c. Huang and C. A. Fierke, "Function and mechanism of zinc

metalloenzymes", *The Journal of Nutrition*, Vol. 130, No. 5, pp. 1437S–1446S, May 2000.

165. Shi, H., W. Liu, Y. Yao, Y. Wei and Z. Chan, "Alcohol dehydrogenase 1 (ADH1) confers both abiotic and biotic stress resistance in Arabidopsis", *Plant Science*, Vol. 262, pp. 24–31, Sep. 2017.

166. Yu, S., X. Zhang, Q. Guan, T. Takano and S. Liu, "Expression of a carbonic anhydrase gene is induced by environmental stresses in Rice (Oryza sativa L.)", *Biotechnology Letters*, Vol. 29, No. 1, pp. 89–94, Jan. 2007.

167. Bowler, C., M. V. Montagu and D. Inze, "Superoxide dismutase and stress tolerance", *Annual Review of Plant Physiology and Plant Molecular Biology*, Vol. 43, No. 1, pp. 83–116, Jun. 1992.

168. Gavalas, N. A. and H. E. Clark, "On the role of manganese in photosynthesis: Kinetics of photoinhibition in manganese-deficent and 3-(4-Chlorophenyl)-1, 1-dimethylurea-inhibited *Euglena gracilis*", *Plant Physiology*, Vol. 47, No. 1, pp. 139–143, Jan. 1971.

169. Husted, S., K. H. Laursen, C. A. Hebbern, S. B. Schmidt, P. Pedas, A. Haldrup and P. E. Jensen, "Manganese deficiency leads to genotype-specific changes in fluorescence induction kinetics and state transitions", *Plant Physiology*, Vol. 150, No. 2, pp. 825–833, Jun. 2009.

170. Schmidt, S. B., D. P. Persson, M. Powikrowska, J. Frydenvang, J. K. Schjoerring, P. E. Jensen and S. Husted, "Metal binding in photosystem II super- and subcomplexes from barley thylakoids", *Plant Physiology*, Vol. 168, No. 4, pp. 1490–1502, Aug. 2015.

171. Batista-Silva, W., B. Heinemann, N. Rugen, A. Nunes[U+2010]Nesi, W. L. Araújo, H.-P. Braun and T. M. Hildebrandt, "The role of amino acid metabolism

during abiotic stress release", *Plant, Cell & Environment*, Vol. 42, No. 5, pp. 1630–1644, 2019.

172. Pires, M. V., A. A. P. Júnior, D. B. Medeiros, D. M. Daloso, P. A. Pham, K. A. Barros, M. K. M. Engqvist, A. Florian, I. Krahnert, V. G. Maurino, W. L. Araújo and A. R. Fernie, "The influence of alternative pathways of respiration that utilize branched-chain amino acids following water shortage in Arabidopsis", *Plant, Cell & Environment*, Vol. 39, No. 6, pp. 1304–1319, 2016.

173. Fujiki, Y., M. Ito, T. Itoh, I. Nishida and A. Watanabe, "Activation of the promoters of Arabidopsis genes for the branched-chain α-keto acid dehydrogenase complex in transgenic tobacco BY-2 cells under sugar starvation", *Plant and Cell Physiology*, Vol. 43, No. 3, pp. 275–280, Mar. 2002.

174. Yadav, A. K., A. J. Carroll, G. M. Estavillo, G. J. Rebetzke and B. J. Pogson, "Wheat drought tolerance in the field is predicted by amino acid responses to glasshouse-imposed drought", *Journal of Experimental Botany*, Vol. 70, No. 18, pp. 4931–4948, Sep. 2019, publisher: Oxford Academic.

175. You, J., Y. Zhang, A. Liu, D. Li, X. Wang, K. Dossa, R. Zhou, J. Yu, Y. Zhang, L. Wang and X. Zhang, "Transcriptomic and metabolomic profiling of drought-tolerant and susceptible sesame genotypes in response to drought stress", *BMC Plant Biology*, Vol. 19, No. 1, p. 267, Jun. 2019.

176. Arruda, P., E. L. Kemper, F. Papes and A. Leite, "Regulation of lysine catabolism in higher plants", *Trends in Plant Science*, Vol. 5, No. 8, pp. 324–330, Aug. 2000.

177. Azevedo, R. A., C. Damerval, J. Landry, P. J. Lea, C. M. Bellato, L. W. Meinhardt, M. L. Guilloux, S. Delhaye, A. A. Toro, S. A. Gaziola and B. D. A. Berdejo, "Regulation of maize lysine metabolism and endosperm protein synthesis by opaque and floury mutations", *European Journal of Biochemistry*, Vol. 270, No. 24, pp. 4898–4908, 2003.

178. Kiyota, E., I. A. Pena and P. Arruda, "The saccharopine pathway in seed development and stress response of maize", *Plant, Cell & Environment*, Vol. 38, No. 11, pp. 2450–2461, 2015.

179. Markovitz, P. J. and D. T. Chuang, "The bifunctional aminoadipic semialdehyde synthase in lysine degradation. Separation of reductase and dehydrogenase domains by limited proteolysis and column chromatography.", *Journal of Biological Chemistry*, Vol. 262, No. 19, pp. 9353–9358, Jul. 1987.

180. Michaletti, A., M. R. Naghavi, M. Toorchi, L. Zolla and S. Rinalducci, "Metabolomics and proteomics reveal drought-stress responses of leaf tissues from spring-wheat", *Scientific Reports*, Vol. 8, No. 1, p. 5710, Apr. 2018.

181. Moulin, M., C. Deleu, F. Larher and A. Bouchereau, "The lysine-ketoglutarate reductase–saccharopine dehydrogenase is involved in the osmo-induced synthesis of pipecolic acid in rapeseed leaf tissues", *Plant Physiology and Biochemistry*, Vol. 44, No. 7, pp. 474–482, Jul. 2006.

182. Brandt, A. B., "In vivo incorporation of [14C] lysine into the endosperm proteins of wild type and high-lysine barley", *FEBS Letters*, Vol. 52, No. 2, pp. 288–291, 1975.

183. Lawrence, J. M. and D. R. Grant, "Incorporation of lysine-C14 into the developing grain of wheat", *Archives of Biochemistry and Biophysics*, Vol. 104, No. 1, pp. 73–78, Jan. 1964.

184. Sodek, L. and C. M. Wilson, "Incorporation of leucine-14C and lysine-14C into protein in the developing endosperm of nomal and opaque-2 corn", *Archives of Biochemistry and Biophysics*, Vol. 140, No. 1, pp. 29–38, Sep. 1970.

185. Hildebrandt, T., A. Nunes Nesi, W. Araújo and H.-P. Braun, "Amino acid catabolism in plants", *Molecular Plant*, Vol. 8, No. 11, pp. 1563–1579, Nov. 2015.

186. Ramos, M. L. G., R. Parsons and J. I. Sprent, "Differences in ureide and amino acid content of water stressed soybean inoculated with Bradyrhizobium japonicum and B. elkanii", *Pesquisa Agropecuária Brasileira*, Vol. 40, No. 5, pp. 453–458, May 2005.

187. Lei, P., X. Pang, X. Feng, S. Li, B. Chi, R. Wang, Z. Xu and H. Xu, "The microbe-secreted isopeptide poly-γ-glutamic acid induces stress tolerance in Brassica napus L. seedlings by activating crosstalk between H 2 O 2 and Ca 2+", *Scientific Reports*, Vol. 7, No. 1, p. 41618, Feb. 2017.

188. Kan, C.-C., T.-Y. Chung, H.-Y. Wu, Y.-A. Juo and M.-H. Hsieh, "Exogenous glutamate rapidly induces the expression of genes involved in metabolism and defense responses in rice roots", *BMC Genomics*, Vol. 18, No. 1, p. 186, Feb. 2017.

189. Qiu, X.-M., Y.-Y. Sun, X.-Y. Ye and Z.-G. Li, "Signaling role of glutamate in plants", *Frontiers in Plant Science*, Vol. 10, 2020.

190. Yoshida, R., I. C. Mori, N. Kamizono, Y. Shichiri, T. Shimatani, F. Miyata, K. Honda and S. Iwai, "Glutamate functions in stomatal closure in Arabidopsis and fava bean", *Journal of Plant Research*, Vol. 129, No. 1, pp. 39–49, Jan. 2016.

191. Lu, S. C., "Glutathione synthesis", *Biochimica et Biophysica Acta (BBA) - General Subjects*, Vol. 1830, No. 5, pp. 3143–3153, May 2013.

192. Kan, C.-C., T.-Y. Chung, Y.-A. Juo and M.-H. Hsieh, "Glutamine rapidly induces the expression of key transcription factor genes involved in nitrogen and stress responses in rice roots", *BMC Genomics*, Vol. 16, No. 1, p. 731, Sep. 2015.

193. James, D., B. Borphukan, D. Fartyal, B. Ram, J. Singh, M. Manna, V. Sheri, V. Panditi, R. Yadav, V. M. M. Achary and M. K. Reddy, "Concurrent overexpression of OsGS1;1 and OsGS2 genes in transgenic rice (Oryza sativa L.): Impact

on tolerance to abiotic stresses", *Frontiers in Plant Science*, Vol. 9, 2018.

194. Lee, H. J., S. E. Abdula, D. W. Jang, S.-H. Park, U.-H. Yoon, Y. J. Jung, K. K. Kang, I. S. Nou and Y.-G. Cho, "Overexpression of the glutamine synthetase gene modulates oxidative stress response in rice after exposure to cadmium stress", *Plant Cell Reports*, Vol. 32, No. 10, pp. 1521–1529, Oct. 2013.

195. Masclaux-Daubresse, C., M. Reisdorf-Cren, K. Pageau, M. Lelandais, O. Grandjean, J. Kronenberger, M.-H. Valadier, M. Feraud, T. Jouglet and A. Suzuki, "Glutamine synthetase-glutamate synthase pathway and glutamate dehydrogenase play distinct roles in the sink-source nitrogen cycle in tobacco", *Plant Physiology*, Vol. 140, No. 2, pp. 444–456, Feb. 2006.

196. Zhang, Z., S. Xiong, Y. Wei, X. Meng, X. Wang and X. Ma, "The role of glutamine synthetase isozymes in enhancing nitrogen use efficiency of N-efficient winter wheat", *Scientific Reports*, Vol. 7, No. 1, p. 1000, Apr. 2017.

197. Lea, P. J., L. Sodek, M. a. J. Parry, P. R. Shewry and N. G. Halford, "Asparagine in plants", *Annals of Applied Biology*, Vol. 150, No. 1, pp. 1–26, 2007.

198. Pate, J. S., "Transport and partitioning of nitrogenous solutes", *Annual Review of Plant Physiology*, Vol. 31, No. 1, pp. 313–340, 1980.

199. Debouba, M., H. Gouia, A. Suzuki and M. H. Ghorbel, "NaCl stress effects on enzymes involved in nitrogen assimilation pathway in tomato "Lycopersicon esculentum" seedlings", *Journal of Plant Physiology*, Vol. 163, No. 12, pp. 1247–1258, Dec. 2006.

200. Gouia, H., M. H. Ghorbal and B. Touraine, "Effects of NaCl on flows of N and mineral ions and on NO3- reduction rate within whole plants of salt-sensitive bean and salt-tolerant cotton", *Plant Physiology*, Vol. 105, No. 4, pp. 1409–1418, Aug. 1994.

201. Gupta, B. and B. Huang, "Mechanism of salinity tolerance in plants: Physiological, biochemical, and molecular characterization", *International Journal of Genomics*, Vol. 2014, pp. 1–18, 2014.

202. Sytar, O., S. Mbarki, M. Zivcak and M. Brestic, "The involvement of different secondary metabolites in salinity tolerance of crops", V. Kumar, S. H. Wani, P. Suprasanna and L.-S. P. Tran (Editors), *Salinity Responses and Tolerance in Plants, Volume 2: Exploring RNAi, Genome Editing and Systems Biology*, pp. 21–48, Springer International Publishing, Cham, 2018.

203. Degenhardt, J., T. G. Köllner and J. Gershenzon, "Monoterpene and sesquiterpene synthases and the origin of terpene skeletal diversity in plants", *Phytochemistry*, Vol. 70, No. 15, pp. 1621–1637, Oct. 2009.

204. Bourgaud, F., A. Gravot, S. Milesi and E. Gontier, "Production of plant secondary metabolites: a historical perspective", *Plant Science*, Vol. 161, No. 5, pp. 839–851, Oct. 2001.

205. Harborne, J. B., "Classes and functions of secondary products from plants", *Chemicals from Plants*, pp. 1–25, World Scientific / Imperial College Press, Mar. 1999.

206. Vaughan, M. M., S. Christensen, E. A. Schmelz, A. Huffaker, H. J. Mcauslane, H. T. Alborn, M. Romero, L. H. Allen and P. E. A. Teal, "Accumulation of terpenoid phytoalexins in maize roots is associated with drought tolerance", *Plant, Cell & Environment*, Vol. 38, No. 11, pp. 2195–2207, 2015.

207. Loreto, F., P. Ciccioli, A. Cecinato, E. Brancaleoni, M. Frattoni, C. Fabozzi and D. Tricoli, "Evidence of the photosynthetic origin of monoterpenes emitted by Quercus ilex L. leaves by 13C labeling", *Plant Physiology*, Vol. 110, No. 4, pp. 1317–1322, Apr. 1996.

208. Sharkey, T. D., E. L. Singsaas, P. J. Vanderveer and C. Geron, "Field measurements of isoprene emission from trees in response to temperature and light", *Tree Physiology*, Vol. 16, No. 7, pp. 649–654, Jul. 1996.

209. Kleine, S. and C. Müller, "Drought stress and leaf herbivory affect root terpenoid concentrations and growth of Tanacetum vulgare", *Journal of Chemical Ecology*, Vol. 40, No. 10, pp. 1115–1125, Oct. 2014.

210. Nogués, I., M. Medori and C. Calfapietra, "Limitations of monoterpene emissions and their antioxidant role in Cistus sp. under mild and severe treatments of drought and warming", *Environmental and Experimental Botany*, Vol. 119, pp. 76–86, Nov. 2015.

211. Peñuelas, J., I. Filella, R. Seco and J. Llusià, "Increase in isoprene and monoterpene emissions after re-watering of droughted Quercus ilex seedlings", *Biologia Plantarum*, Vol. 53, No. 2, pp. 351–354, Jun. 2009.

212. Šimpraga, M., H. Verbeeck, M. Demarcke, O. Pokorska, C. Amelynck, N. Schoon, J. Dewulf, H. Van Langenhove, B. Heinesch, M. Aubinet, Q. Laffineur, J. F. Müller and K. Steppe, "Clear link between drought stress, photosynthesis and biogenic volatile organic compounds in Fagus sylvatica L.", *Atmospheric Environment*, Vol. 45, No. 30, pp. 5254–5259, Sep. 2011.

213. Isah, T., "Stress and defense responses in plant secondary metabolites production", *Biological Research*, Vol. 52, No. 1, p. 39, Dec. 2019.

214. Centritto, M., F. Loreto and K. Chartzoulakis, "The use of low CO2 to estimate diffusional and non-diffusional limitations of photosynthetic capacity of salt-stressed olive saplings", *Plant, Cell and Environment*, Vol. 26, No. 4, pp. 585–594, Apr. 2003.

215. Flowers, T. J., "Salt tolerance in Suaeda maritima (L.) Dum: A comparison

of mitochondria isolated from green tissues of Sueada and Pisum", *Journal of Experimental Botany*, Vol. 25, No. 1, pp. 101–110, Feb. 1974.

216. Jacoby, R. P., N. L. Taylor and A. H. Millar, "The role of mitochondrial respiration in salinity tolerance", *Trends in Plant Science*, Vol. 16, No. 11, pp. 614–623, Nov. 2011.

217. Kasai, K., H. Fukayama, N. Uchida, N. Mori, T. Yasuda, Y. Oji and C. Nakamura, "Salinity tolerance in Triticum aestivum-Lophopyrum elongatum amphiploid and 5E disomic addition line evaluated by NaCl effects on photosynthesis and respiration", *Cereal Research Communications*, Vol. 26, No. 3, pp. 281–287, Sep. 1998.

218. Bondy, S. C., "Ethanol toxicity and oxidative stress", *Toxicology Letters*, Vol. 63, No. 3, pp. 231–241, Dec. 1992.

219. Zhang, M., S. Nagata, K. Miyazawa, H. Kikuchi and Y. Esashi, "A Competitive enzyme-linked immunosorbent assay to quantify acetaldehyde-protein adducts that accumulate in dry seeds during aging", *Plant Physiology*, Vol. 113, No. 2, pp. 397–402, Feb. 1997.

220. Conley, T. R., H.-P. Peng and M.-C. Shih, "Mutations affecting induction of glycolytic and fermentative genes during germination and environmental stresses in Arabidopsis", *Plant Physiology*, Vol. 119, No. 2, pp. 599–608, Feb. 1999.

221. Yi, S. Y., S. S. Ku, H.-J. Sim, S.-K. Kim, J. H. Park, J. I. Lyu, E. J. So, S. Y. Choi, J. Kim, M. S. Ahn, S. W. Kim, H. Park, W. J. Jeong, Y. P. Lim, S. R. Min and J. R. Liu, "An alcohol dehydrogenase gene from Synechocystis sp. confers salt tolerance in transgenic tobacco", *Frontiers in Plant Science*, Vol. 8, p. 1965, Nov. 2017.

222. Alpaslan, M., E. Boydak, M. Hayta, S. Gerçek and M. Simsek, "Effect of row

space and irrigation on seed composition of Turkish sesame (Sesamum indicum L.)", *Journal of the American Oil Chemists' Society*, Vol. 78, No. 9, pp. 933–935, Sep. 2001.

223. Yordanov, I., V. Velikova and T. Tsonev, "Plant responses to drought, acclimation, and stress tolerance", *Photosynthetica*, Vol. 38, No. 2, pp. 171–186, Nov. 2000.

224. Sun, X., C. Hu, Q. Tan, J. Liu and H. Liu, "Effects of molybdenum on expression of cold-responsive genes in abscisic acid (ABA)-dependent and ABA-independent pathways in winter wheat under low-temperature stress", *Annals of Botany*, Vol. 104, No. 2, pp. 345–356, Aug. 2009.

225. Sun, X., Q. Tan, Z. Nie, C. Hu and Y. An, "Differential expression of proteins in response to molybdenum deficiency in winter wheat leaves under low-temperature stress", *Plant Molecular Biology Reporter*, Vol. 32, No. 5, pp. 1057–1069, Oct. 2014.

226. Wu, S., C. Hu, Q. Tan, Z. Nie and X. Sun, "Effects of molybdenum on water utilization, antioxidative defense system and osmotic-adjustment ability in winter wheat (Triticum aestivum) under drought stress", *Plant Physiology and Biochemistry*, Vol. 83, pp. 365–374, Oct. 2014.

227. Zhang, M., C. Hu, X. Zhao, Q. Tan, X. Sun, A. Cao, M. Cui and Y. Zhang, "Molybdenum improves antioxidant and osmotic-adjustment ability against salt stress in Chinese cabbage (Brassica campestris L. ssp. Pekinensis)", *Plant and Soil*, Vol. 355, No. 1, pp. 375–383, Jun. 2012.

228. Zhang, M., C. Hu, X. Sun, X. Zhao, Q. Tan, Y. Zhang and N. Li, "Molybdenum affects photosynthesis and ionic homeostasis of Chinese cabbage under salinity stress", *Communications in Soil Science and Plant Analysis*, Vol. 45, No. 20, pp. 2660–2672, Nov. 2014.

229. Gibson, S. I., "Control of plant development and gene expression by sugar signaling", *Current Opinion in Plant Biology*, Vol. 8, No. 1, pp. 93–102, Feb. 2005.

230. Rosa, M., C. Prado, G. Podazza, R. Interdonato, J. A. González, M. Hilal and F. E. Prado, "Soluble sugars: Metabolism, sensing and abiotic stress: A complex network in the life of plants", *Plant Signaling & Behavior*, Vol. 4, No. 5, pp. 388–393, May 2009.

231. Braun, D. M., L. Wang and Y.-L. Ruan, "Understanding and manipulating sucrose phloem loading, unloading, metabolism, and signalling to enhance crop yield and food security", *Journal of Experimental Botany*, Vol. 65, No. 7, pp. 1713–1735, Apr. 2014.

232. Hennion, N., M. Durand, C. Vriet, J. Doidy, L. Maurousset, R. Lemoine and N. Pourtau, "Sugars en route to the roots. Transport, metabolism and storage within plant roots and towards microorganisms of the rhizosphere", *Physiologia Plantarum*, Vol. 165, No. 1, pp. 44–57, Jan. 2019.

233. Weber, H., L. Borisjuk and U. Wobus, "Sugar import and metabolism during seed development", *Trends in Plant Science*, Vol. 2, No. 5, pp. 169–174, May 1997.

234. Cheng, W.-H. and P. S. Chourey, "Genetic evidence that invertase-mediated release of hexoses is critical for appropriate carbon partitioning and normal seed development in maize:", *Theoretical and Applied Genetics*, Vol. 98, No. 3-4, pp. 485–495, Mar. 1999.

235. Babb, V. M. and C. H. Haigler, "Sucrose phosphate synthase activity rises in correlation with high-rate cellulose synthesis in three heterotrophic systems", *Plant Physiology*, Vol. 127, No. 3, pp. 1234–1242, Nov. 2001.

236. Birmingham, A., E. M. Anderson, A. Reynolds, D. Ilsley-Tyree, D. Leake, Y. Fedorov, S. Baskerville, E. Maksimova, K. Robinson, J. Karpilow, W. S. Marshall

and A. Khvorova, "3′ UTR seed matches, but not overall identity, are associated with RNAi off-targets", *Nature Methods*, Vol. 3, No. 3, pp. 199–204, Mar. 2006.

237. Jackson, A. L., "Widespread siRNA "off-target" transcript silencing mediated by seed region sequence complementarity", *RNA*, Vol. 12, No. 7, pp. 1179–1187, May 2006.

238. Saxena, S., Z. O. Jónsson and A. Dutta, "Small RNAs with imperfect match to endogenous mRNA repress translation", *Journal of Biological Chemistry*, Vol. 278, No. 45, pp. 44312–44319, Nov. 2003.

239. Aleman, L. M., J. Doench and P. A. Sharp, "Comparison of siRNA-induced off-target RNA and protein effects", *RNA*, Vol. 13, No. 3, pp. 385–395, Feb. 2007.

240. Chiou, T.-J. and D. R. Bush, "Sucrose is a signal molecule in assimilate partitioning", *Proceedings of the National Academy of Sciences*, Vol. 95, No. 8, pp. 4784–4788, Apr. 1998.

241. Moore, B., "Role of the Arabidopsis glucose sensor HXK1 in nutrient, light, and hormonal signaling", *Science*, Vol. 300, No. 5617, pp. 332–336, Apr. 2003.

242. Sarowar, S., J. Y. Lee, E. R. Ahn and H. S. Pai, "A role of hexokinases in plant resistance to oxidative stress and pathogen infection", *Journal of Plant Biology*, Vol. 51, No. 5, pp. 341–346, Sep. 2008.

243. Cho, J.-I., N. Ryoo, J.-S. Eom, D.-W. Lee, H.-B. Kim, S.-W. Jeong, Y.-H. Lee, Y.-K. Kwon, M.-H. Cho, S. H. Bhoo, T.-R. Hahn, Y.-I. Park, I. Hwang, J. Sheen and J.-S. Jeon, "Role of the rice hexokinases OsHXK5 and OsHXK6 as Glucose Sensors", *Plant Physiology*, Vol. 149, No. 2, pp. 745–759, Feb. 2009.

244. Tauzin, A. S. and T. Giardina, "Sucrose and invertases, a part of the plant defense response to the biotic stresses", *Frontiers in Plant Science*, Vol. 5, 2014.

245. Martínez-Noël, G. M. and J. A. Tognetti, "Sugar signaling under abiotic stress in plants", *Plant Metabolites and Regulation Under Environmental Stress*, pp. 397–406, Elsevier, 2018.

246. Ahmad, I. Z., "Role of sugars in abiotic stress signaling in plants", *Plant Signaling Molecules*, pp. 207–217, Elsevier, 2019.

247. Koch, K. E., K. D. Nolte, E. R. Duke, D. R. McCarty and W. T. Avigne, "Sugar levels modulate differential expression of Maize sucrose synthase genes", *The Plant Cell*, pp. 59–69, Jan. 1992.

248. Roitsch, T., M. Bittner and D. E. Godt, "Induction of apoplastic invertase of Chenopodium rubrum by D-glucose and a glucose analog and tissue-specific expression suggest a role in sink-source Regulation", *Plant Physiology*, Vol. 108, No. 1, pp. 285–294, May 1995.

249. Stitt, M. and V. Hurry, "A plant for all seasons: alterations in photosynthetic carbon metabolism during cold acclimation in Arabidopsis", *Current Opinion in Plant Biology*, Vol. 5, No. 3, pp. 199–206, Jun. 2002.

250. Slama, I., C. Abdelly, A. Bouchereau, T. Flowers and A. Savouré, "Diversity, distribution and roles of osmoprotective compounds accumulated in halophytes under abiotic stress", *Annals of Botany*, Vol. 115, No. 3, pp. 433–447, Feb. 2015.

251. Franz, S. L. and T. A. Tattar, "Effect of sugars and amino acids on membrane potential in two clones of sugarcane", *Plant Physiology*, Vol. 67, No. 1, pp. 150–155, Jan. 1981.

252. Geiger, M., M. Stitt and P. Geigenberger, "Metabolism in slices from growing potato tubers responds differently to addition of sucrose and glucose", *Planta*, Vol. 206, No. 2, pp. 234–244, Aug. 1998.

253. Miedema, H., J. H. Bothwell, C. Brownlee and J. M. Davies, "Calcium uptake

by plant cells – channels and pumps acting in concert", *Trends in Plant Science*, Vol. 6, No. 11, pp. 514–519, Nov. 2001.

254. Miedema, H., V. Demidchik, A. Véry, J. H. F. Bothwell, C. Brownlee and J. M. Davies, "Two voltage[U+2010]dependent calcium channels co[U+2010]exist in the apical plasma membrane of *Arabidopsis thaliana* root hairs", *New Phytologist*, Vol. 179, No. 2, pp. 378–385, Jul. 2008.

255. Mito, N., L. E. Wimmers and A. B. Bennett, "Sugar regulates mRNA abundance of H+-ATPase gene family members in tomato", *Plant Physiology*, Vol. 112, No. 3, pp. 1229–1236, Nov. 1996.

256. Nieves-Cordones, M., F. Alemán, V. Martínez and F. Rubio, "K+ uptake in plant roots. The systems involved, their regulation and parallels in other organisms", *Journal of Plant Physiology*, Vol. 171, No. 9, pp. 688–695, May 2014.

257. Roden, L. C. and R. A. Ingle, "Lights, rhythms, infection: The role of light and the circadian clock in determining the outcome of plant–pathogen interactions", *The Plant Cell*, Vol. 21, No. 9, pp. 2546–2552, Sep. 2009.

258. Bolouri Moghaddam, M. R. and W. Van den Ende, "Sweet immunity in the plant circadian regulatory network", *Journal of Experimental Botany*, Vol. 64, No. 6, pp. 1439–1449, Apr. 2013.

259. Haydon, M. J., O. Mielczarek, F. C. Robertson, K. E. Hubbard and A. A. R. Webb, "Photosynthetic entrainment of the Arabidopsis thaliana circadian clock", *Nature*, Vol. 502, No. 7473, pp. 689–692, Oct. 2013.

260. Voß, U., M. H. Wilson, K. Kenobi, P. D. Gould, F. C. Robertson, W. A. Peer, M. Lucas, K. Swarup, I. Casimiro, T. J. Holman, D. M. Wells, B. Péret, T. Goh, H. Fukaki, T. C. Hodgman, L. Laplaze, K. J. Halliday, K. Ljung, A. S. Murphy, A. J. Hall, A. A. R. Webb and M. J. Bennett, "The circadian clock rephases during

lateral root organ initiation in Arabidopsis thaliana", *Nature Communications*, Vol. 6, No. 1, p. 7641, Nov. 2015.

261. Marten, I., G. Lohse and R. Hedrich, "Plant growth hormones control voltage-dependent activity of anion channels in plasma membrane of guard cells", *Nature*, Vol. 353, No. 6346, pp. 758–762, Oct. 1991.

262. Lohse, G. and R. Hedrich, "Characterization of the plasma-membrane H+-ATPase from Vicia faba guard cells: Modulation by extracellular factors and seasonal changes", *Planta*, Vol. 188, No. 2, pp. 206–214, Sep. 1992.

263. Philippar, K., I. Fuchs, H. Luthen, S. Hoth, C. S. Bauer, K. Haga, G. Thiel, K. Ljung, G. Sandberg, M. Bottger, D. Becker and R. Hedrich, "Auxin-induced K+ channel expression represents an essential step in coleoptile growth and gravitropism", *Proceedings of the National Academy of Sciences*, Vol. 96, No. 21, pp. 12186–12191, Oct. 1999.

264. Shishova, M. and S. Lindberg, "Auxin induces an increase of Ca2+ concentration in the cytosol of wheat leaf protoplasts", *Journal of Plant Physiology*, Vol. 161, No. 8, pp. 937–945, Aug. 2004.

265. Kirpichnikova, A., E. Rudashevskaya, V. Yemelyanov and M. Shishova, "Ca2+-transport through plasma membrane as a test of auxin sensitivity", *Plants*, Vol. 3, No. 2, pp. 209–222, Mar. 2014.

266. Tang, R.-J. and S. Luan, "Regulation of calcium and magnesium homeostasis in plants: from transporters to signaling network", *Current Opinion in Plant Biology*, Vol. 39, pp. 97–105, Oct. 2017.

267. Epstein, E., "The essential role of calcium in selective cation transport by plant cells", *Plant Physiology*, Vol. 36, No. 4, pp. 437–444, Jul. 1961.

268. Rains, D. W. and E. Epstein, "Sodium absorption by Barley roots: Its mediation

by mechanism 2 of alkali cation transport", *Plant Physiology*, Vol. 42, No. 3, pp. 319–323, Mar. 1967.

269. Zhu, J.-K., "Salt and drought stress signal transduction in plants", *Annual Review of Plant Biology*, Vol. 53, No. 1, pp. 247–273, Jun. 2002.

270. James, A. B., J. A. Monreal, G. A. Nimmo, C. L. Kelly, P. Herzyk, G. I. Jenkins and H. G. Nimmo, "The circadian clock in Arabidopsis roots is a simplified slave version of the clock in shoots", *Science*, Vol. 322, No. 5909, pp. 1832–1835, Dec. 2008.

271. Ivashikina, N., R. Deeken, S. Fischer, P. Ache and R. Hedrich, "AKT2/3 subunits render guard cell K+ channels Ca2+ sensitive", *Journal of General Physiology*, Vol. 125, No. 5, pp. 483–492, May 2005.

272. Cheong, Y. H., G. K. Pandey, J. J. Grant, O. Batistic, L. Li, B.-G. Kim, S.-C. Lee, J. Kudla and S. Luan, "Two calcineurin B-like calcium sensors, interacting with protein kinase CIPK23, regulate leaf transpiration and root potassium uptake in Arabidopsis: CBL-CIPK network in drought and low-K responses", *The Plant Journal*, Vol. 52, No. 2, pp. 223–239, Aug. 2007.

273. Lan, W.-Z., S.-C. Lee, Y.-F. Che, Y.-Q. Jiang and S. Luan, "Mechanistic analysis of AKT1 regulation by the CBL–CIPK–PP2CA interactions", *Molecular Plant*, Vol. 4, No. 3, pp. 527–536, May 2011.

274. Ren, X.-L., G.-N. Qi, H.-Q. Feng, S. Zhao, S.-S. Zhao, Y. Wang and W.-H. Wu, "Calcineurin B-like protein CBL10 directly interacts with AKT1 and modulates K+ homeostasis in Arabidopsis", *The Plant Journal*, Vol. 74, No. 2, pp. 258–266, Apr. 2013.

275. Masuda, T., "Recent overview of the Mg branch of the tetrapyrrole biosynthesis leading to chlorophylls", *Photosynthesis Research*, Vol. 96, No. 2, pp. 121–143,

May 2008.

276. Portis, A. R. and Jr., "Rubisco activase – rubisco's catalytic chaperone", *Photosynthesis Research*, Vol. 75, No. 1, pp. 11–27, 2003.

277. Kwon, M. C., Y. X. Kim, S. Lee, E. S. Jung, D. Singh, J. Sung and C. H. Lee, "Comparative metabolomics unravel the effect of magnesium oversupply on tomato fruit quality and associated plant metabolism", *Metabolites*, Vol. 9, No. 10, p. 231, Oct. 2019.

278. Wang, Q., S. Yang, S. Wan and X. Li, "The significance of calcium in photosynthesis", *International Journal of Molecular Sciences*, Vol. 20, No. 6, p. 1353, Mar. 2019.

279. Stael, S., B. Wurzinger, A. Mair, N. Mehlmer, U. C. Vothknecht and M. Teige, "Plant organellar calcium signalling: an emerging field", *Journal of Experimental Botany*, Vol. 63, No. 4, pp. 1525–1542, Feb. 2012.

280. Parre, E., M. A. Ghars, A.-S. Leprince, L. Thiery, D. Lefebvre, M. Bordenave, L. Richard, C. Mazars, C. Abdelly and A. Savouré, "Calcium signaling via phospholipase C is essential for proline accumulation upon ionic but not nonionic hyperosmotic stresses in Arabidopsis", *Plant Physiology*, Vol. 144, No. 1, pp. 503–512, May 2007.

281. de Azevedo Neto, A. D., J. T. Prisco, J. Enéas-Filho, C. E. B. d. Abreu and E. Gomes-Filho, "Effect of salt stress on antioxidative enzymes and lipid peroxidation in leaves and roots of salt-tolerant and salt-sensitive maize genotypes", *Environmental and Experimental Botany*, Vol. 56, No. 1, pp. 87–94, May 2006.

282. Noctor, G., "Drought and oxidative load in the leaves of C3 plants: A predominant role for photorespiration?", *Annals of Botany*, Vol. 89, No. 7, pp. 841–850, Jun. 2002.

283. Laxa, M., M. Liebthal, W. Telman, K. Chibani and K.-J. Dietz, "The role of the plant antioxidant system in drought tolerance", *Antioxidants*, Vol. 8, No. 4, p. 94, Apr. 2019.

284. Öztürk, L. and Y. Demir, "In vivo and in vitro protective role of proline", *Plant Growth Regulation*, Vol. 38, No. 3, pp. 259–264, 2002.

285. Gill, S. S. and N. Tuteja, "Reactive oxygen species and antioxidant machinery in abiotic stress tolerance in crop plants", *Plant Physiology and Biochemistry*, Vol. 48, No. 12, pp. 909–930, Dec. 2010.

286. Ben Amor, N., W. Megdiche, A. Jiménez, F. Sevilla and C. Abdelly, "The effect of calcium on the antioxidant systems in the halophyte Cakile maritima under salt stress", *Acta Physiologiae Plantarum*, Vol. 32, No. 3, pp. 453–461, May 2010.

287. Seifikalhor, M., S. Aliniaeifard, A. Shomali, N. Azad, B. Hassani, O. Lastochkina and T. Li, "Calcium signaling and salt tolerance are diversely entwined in plants", *Plant Signaling & Behavior*, Vol. 14, No. 11, p. 1665455, Nov. 2019.

288. Blokhina, O., "Antioxidants, oxidative damage and oxygen deprivation stress: A review", *Annals of Botany*, Vol. 91, No. 2, pp. 179–194, Jan. 2003.

APPENDIX A: SUPPLEMENTARY INFORMATION FOR THE OMICS STUDY

Table A.1. Leaf specific genes for intensity difference analysis. FC: Fold change.

ID	IL $\log_2$ FC	TL $\log_2$ FC	Annotation
Phvul.001G004900	-3.63	0	Domain of unknown function
Phvul.001G021750	-3.50	0	EF hand
Phvul.001G026700	-2.39	0	Zinc finger protein AZF3-related
Phvul.001G048600	-3.67	0	Protein kinase domain
Phvul.001G126700	-3.41	0	Calcium-binding protein CML24-related
Phvul.001G155150	-5.06	0	Cation transporting atpase, c-terminus
Phvul.001G155201	-5.51	0	E1-E2 ATPase
Phvul.001G165200	6.62	0	Photosystem II 13kda protein
Phvul.001G220100	-3.60	0	Cathepsin B
Phvul.001G225000	-2.64	0	Nicotianamine synthase
Phvul.001G242100	3.47	0	Chlorophyll a-b binding protein CP29.3
Phvul.002G025600	3.39	0	Quinate o-hydroxycinnamoyltransferase
Phvul.002G083600	4.06	0	Pollen allergen
Phvul.002G122600	3.62	0	Long-chain-alcohol oxidase FAO4a
Phvul.002G155300	3.51	0	Heat stress transcription factor b-2b
Phvul.002G196200	-7.55	0	LRR receptor-like serine/threonine-protein kinase FLS2
Phvul.002G235600	-2.84	0	Amino acid transporter
Phvul.002G275000	-3.56	0	NAC domain-containing protein 2
Phvul.002G285100	4.18	0	11-beta-hydroxysteroid dehydrogenase
Phvul.002G285600	3.67	0	Farnesylated protein 3-related
Phvul.002G292900	-2.62	0	Copper transport protein ATOX1-related
Phvul.002G306200	-2.71	0	Inositol oxygenase
Phvul.003G050600	6.26	0	Protein eceriferum 26-related
Phvul.003G061900	6.62	0	Angiotensin-converting enzyme 2
Phvul.003G101100	-3.47	0	Nitrate, fromate, iron dehydrogenase
Phvul.003G140200	-3.33	0	E1-E2 ATPase
Phvul.003G149500	-3.93	0	Glutamate receptor 2.5-related
Phvul.003G151700	4.37	0	EamA-like transporter family

Table A.1. Leaf specific genes for intensity difference analysis. (cont.)

Phvul.003G228000	-2.79	0	Pollen allergen
Phvul.004G021000	-3.2512409999999998	0	Matrilysin

Table A.1. Leaf specific genes for intensity difference analysis. (cont.)

ID	IL $\log_2$ FC	TL $\log_2$ FC	Annotation
Phvul.004G029100	4.47	0	Starch synthase
Phvul.004G102800	2.62	0	S-type anion channel SLAH2-related
Phvul.004G111900	-4.29	0	Solute carrier family 13 member
Phvul.005G078500	-3.77	0	Protein kinase domain
Phvul.005G109000	-7.78	0	Transferase family
Phvul.006G046000	7.46	0	Small heat-shock protein HSP20 family
Phvul.006G098600	5.30	0	(z)-3-hexen-1-ol acetyltransferase
Phvul.006G147800	-2.86	0	WRKY DNA-binding domain
Phvul.006G197900	4.00	0	Squalene monooxygenase
Phvul.007G050400	-4.03	0	Salt stress response/antifungal
Phvul.007G062000	5.86	0	Early light-induced protein 1
Phvul.007G087500	-5.15	0	Leucine rich repeat n-terminal domain
Phvul.007G202800	4.80	0	Protein of unknown function, DUF538
Phvul.007G215600	-2.58	0	Alpha/beta-hydrolases superfamily protein
Phvul.007G260400	-4.24	0	L-type lectin-domain containing receptor kinase S.5-related
Phvul.008G011500	-7.77	0	Thioredoxin
Phvul.008G037300	-5.14	0	Calmodulin
Phvul.008G069400	4.54	0	SPX domain
Phvul.008G086800	-3.60	0	Peroxidase / lactoperoxidase
Phvul.008G087000	2.40	0	Protease inhibitor/seed storage/LTP family
Phvul.008G109200	-2.67	0	Polygalacturonase / pectinase
Phvul.008G109600	-4.17	0	Leucine rich repeat
Phvul.008G166000	5.64	0	Flavonol synthase 3-related
Phvul.008G210100	4.40	0	Beta-d-glucan exohydrolase-like protein-related
Phvul.008G220600	-4.40	0	Abscisic acid receptor PYL5
Phvul.008G229500	3.49	0	Proprotein convertase subtilisin/kexin
Phvul.008G237500	8.29	0	Glutamine synthetase
Phvul.009G018100	5.22	0	Zinc finger FYVE domain containing protein
Phvul.009G061500	-2.78	0	Cytochrome p450 CYP2 subfamily
Phvul.009G068100	-3.48	0	Protein kinase domain
Phvul.009G108300	-3.90	0	Adenosylhomocysteine nucleosidase
Phvul.009G116500	-2.99	0	Basic endochitinase b

Table A.1. Leaf specific genes for intensity difference analysis. (cont.)

ID	IL $\log_2$ FC	TL $\log_2$ FC	Annotation
Phvul.009G225500	3.049	0	Chlorophyll a/b binding protein
Phvul.009G240666	-5.39	0	Ankyrin repeats
Phvul.010G006400	2.84	0	Tubulin
Phvul.010G012900	4.13	0	Isoflavone 2'-hydroxylase
Phvul.010G065400	-3.09	0	Abscisic acid receptor PYL4
Phvul.011G085300	-3.20	0	Glucuronoxylan glucuronosyltransferase F8H-related
Phvul.011G107700	7.56	0	Beta-amylase 5-related
Phvul.011G136600	4.29	0	GMC oxidoreductase
Phvul.011G183766	3.13	0	Pathogenesis-related protein bet v I family
Phvul.011G183832	3.29	0	Pathogenesis-related protein bet v I family
Phvul.011G183900	3.45	0	Pathogenesis-related protein bet v I family
Phvul.L005001	3.20	0	Methionine-gamma-lyase
Phvul.L001658	4.42	0	Plant protein of unknown function

Table A.2. Root specific genes for intensity difference analysis. FC: Fold change.

ID	IR $\log_2$ FC	TR $\log_2$ FC	Annotation
Phvul.001G019500	3.25	0	Serine protease family S10 serine carboxypeptidase
Phvul.001G020200	1.74	0	Ca2+-independent phospholipase A2
Phvul.001G077000	4.11	0	Amino acid permease 1-related
Phvul.001G126400	-2.24	0	Achaete-scute homolog 3
Phvul.001G130700	-4.01	0	ATP-binding cassette transporter
Phvul.001G154200	1.70	0	Sulfate transporter 3.1-related
Phvul.001G180500	6.24	0	Uncharacterized nodulin-like protein
Phvul.001G194600	2.13	0	Harpin-induced protein-like-related
Phvul.001G218600	2.39	0	Chitinase-related
Phvul.001G243300	2.05	0	Phosphatidylinositol phospholipase C, delta
Phvul.002G017800	-2.01	0	Nicotinate phosphoribosyltransferase
Phvul.002G081400	-3.83	0	CLAVATA3/ESR (CLE)-related protein 10-related

Table A.2. Root specific genes for intensity difference analysis. (cont.)

ID	IR $\log_2$ FC	TR $\log_2$ FC	Annotation
Phvul.002G110600	4.59	0	CAMP-response element binding protein-related
Phvul.002G112600	2.64	0	Thiosulfate sulfurtransferase / thiosulfate thiotransferase
Phvul.002G134900	-6.41	0	CGI-141-related/lipase containing protein
Phvul.002G151300	-2.22	0	ACR7-related
Phvul.002G160700	1.84	0	Respiratory burst oxidase homolog protein F-related
Phvul.002G312600	3.68	0	Dynein light chain
Phvul.002G318500	2.96	0	Pectinesterase/pectinesterase inhibitor 6-related
Phvul.003G011800	2.78	0	6-beta-hydroxyhyoscyamine epoxidase/hydroxyhyoscyamine dioxygenase
Phvul.003G021300	-2.95	0	Cation efflux protein/zinc transporter
Phvul.003G049100	-5.06	0	Chitinase
Phvul.003G096700	7.22	0	Late embryogenesis abundant 3 (lea3) family protein
Phvul.003G117100	3.81	0	Cell wall / vacuolar inhibitor of fructosidase 1-related
Phvul.003G151700	2.63	0	EamA-like transporter family
Phvul.003G154800	3.64	0	Heat shock 70 kda protein 5
Phvul.003G164000	3.95	0	Protein NRT1/ PTR family 6.2
Phvul.003G209000	7.33	0	EMB
Phvul.003G224800	3.61	0	Expansin-like b1
Phvul.003G238600	-2.38	0	Natural resistance-associated macrophage protein
Phvul.003G268700	2.22	0	FI18644P1-related
Phvul.003G284000	-3.80	0	MYB domain protein 9
Phvul.004G005400	3.32	0	Alkane hydroxylase cyp96a15-related
Phvul.004G021200	5.25	0	Cytochrome p450 CYP2 subfamily
Phvul.004G059200	-3.81	0	Pectate lyase 11-related
Phvul.004G102700	-3.11	0	Membrane-associated kinase regulator 6-related
Phvul.004G107700	1.80	0	Heat shock protein 90
Phvul.004G110200	-2.17	0	C2 domain
Phvul.004G122000	4.09	0	Dehydration-responsive element-binding protein 1A-related
Phvul.004G129400	5.13	0	22.0 kda heat shock protein
Phvul.004G158100	-11.40	0	Legume lectin domain

Table A.2. Root specific genes for intensity difference analysis. (cont.)

ID	IR $\log_2$ FC	TR $\log_2$ FC	Annotation
Phvul.005G002600	3.83	0	Sucrose-phosphate synthase 4-related
Phvul.005G007600	2.26	0	Pectinesterase / pectin methylesterase
Phvul.005G060000	-3.90	0	F3O9.29 protein-related
Phvul.005G061066	-3.64	0	Feruloyl-CoA ortho-hydroxylase
Phvul.005G061132	-3.68	0	Genomic dna, chromosome 3, p1 clone:mjm20
Phvul.005G065700	2.11	0	Comitin
Phvul.005G130900	3.35	0	Xyloglucan-specific endo-beta-1,4-glucanase / xyloglucanendohydrolase
Phvul.005G151000	-1.93	0	Dienelactone hydrolase-like protein
Phvul.005G160800	-2.87	0	Phosphoethanolamine/phosphocholine phosphatase
Phvul.005G162300	-4.56	0	Leucine-rich repeat protein kinase-related
Phvul.005G162400	-2.84	0	Leucine rich repeat
Phvul.005G171200	-2.72	0	F18B13.4 protein
Phvul.005G176100	-2.80	0	Lactoylglutathione lyase glyoxalase I
Phvul.005G184400	-2.74	0	Pectinesterase
Phvul.006G077100	2.59	0	Serine/threonine-protein kinase wnk4-related
Phvul.006G084400	2.98	0	Salt stress response/antifungal
Phvul.006G148000	-3.03	0	Mitogen-activated protein kinase kinase kinase 15-related
Phvul.006G153100	2.22	0	Eukaryotic aspartyl protease family protein
Phvul.006G178300	-3.27	0	N-hydroxycinnamoyl/benzoyltransferase, putative-related
Phvul.006G205400	2.18	0	2-nitropropane dioxygenase-like protein
Phvul.007G011400	3.23	0	Oxoglutarate dehydrogenase
Phvul.007G061000	3.63	0	Ring zinc finger protein
Phvul.007G065100	3.61	0	Mads box protein
Phvul.007G084600	1.94	0	Pollen proteins Ole e I like
Phvul.007G100900	2.29	0	ABC transporter G family member 21
Phvul.007G103300	-2.39	0	Predicted transporter ADD1
Phvul.007G106300	4.20	0	Geraniol 8-hydroxylase
Phvul.007G225200	4.89	0	Late embryogenesis abundant protein -related
Phvul.007G231700	2.75	0	Ammonium transporter 1 member 2

Table A.2. Root specific genes for intensity difference analysis. (cont.)

ID	IR $\log_2$ FC	TR $\log_2$ FC	Annotation
Phvul.007G276900	-3.59	0	Protein phosphatase 2C-like protein 44-related
Phvul.008G069400	-1.97	0	SPX domain
Phvul.008G087600	1.83	0	Alanine-glyoxylate transaminase
Phvul.008G112700	1.55	0	Alpha crystallins
Phvul.008G155000	3.15	0	Cytochrome p450 71b21-related
Phvul.008G244200	-3.12	0	Metal tolerance protein C3-related
Phvul.008G247600	2.80	0	O-methyltransferase
Phvul.009G024301	3.54	0	Protein of unknown function
Phvul.009G053500	-2.07	0	Plastid-lipid-associated protein 14, chloroplastic-related
Phvul.009G061600	-3.36	0	Cytochrome p450 82C2-related
Phvul.009G080200	4.96	0	17.6 kda class II heat shock protein-related
Phvul.009G116600	2.56	0	Basic endochitinase B
Phvul.009G127900	-3.35	0	Manganese transporter
Phvul.009G128000	-2.80	0	Protein of unknown function
Phvul.009G131000	9.27	0	Naringenin-chalcone synthase/flavonone synthase
Phvul.009G132900	2.20	0	3-methyl-2-oxobutanoate dehydrogenase
Phvul.009G199200	2.24	0	PHYB activation tagged suppressor 1
Phvul.009G207800	2.32	0	Aldo/keto reductase-related
Phvul.009G211000	3.56	0	Extensin-like protein repeat
Phvul.009G233200	1.86	0	Xyloglucan:xyloglucosyl transferase
Phvul.009G234500	1.62	0	Ras suppressor protein
Phvul.009G244200	3.61	0	Isoflavone 2'-hydroxylase
Phvul.010G005900	3.78	0	Laccase-7-related
Phvul.010G009400	2.20	0	Protein NRT1/PTR family 5.5-related
Phvul.010G016000	4.32	0	Ribulose bisphosphate carboxylase/ oxygenase activase, chloroplastic
Phvul.010G036100	-3.32	0	Feruloyl-CoA ortho-hydroxylase
Phvul.010G078258	2.10	0	Alanine-glyoxylate transaminase
Phvul.010G083700	3.15	0	Myeloid leukemia factor
Phvul.010G087800	-1.76	0	Protein Y45F10A.7, isoform A
Phvul.010G101500	-3.42	0	Ferric reduction oxidase 2-related

Table A.2. Root specific genes for intensity difference analysis. (cont.)

ID	IR $\log_2$ FC	TR $\log_2$ FC	Annotation
Phvul.010G133300	1.97	0	Nuclear transcription factor Y subunit A3-related
Phvul.011G010200	-4.19	0	Cation/H(+) antiporter 28
Phvul.011G019300	-1.79	0	(s)-norcoclaurine synthase
Phvul.011G022300	-2.57	0	Cinnamyl-alcohol dehydrogenase
Phvul.011G046300	1.94	0	Burp domain
Phvul.011G055700	2.12	0	Beta-glucosidase
Phvul.011G077900	4.42	0	Glucan endo-1,3-beta-D-glucosidase/laminarinase
Phvul.011G083500	-3.97	0	MFS transporter, NNP family, nitrate/nitrite transporter
Phvul.011G085200	1.95	0	Xyloglucan:xyloglucosyl transferase
Phvul.011G122900	1.74	0	Monothiol glutaredoxin-s13
Phvul.011G125200	1.97	0	AP2 domain
Phvul.011G157500	3.76	0	Aminotransferase TAT2-related
Phvul.011G169900	5.84	0	Trypsin and protease inhibitor
Phvul.011G183000	2.52	0	Pathogenesis-related protein bet v I family
Phvul.011G189900	2.71	0	Permease of the major facilitator superfamily
Phvul.011G194300	3.24	0	G-type lectin S-receptor-like serine/threonine-protein kinase B120
Phvul.L005001	1.76	0	Methionine-gamma-lyase

Table A.3. Enriched GO terms for Ispir leaf tissues. At least five DEGs were detected for each term. P: Biological process; F: Molecular function; C: Cellular component. Z-score.

GO Information					Z-score	Mean	FDRnbsp;
No	**GO Term**	**Onto**	**Number**	**Description**			
1	GO:0015979	P	14	photosynthesis	3.3	2.4	0.0083
2	GO:0045087	P	17	innate immune response	-2.8	-2.5	0.032
3	GO:0006955	P	17	immune response	-2.8	-2.5	0.032
4	GO:0002376	P	17	immune system process	-2.8	-2.5	0.032
5	GO:0044036	P	14	cell wall macromolecule metabolic process	-3.4	-3.2	0.0068
6	GO:0016998	P	14	cell wall macromolecule catabolic process	-3.4	-3.2	0.0068
7	GO:0012501	P	43	programmed cell death	-3.6	-2.1	0.0028
8	GO:0006915	P	43	apoptosis	-3.6	-2.1	0.0028
9	GO:0016265	P	44	death	-3.7	-2.1	0.0022
10	GO:0008219	P	44	cell death	-3.7	-2.1	0.0022
11	GO:0006952	P	40	defense response	-3.8	0.0022	0.0022
12	GO:0019538	P	318	protein metabolic process	-3.9	-1	0.0016
13	GO:0043170	P	554	macromolecule metabolic process	-3.9	-0.88	0.0014
14	GO:0044260	P	484	cellular macromolecule metabolic process	-3.9	-0.92	0.0014
15	GO:0044267	P	263	cellular protein metabolic process	-4.5	-1.2	0.00014
16	GO:0006796	P	218	phosphate metabolic process	-5.8	-1.6	0.00000019
17	GO:0006793	P	218	phosphorus metabolic process	-5.8	-1.6	0.00000019

Table A.3. Enriched GO terms for Ispir leaf tissues. (cont.)

GO Information					Z-score	Mean	FDRnbsp;
No	**GO Term**	**Onto**	**Number**	**Description**			
18	GO:0016310	P	214	phosphorylation	-5.8	-1.6	0.00000019
19	GO:0043412	P	233	macromolecule modification	-5.8	-1.6	0.00000019
20	GO:0006468	P	212	protein amino acid phosphorylation	-5.9	-1.6	0.00000019
21	GO:0006464	P	229	protein modification process	-5.9	-1.6	0.00000019
22	GO:0043687	P	224	post-translational protein modification	-6.1	-1.6	0.00000019
23	GO:0004857	F	12	enzyme inhibitor activity	3.6	3	0.0023
24	GO:0030234	F	19	enzyme regulator activity	3.5	2.20	0.0039
25	GO:0030599	F	10	pectinesterase activity	3	2.6	0.017
26	GO:0004888	F	22	transmembrane receptor activity	-3.1	-2.4	0.012
27	GO:0004872	F	22	receptor activity	-3.1	-2.4	0.012
28	GO:0016740	F	405	transferase activity	-3.4	-0.89	0.0039
29	GO:0005488	F	1012	binding	-3.8	-0.73	0.00098
30	GO:0017076	F	376	purine nucleotide binding	-4.40	-1.10	0.00011
31	GO:0000166	F	392	nucleotide binding	-4.5	-1.10	0.000061
32	GO:0043531	F	40	ADP binding	-4.60	-2.7	0.000035
33	GO:0030554	F	358	adenyl nucleotide binding	-4.7	-1.10	0.000027
34	GO:0001883	F	358	purine nucleoside binding	-4.7	-1.10	0.000027
35	GO:0001882	F	358	nucleoside binding	-4.7	-1.10	0.000027

Table A.3. Enriched GO terms for Ispir leaf tissues. (cont.)

GO Information					Z-score	Mean	FDRnbsp;
No	**GO Term**	**Onto**	**Number**	**Description**			
36	GO:0032555	F	340	purine ribonucleotide binding	-5.10	-1.2	0.0000054
37	GO:0032553	F	340	ribonucleotide binding	-5.10	-1.2	0.0000054
38	GO:0016772	F	232	transferase activity, transferring phosphorus-containing groups	-5.5	-1.5	0.0000007
39	GO:0032559	F	324	adenyl ribonucleotide binding	-5.5	-1.3	0.0000007
40	GO:0005524	F	324	ATP binding	-5.5	-1.3	0.0000007
41	GO:0016773	F	221	phosphotransferase activity, alcohol group as acceptor	-5.6	-1.5	0.0000007
42	GO:0016301	F	221	kinase activity	-5.6	-1.5	0.0000007
43	GO:0004672	F	214	protein kinase activity	-5.8	-1.6	0.0000007
44	GO:0043229	C	110	intracellular organelle	4.60	1	0.000056
45	GO:0043226	C	110	organelle	4.60	1	0.000056
46	GO:0044424	C	144	intracellular part	4.2	0.77	0.00022
47	GO:0043231	C	82	intracellular membrane-bounded organelle	4	1.10	0.00029
48	GO:0043227	C	82	membrane-bounded organelle	4	1.10	0.00029
49	GO:0005634	C	63	nucleus	3.9	1.2	0.00038
50	GO:0005622	C	180	intracellular	3	0.36	0.011
51	GO:0009579	C	10	thylakoid	2.8	2.5	0.016

Table A.4. Enriched GO terms for Ispir root tissues. At least five DEGs were detected for each term. P: Biological process; F: Molecular function; C: Cellular component. Z-score.

GO Information					Z-score	Mean	FDRnbsp;
No	**GO Term**	**Onto**	**Number**	**Description**			
1	GO:0032501	P	15	multicellular organismal process	2	1.8	0.041
13	GO:0009309	P	24	amine biosynthetic process	-2	-0.41	0.046
14	GO:0044271	P	27	cellular nitrogen compound biosynthetic process	-2.1	-0.38	0.04
15	GO:0034641	P	43	cellular nitrogen compound metabolic process	0.0022	-0.24	0.027
16	GO:0044282	P	16	small molecule catabolic process	-2.4	-0.9	0.014
17	GO:0044265	P	15	cellular macromolecule catabolic process	-2.6	-1	0.0099
18	GO:0006066	P	21	alcohol metabolic process	-2.6	-0.8	0.0092
19	GO:0044248	P	27	cellular catabolic process	-2.7	-0.66	0.008
20	GO:0046164	P	11	alcohol catabolic process	-2.7	-1.4	0.007
21	GO:0044275	P	11	cellular carbohydrate catabolic process	-2.7	-1.4	0.007
22	GO:0016747	F	30	transferase activity, transferring acyl groups other than amino-acyl groups	2.7	1.7	0.0076
23	GO:0016746	F	30	transferase activity, transferring acyl groups	2.7	1.7	0.0076
24	GO:0008762	F	12	UDP-N-acetylmuramate dehydrogenase activity	1.9	1.9	0.049
25	GO:0016758	F	42	transferase activity, transferring hexosyl groups	1.8	1.2	0.079

Table A.4. Enriched GO terms for Ispir root tissues. (cont.)

GO Information					Z-score	Mean	FDRnbsp;
No	**GO Term**	**Onto**	**Number**	**Description**			
26	GO:0004091	F	20	carboxylesterase activity	-2	-0.49	0.049
27	GO:0008270	F	33	zinc ion binding	-2	-0.29	0.041
28	GO:0042578	F	13	phosphoric ester hydrolase activity	-2	-0.79	0.041
29	GO:0043531	F	21	ADP binding	-2.1	-0.52	0.038
30	GO:0070035	F	11	purine NTP-dependent helicase activity	-2.1	-0.99	0.032
31	GO:0008026	F	11	ATP-dependent helicase activity	-2.1	-0.99	0.032
32	GO:0004386	F	16	helicase activity	-2.4	-0.87	0.017
33	GO:0016298	F	10	lipase activity	-2.6	-1.4	0.0093
34	GO:0016788	F	52	hydrolase activity, acting on ester bonds	-2.6	-0.3	0.0091
35	GO:0008324	F	22	cation transmembrane transporter activity	-2.9	-0.93	0.0035
36	GO:0046873	F	13	metal ion transmembrane transporter activity	-3	-1.4	0.0031
37	GO:0022891	F	40	substrate-specific transmembrane transporter activity	-3.2	-0.64	0.0015
38	GO:0022892	F	41	substrate-specific transporter activity	-3.3	-0.66	0.0011
39	GO:0015075	F	35	ion transmembrane transporter activity	-3.3	-0.78	0.00086
40	GO:0005737	C	39	cytoplasm	-2	-0.19	0.049

Table A.5. Enriched GO terms for TR43477 leaf tissues. At least five DEGs were detected for each term. P - Biological process; F - Molecular function; C - Cellular component. Z-score is derived from the number of genes and fold changes.

GO Information					Z-score	Mean	FDRnbsp;
No	**GO Term**	**Onto**	**Number**	**Description**			
1	GO:0032501	P	10	multicellular organismal process	3.2	3.4	0.016
2	GO:0080090	P	139	regulation of primary metabolic process	3.1	0.43	0.016
3	GO:0031326	P	139	regulation of cellular biosynthetic process	3.1	0.43	0.016
4	GO:0010556	P	139	regulation of macromolecule biosynthetic process	3.1	0.43	0.016
5	GO:0009889	P	139	regulation of biosynthetic process	3.1	0.43	0.016
6	GO:0031323	P	143	regulation of cellular metabolic process	3.1	0.41	0.016
7	GO:0051252	P	138	regulation of RNA metabolic process	3.1	0.42	0.016
8	GO:0051171	P	138	regulation of nitrogen compound metabolic process	3.1	0.42	0.016
9	GO:0045449	P	138	regulation of transcription	3.1	0.42	0.016
10	GO:0019219	P	138	regulation of nucleobase, nucleoside, nucleotide and nucleic acid metabolic process	3.1	0.42	0.016
11	GO:0006355	P	138	regulation of transcription, DNA-dependent	3.1	0.42	0.016
12	GO:0060255	P	140	regulation of macromolecule metabolic process	3.1	0.41	0.016
13	GO:0010468	P	140	regulation of gene expression	3.1	0.41	0.016
14	GO:0019222	P	144	regulation of metabolic process	3.1	0.39	0.016
15	GO:0032774	P	141	RNA biosynthetic process	3	0.4	0.016

Table A.5. Enriched GO terms for TR43477 leaf tissues. (cont.)

GO Information					Z-score	Mean	FDRnbsp;
No	**GO Term**	**Onto**	**Number**	**Description**			
16	GO:0006351	P	141	transcription, DNA-dependent	3	0.4	0.016
17	GO:0006350	P	141	transcription	3	0.4	0.016
18	GO:0050794	P	182	regulation of cellular process	2.8	0.2	0.034
19	GO:0050789	P	186	regulation of biological process	2.7	0.16	0.048
20	GO:0044264	P	22	cellular polysaccharide metabolic process	-2.7	-2.9	0.041
21	GO:0044042	P	14	glucan metabolic process	-3.4	-4.10	0.016
22	GO:0005976	P	30	polysaccharide metabolic process	-3.4	-3.1	0.016
23	GO:0006073	P	13	cellular glucan metabolic process	-3.5	-4.3	0.016
24	GO:0006091	P	31	generation of precursor metabolites and energy	-4.60	-3.9	0.00015
25	GO:0019684	P	23	photosynthesis, light reaction	-5.2	-4.8	0.000013
26	GO:0009765	P	21	photosynthesis, light harvesting	-5.2	-5.10	0.000013
27	GO:0015979	P	54	photosynthesis	-5.6	-3.6	0.0000028
28	GO:0016747	F	32	transferase activity, transferring acyl groups other than amino-acyl groups	3.9	2.1	0.004
29	GO:0016746	F	36	transferase activity, transferring acyl groups	3.6	1.7	0.0088
30	GO:0030554	F	270	adenyl nucleotide binding	2.9	0.078	0.035
31	GO:0001883	F	270	purine nucleoside binding	2.9	0.078	0.035

Table A.5. Enriched GO terms for TR43477 leaf tissues. (cont.)

GO Information					Z-score	Mean	FDRnbsp;
No	**GO Term**	**Onto**	**Number**	**Description**			
32	GO:0032559	F	246	adenyl ribonucleotide binding	2.9	0.11	0.035
33	GO:0005524	F	246	ATP binding	2.9	0.11	0.035
34	GO:0001882	F	271	nucleoside binding	2.8	0.067	0.035
35	GO:0043565	F	48	sequence-specific DNA binding	2.8	0.97	0.035
36	GO:0000166	F	308	nucleotide binding	2.8	0.013	0.035
37	GO:0017076	F	287	purine nucleotide binding	2.8	0.03	0.035
38	GO:0032555	F	263	purine ribonucleotide binding	2.7	0.053	0.035
39	GO:0032553	F	263	ribonucleotide binding	2.7	0.053	0.035
40	GO:0004252	F	13	serine-type endopeptidase activity	-2.5	-3.4	0.047
41	GO:0043169	F	188	cation binding	-2.6	-1.3	0.046
42	GO:0043167	F	188	ion binding	-2.6	-1.3	0.046
43	GO:0008194	F	12	UDP-glycosyltransferase activity	-2.6	-3.6	0.043
44	GO:0016684	F	12	oxidoreductase activity, acting on peroxide as acceptor	-2.6	-3.6	0.043
45	GO:0004601	F	12	peroxidase activity	-2.6	-3.6	0.043
46	GO:0070011	F	51	peptidase activity, acting on L-amino acid peptides	-2.7	-2.1	0.043
47	GO:0017171	F	25	serine hydrolase activity	-2.8	-2.8	0.035
48	GO:0008236	F	25	serine-type peptidase activity	-2.8	-2.8	0.035

Table A.5. Enriched GO terms for TR43477 leaf tissues. (cont.)

GO Information					Z-score	Mean	FDRnbsp;
No	**GO Term**	**Onto**	**Number**	**Description**			
49	GO:0000287	F	16	magnesium ion binding	-2.8	-3.3	0.035
50	GO:0016835	F	18	carbon-oxygen lyase activity	-3.1	-3.4	0.027
51	GO:0016701	F	12	oxidoreductase activity, acting on single donors with incorporation of molecular oxygen	-3.1	-4.1	0.027
52	GO:0016838	F	12	carbon-oxygen lyase activity, acting on phosphates	-3.3	-4.3	0.016
53	GO:0010333	F	12	terpene synthase activity	-3.3	-4.3	0.016
54	GO:0051213	F	10	dioxygenase activity	-3.5	-5	0.0088
55	GO:0016702	F	10	oxidoreductase activity, acting on single donors with incorporation of molecular oxygen, incorporation of two atoms of oxygen	-3.5	-5	0.0088
56	GO:0004857	F	21	enzyme inhibitor activity	-5.5	-5.3	0.0000026
57	GO:0030234	F	26	enzyme regulator activity	-6	-5.2	0.00000028

Table A.6. Enriched GO terms for TR43477 root tissues. At least five DEGs were detected for each term. P - Biological process; F - Molecular function; C - Cellular component. Z-score is derived from the number of genes and fold changes.

GO Information					Z-score	Mean	FDRnbsp;
No	**GO Term**	**Onto**	**Number**	**Description**			
1	GO:0032501	P	10	multicellular organismal process	2.6	2.3	0.0081
7	GO:0006950	P	31	response to stress	-2.1	-1.3	0.0033
8	GO:0050896	P	36	response to stimulus	-2.5	-1.4	0.014
9	GO:0006979	P	16	response to oxidative stress	-2.8	-2.3	0.005
10	GO:0042221	P	22	response to chemical stimulus	-2.9	-2.1	0.0033
11	GO:0003677	F	74	DNA binding	2	0.49	0.048
18	GO:0060089	F	11	molecular transducer activity	-2.1	-2.1	0.035
19	GO:0004871	F	11	signal transducer activity	-2.1	-2.1	0.035
20	GO:0016209	F	18	antioxidant activity	-2.6	-2	0.01
21	GO:0016684	F	16	oxidoreductase activity, acting on peroxide as acceptor	-2.8	-2.3	0.005
22	GO:0004601	F	16	peroxidase activity	-2.8	-2.3	0.005
23	GO:0043231	C	18	intracellular membrane-bounded organelle	2.3	1.4	0.024
24	GO:0043227	C	19	membrane-bounded organelle	2.1	1.2	0.038

Table A.7. Enriched KEGG pathways for Ispir leaf tissues. At least five DEGs were detected for each pathway. Upregulated and downregulated genes were analysed separately. Main groups are highlighted in yellow and not displayed in the graph.

Up	
Enrichment FDR	**Functional Category**
0.00000000098	Biosynthesis of secondary metabolites
0.00000025	Metabolic pathways
0.00058	Carbon fixation in photosynthetic organisms
0.00058	Protein processing in endoplasmic reticulum
0.00099	Photosynthesis
0.0033	Starch and sucrose metabolism
0.0044	Porphyrin and chlorophyll metabolism
0.0044	Carotenoid biosynthesis
0.0045	Cutin, suberine and wax biosynthesis
0.0061	Carbon metabolism
0.0082	Glyoxylate and dicarboxylate metabolism
Down	
Enrichment FDR	**Functional Category**
0.000000000048	Plant-pathogen interaction
0.0000000012	MAPK signaling pathway
0.0031	Phenylpropanoid biosynthesis
0.018	Plant hormone signal transduction
0.051	Circadian rhythm

Table A.8. Enriched KEGG pathways for TR43477 leaf tissues. At least five DEGs were detected for each pathway. Upregulated and downregulated genes were analysed separately. Main groups are highlighted in yellow and not displayed in the graph.

Up	
Enrichment FDR	**Functional Category**
0.00001	Beta-Alanine metabolism
0.00018	Cutin, suberine and wax biosynthesis
0.00022	Valine, leucine and isoleucine degradation

Table A.8. Enriched KEGG pathways for TR43477 leaf tissues. (cont.)

Enrichment FDR	**Functional Category**
0.00038	Fatty acid degradation
0.0034	Protein processing in endoplasmic reticulum
0.021	Galactose metabolism
0.021	Alpha-Linolenic acid metabolism
0.021	Metabolic pathways
0.024	Isoquinoline alkaloid biosynthesis
0.026	Tyrosine metabolism
0.026	Biosynthesis of secondary metabolites
0.026	Peroxisome
0.027	Carotenoid biosynthesis
0.027	Plant hormone signal transduction
0.03	Tropane, piperidine and pyridine alkaloid biosynthesis
0.032	Arginine and proline metabolism
0.032	Fatty acid metabolism
0.053	Arginine biosynthesis
0.053	Phenylalanine metabolism
Down	
Enrichment FDR	**Functional Category**
0.00000000000000011	Photosynthesis
0.00000000000000037	Metabolic pathways
0.00000000000019	Photosynthesis
0.00000000000061	Biosynthesis of secondary metabolites
0.00000057	Ribosome biogenesis in eukaryotes
0.0005	DNA replication
0.00067	Carbon fixation in photosynthetic organisms
0.0042	Carbon metabolism
0.0063	Starch and sucrose metabolism
0.0098	Steroid biosynthesis
0.0099	Porphyrin and chlorophyll metabolism
0.01	Terpenoid backbone biosynthesis
0.012	Glyoxylate and dicarboxylate metabolism
0.015	Biosynthesis of amino acids
0.017	Glycine, serine and threonine metabolism
0.021	Sulfur metabolism

Table A.8. Enriched KEGG pathways for TR43477 leaf tissues. (cont.)

Enrichment FDR	**Functional Category**
0.032	Glutathione metabolism
0.049	Thiamine metabolism
0.05	Alpha-Linolenic acid metabolism
0.052	Nitrogen metabolism
0.054	Cysteine and methionine metabolism

Table A.9. Enriched KEGG pathways for Ispir root tissues. At least five DEGs were detected for each pathway. Upregulated and downregulated genes were analysed separately. Main groups are highlighted in yellow and not displayed in the graph.

Up	
Enrichment FDR	**Functional Category**
0.0000024	Galactose metabolism
0.0000032	Metabolic pathways
0.0003	Biosynthesis of secondary metabolites
0.0016	Phenylpropanoid biosynthesis
0.023	Photosynthesis
0.023	Tryptophan metabolism
0.023	Starch and sucrose metabolism
0.023	MAPK signaling pathway
0.025	Carotenoid biosynthesis
0.029	Diterpenoid biosynthesis
0.032	Protein processing in endoplasmic reticulum
0.035	Amino sugar and nucleotide sugar metabolism
0.045	Monoterpenoid biosynthesis
0.049	Plant hormone signal transduction
0.053	Fatty acid degradation
Down	
Enrichment FDR	**Functional Category**
0.00019	Phenylpropanoid biosynthesis
0.00019	Metabolic pathways
0.00049	Biosynthesis of secondary metabolites

Table A.9. Enriched KEGG pathways for Ispir root tissues. (cont.)

Enrichment FDR	**Functional Category**
0.0005	Phenylalanine metabolism
0.0058	Biosynthesis of amino acids
0.0067	Nitrogen metabolism
0.0067	Ribosome biogenesis in eukaryotes
0.051	Cysteine and methionine metabolism

Table A.10. Enriched KEGG pathways for TR43477 root tissues. At least five DEGs were detected for each pathway. Upregulated and downregulated genes were analysed separately. Main groups are highlighted in yellow and not displayed in the graph.

Up	
Enrichment FDR	**Functional Category**
0.00046	MAPK signaling pathway
0.0032	Galactose metabolism
0.0034	Phenylpropanoid biosynthesis
0.0042	Plant hormone signal transduction
0.01	Biosynthesis of secondary metabolites
0.029	Starch and sucrose metabolism
0.031	Alanine, aspartate and glutamate metabolism
0.041	Metabolic pathways
Down	
Enrichment FDR	**Functional Category**
0.000000042	Phenylpropanoid biosynthesis
0.00000083	Metabolic pathways
0.0000087	Photosynthesis
0.0003	Biosynthesis of secondary metabolites
0.0022	Circadian rhythm
0.0084	Nitrogen metabolism

Table A.11. Ispir leaf metabolites list. RT: Retention time; MW: Molecular Weight; Cont: Control; Tre: Treatment; Av: Average; SD: Standard deviation; FC: Fold change. Average values display the mean area of the representative peak in the spectrum.

Metabolite	**RT**	**MW**	**KEGG/ Pubchem ID**	**Cont. Av.**	**Cont. SD**	**Tre. Av.**	**Tre. SD**	***p*-value**	**FC**	**log2 FC**
L-proline	6.413	259	C00148	48.45	96.91	821.11	165.51	0	16.94	4.08
D-mannitol	11.621	614	C00392	436.02	113.04	7768.69	1362.74	0	17.81	4.15
L-serine	7.028	321	C00065	926.42	239.51	4986.85	978.31	0	5.38	2.42
Veratric acid	8.115	222	CID7121	1225.57	276.6	330.53	161.81	0	0.26	-1.89
Lauric acid	9.152	242	C02679	483.8	175.19	1287.72	253.88	0	2.66	1.41
Beta-alanine	7.605	305	C00099	119.26	91.47	591.81	170.88	0	4.96	2.31
L-norvaline	2.744	261	C01826	15324.07	2067.26	9898.17	1156.68	0	0.64	-0.63
L-threonine	7.278	335	C00188	477.16	68.75	760.53	108.46	0	1.59	0.67
myo-Inositol	12.588	612	C00137	38980.88	10986.07	90474.46	20197.27	0	2.32	1.21
D-xylose	11.898	512	C00181	955.63	218.21	1515.21	182.42	0	1.58	0.66
L-isoleucine	6.375	275	C00407	238.31	85.01	0	0	0	0	-3.06
Glutamate	9.2	363	C00025	980.42	255.43	1968.03	418.71	0	2	1
Propanedioic acid	5.46	248	C00383	11285.81	3423.13	3607.33	2133.59	0	0.31	-1.64
Sucrose	15.723	918	C00089	69011.23	16964.01	253407.98	77474.16	0	3.67	1.87
Glycolate	4.048	220	C00160	601.66	92.24	385.27	20.93	0	0.64	-0.64
L-tryptophan	2.905	232	C00078	669.28	187	257.92	79.36	0	0.38	-1.37
Benzoic acid	5.859	194	C00180	395.64	106.7	182.25	76.99	0.01	0.46	-1.11
Hexanoic acid	3.974	188	C01585	543.1	176.97	181.1	33.38	0.01	0.33	-1.58
Threose	8.997	423	C00279	6672.66	3399.82	14157.41	3842.86	0.01	2.12	1.08

Table A.11. Ispir leaf metabolites list. (cont.)

Metabolite	**RT**	**MW**	**KEGG/ Pubchem ID**	**Cont. Av.**	**Cont. SD**	**Tre. Av.**	**Tre. SD**	***p*-value**	**FC**	**log2 FC**
Lactic acid	3.885	234	C00186	1179.3	245.08	753.08	42.59	0.02	0.63	-0.64
Sorbitol	12.754	614	C00794	678.03	423.96	1414.43	367.63	0.03	2.08	1.06
D-glucose	11.573	540	C00031	1569.37	153.84	2180.83	403.83	0.03	1.38	0.47
Beta-gentiobiose	13.142	540	C08240	692.61	216.03	1321.28	424.66	0.03	1.9	0.93
2-Coumerate	3.589	308	C01772	158.89	80.64	275.26	40	0.04	1.73	0.79
L-asparagine	9.607	348	C00152	435.29	117.69	882.84	321.35	0.04	2.02	1.02
D-galactose	11.351	569	C00124, C00984	1143.66	563.57	2389.54	870.53	0.04	2.08	1.06
Succinate	6.53	262	C00042	887.94	404.07	361.24	45.1	0.05	0.4	-1.29
m-Toluic acid	6.987	208	C07211	346.57	163.61	146.76	53.71	0.06	0.42	-1.23
Myristic acid	10.787	300	C06424	429.94	50.67	603.85	146.68	0.07	1.4	0.49
Terephthalic acid	10.443	310	C06337	3807.16	853.05	2567.74	897.86	0.08	0.67	-0.56
Fumaric acid	6.832	260	C00122	635	159.86	444.36	103.8	0.08	0.69	-0.51
Malic acid	8.152	350	C00149	11772.85	5806.72	5333.73	3051.07	0.09	0.45	-1.14
Galactitol	9.893	614	C01697	1252.05	128.92	1456.29	177.8	0.1	1.16	0.21
D-fructose	11.172	569	C00095, C02336	1158.46	550.2	1776.44	483.6	0.13	1.53	0.61
D(-)ribofuranose	10.199	438	C16639	3610.19	1260.3	2469.52	328.69	0.14	0.68	-0.54
D-tagatose	11.241	569	C00795	827.58	413.57	1399.49	578.59	0.15	1.69	0.75
Boric acid	3.075	278	C12486	2079.79	764.47	1474.05	238.94	0.19	0.7	-0.49
(R)-3-Hydroxybutanoate	6.755	322	C01089	600.68	267.12	405.31	33.12	0.21	0.67	-0.56
GABA	8.471	319	C00334	2124.44	491.15	1770.43	155.75	0.23	0.83	-0.26

Table A.11. Ispir leaf metabolites list. (cont.)

Metabolite	**RT**	**MW**	**KEGG/ Pubchem ID**	**Cont. Av.**	**Cont. SD**	**Tre. Av.**	**Tre. SD**	***p*-value**	**FC**	**log2 FC**
Octadecanoic acid	13.278	356	C01530	3164.52	504.64	2829.25	89.59	0.25	0.89	-0.16
Glycine	6.497	291	C00037	1045.52	324.29	845.17	113.83	0.29	0.8	-0.3
Caffeic acid	12.724	396	C01197	1938.01	536.39	1552.97	753	0.43	0.8	-0.31
L-alanine	4.359	233	C00041	568.28	199.46	476.01	97.85	0.43	0.83	-0.25
L-aspartic acid	8.42	349	C00049	750.86	325.79	905.02	197.18	0.44	1.2	0.26
Melibiose	14.987	918	C05402	1850.31	633.72	2138.79	644.91	0.54	1.15	0.2
L-valine	5.59	261	C00183	311.6	215.08	381.92	60.38	0.55	1.22	0.29
Galactonic acid	12.23	628	C00880	2853.61	531.2	2574.88	1011.95	0.64	0.9	-0.14
L-leucine	6.16	275	C00123	266.08	91.61	245.97	38.19	0.7	0.92	-0.11
Citrate	10.946	480	C00158	1171.23	785.64	999.9	425.48	0.71	0.85	-0.22
Palmitate	12.085	328	C00249	2095.11	392.72	2018.43	193.94	0.73	0.96	-0.05
Maleic acid	6.458	260	C01384	227.87	107.01	269.21	226.45	0.75	1.18	0.24
Ethanolamine	6.101	277	C00189	1357.16	441.79	1283.8	271.99	0.78	0.94	-0.08
m-Coumaric acid	11.45	308	C00811	740.22	148.44	683.51	402.2	0.8	0.92	-0.11
L-phenylalanine	9.255	309	C00079	502.88	445.35	483.59	89.03	0.93	0.96	-0.05
Ethandioic acid	4.786	234	C00209	4793.21	3003.27	4821.42	1002.53	0.98	1	0

Table A.12. Ispir root metabolites list. RT: Retention time; MW: Molecular Weight; Cont: Control; Tre: Treatment; Av: Average; SD: Standard deviation; FC: Fold change. Average values display the mean area of the representative peak in the spectrum.

Metabolite	**RT**	**MW**	**KEGG/ Pubchem ID**	**Cont. Av.**	**Cont. SD**	**Tre. Av.**	**Tre. SD**	***p*-value**	**FC**	**log2 FC**
Veratric acid	8.12	222	CID7121	949.93	85.12	333.23	107.41	0	0.35	-1.51
Glycolate	4.074	220	C00160	543.83	37.08	386.2	42.53	0	0.71	-0.49
Hexanoic acid	4.001	188	C01585	2136.57	383.45	775.39	160.33	0	0.36	-1.46
L-asparagine	9.609	348	C00152	1293.14	446.83	3607.86	765.24	0	2.78	1.48
Octanoic acid	6.028	216	C06423	230.08	57.1	53.71	47.82	0	0.23	-2.09
L-aspartic acid	8.42	349	C00049	1409.25	370.8	3486	751.05	0	2.47	1.3
Glutamate	9.205	363	C00025	1736.37	453.6	4236.94	907.08	0	2.44	1.28
L-proline	6.413	259	C00148	55.78	84.16	587.39	204.25	0	10.53	3.39
Ethanolamine	6.118	277	C00189	2677.55	286.34	1664.33	418.93	0	0.62	-0.68
D-mannitol	11.62	614	C00392	730.1	947.54	4930.6	1834.55	0	6.75	2.75
Benzoic acid	5.876	194	C00180	308.1	32.03	214.31	40.34	0	0.69	-0.52
L-isoleucine	6.389	275	C00407	247.46	43.22	109.57	63.93	0	0.44	-1.17
D-galactose	11.352	569	C00124, C00984	4514.1	843.95	6346.17	654.55	0	1.4	0.49
D-fructose	11.173	569	C00095, C02336	1357.61	449.43	2809.82	764.9	0.01	2.06	1.04
Boric acid	3.105	278	C12486	1043.03	151.89	764.87	64.25	0.01	0.73	-0.44
Galactitol	9.89	614	C01697	1659.84	199.3	1217.49	262.73	0.02	0.73	-0.44
L-serine	7.039	321	C00065	642.24	116.26	1234.58	385.23	0.03	1.92	0.94
Sucrose	15.72	918	C00089	56693.84	32679.65	140474.38	53920.2	0.03	2.47	1.3
D-tagatose	11.241	569	C00795	1430.69	801.92	2881.15	846.64	0.03	2.009	1

Table A.12. Ispir root metabolites list. (cont.)

Metabolite	**RT**	**MW**	**KEGG/ Pubchem ID**	**Cont. Av.**	**Cont. SD**	**Tre. Av.**	**Tre. SD**	***p*-value**	**FC**	**log2 FC**
myo-Inositol	12.587	612	C00137	3993.99	3937.76	22735.95	12688.13	0.03	5.69	2.5
2-Coumerate	3.589	308	C01772	104.25	37.38	164.14	31	0.03	1.57	0.65
Lauric acid	9.152	242	C02679	1081.78	570.809	2104.989	617.34	0.04	1.94	0.96
Alpha-D-xylose	11.89	512	C01394	1178.08	278.74	734.94	240.35	0.04	0.62	-0.68
Palmitate	12.085	328	C00249	2156.42	369.7	1648.57	167.98	0.04	0.76	-0.38
Beta-D-mannopyranose	14.455	540	C02209	2060.6	733.19	1054.32	575.42	0.06	0.51	-0.96
GABA	8.48	319	C00334	2301.01	453.47	4050.41	1433.24	0.06	1.76	0.81
Octadecanoic acid	13.494	356	C01530	3209.46	737.88	2418.27	337.47	0.1	0.75	-0.4
L-tyrosine	11.506	397	C00082	175.96	113.68	45.94	91.89	0.11	0.26	-1.93
Terephthalic acid	10.446	310	C06337	6056.1	4947.92	1111.11	356.53	0.11	0.18	-2.44
Citrate	10.946	480	C00158	23447.32	12715.38	41613.23	16554.31	0.12	1.77	0.82
L-alanine	4.383	233	C00041	542.45	92.96	731.88	206.1	0.14	1.34	0.43
L-norvaline	2.77	261	C01826	12698.79	998.11	11050.49	1748.68	0.14	0.87	-0.2
D-gluconic acid	12.015	628	C00257	1745.24	417.48	1297.78	386.26	0.15	0.74	-0.42
Glycerol	6.22	308	C00116	3192.85	771.44	2552.04	167.98	0.17	0.79	-0.32
L-phenylalanine	9.26	309	C00079	444.54	123.12	572.61	122.21	0.17	1.28	0.36
m-Coumaric acid	11.453	308	C00811	131.24	167.7	0	0	0.19	0	-3.06
Methyl-α-D-glucopyranoside	13.55	482	CID64947	1736.92	614.19	1108.28	651.25	0.19	0.63	-0.64
Propanedioic acid	5.46	248	C00383	191.17	61.6	143.28	17.14	0.19	0.74	-0.41
Sorbitol	12.754	614	C00794	1142.02	579.07	682.95	301.08	0.2	0.59	-0.74

Table A.12. Ispir root metabolites list. (cont.)

Metabolite	**RT**	**MW**	**KEGG/ Pubchem ID**	**Cont. Av.**	**Cont. SD**	**Tre. Av.**	**Tre. SD**	***p*-value**	**FC**	**log2 FC**
Succinate	6.543	262	C00042	786.04	227.9	589.55	188.55	0.22	0.75	-0.41
Caffeic acid	12.724	396	C01197	84.9	119.41	0	0	0.22	0	-3.06
Glycine	6.51	291	C00037	1373.07	557.57	971.36	211.69	0.23	0.7	-0.49
D-glucose	11.574	540	C00031	741	272.12	530.79	184.45	0.24	0.71	-0.48
L-valine	5.61	261	C00183	493.81	60.26	596.28	143.99	0.24	1.2	0.27
L-threonine	7.29	335	C00188	323.27	97.53	394.7	71.66	0.27	1.22	0.28
Lactic acid	3.91	234	C00186	4168.28	2357.14	2645	796.62	0.27	0.63	-0.65
L-leucine	6.176	275	C00123	303.02	44.29	265.5	49.38	0.29	0.87	-0.19
Beta-alanine	7.605	305	C00099	168.56	69.08	219.8	61.08	0.29	1.3	0.38
Maltose	14.631	918	C00897	1614.15	433.55	1204.38	595.51	0.3	0.74	-0.42
D-L-arabinose	9.75	512	C00259	618.24	135.02	534.72	94.35	0.34	0.86	-0.2
D-xylose	11.29	438	C00181	2912.63	651.03	2458.49	682.03	0.36	0.84	-0.24
D-Lyxose	11.86	438	C00476	380.97	144.85	279.61	176.75	0.4	0.73	-0.44
Melibiose	14.987	918	C05402	600.38	417.37	355.71	363.91	0.4	0.59	-0.75
Threose	8.99	423	C00279	421.82	230.94	553.79	190.86	0.4	1.31	0.39
Ethandioic acid	4.808	234	C00209	4807.77	2317.57	3665.1	2032.73	0.48	0.76	-0.39
Beta-gentiobiose	13.141	540	C08240	226.31	193.65	146.9	170.85	0.55	0.64	-0.62
Maleic acid	6.458	260	C01384	89.64	53.95	69.4	42.15	0.57	0.77	-0.36
D-galactose 1E	11.475	569	C00962	1335.45	352.51	1461.2	244.76	0.57	1.09	0.12
D(-)ribofuranose	10.202	438	C16639	872.85	179.06	731.79	438.51	0.57	0.83	-0.25

Table A.12. Ispir root metabolites list. (cont.)

Metabolite	**RT**	**MW**	**KEGG/ Pubchem ID**	**Cont. Av.**	**Cont. SD**	**Tre. Av.**	**Tre. SD**	***p*-value**	**FC**	**log2 FC**
m-Toluic acid	7.001	208	C07211	104.53	49.77	121.77	47.68	0.63	1.16	0.22
Fumaric acid	6.84	260	C00122	392.32	90.87	354.43	125.1	0.63	0.9	-0.14
Urea	5.78	204	C00086	1325.47	432.4	1217.11	168.08	0.65	0.91	-0.12
Myristic acid	10.79	300	C06424	149.59	153.82	189.31	286.98	0.81	1.26	0.33
Malic acid	8.16	350	C00149	9315.129	3989.7	9244.51	4276.1	0.98	0.99	-0.01
L-tryptophan	2.933	232	C00078	386.77	86.23	386.41	182.06	0.99	0.99	0

Table A.13. TR43477 leaf metabolites list. RT: Retention time; MW: Molecular Weight; Cont: Control; Tre: Treatment; Av: Average; SD: Standard deviation; FC: Fold change. Average values display the mean area of the representative peak in the spectrum.

Metabolite	**RT**	**MW**	**KEGG/ Pubchem ID**	**Cont. Av.**	**Cont. SD**	**Tre. Av.**	**Tre. SD**	***p*-value**	**FC**	**log2 FC**
Fumaric acid	7.023	260	C00122	305.29	15.21	140.46	27.43	0	0.46	-1.12
Nonanoic acid	7.13	230	C01601	986.18	109.36	447.48	72.56	0	0.45	-1.14
Benzoic acid	6.053	194	C00180	710.46	59.99	462.3	50.73	0	0.65	-0.61
Myristic acid	10.99	300	C06424	22885.57	435.37	15126.27	1615.32	0	0.66	-0.59
Hexadeconoic acid	12.297	328	C00249	3573.87	376.39	2205.92	298.63	0	0.61	-0.69
(R)-3-Hydroxybutanoate	7.403	248	C01089	327.17	35.42	192.95	39.87	0	0.58	-0.76

Table A.13. TR43477 leaf metabolites list. (cont.)

Metabolite	**RT**	**MW**	**KEGG/ Pubchem ID**	**Cont. Av.**	**Cont. SD**	**Tre. Av.**	**Tre. SD**	***p*-value**	**FC**	**log2 FC**
L-serine	7.225	321	C00065	941.17	573.67	6395.07	1540.3	0	6.79	2.76
Octadeconoic acid	13.49	356	C01530	3315.78	280.82	2158.42	392.55	0	0.65	-0.61
Dihydroxymandelic acid	7.715	356	C05580	1828.25	159.87	1339.07	150.22	0	0.73	-0.44
L-threonine	7.478	335	C00188	638.36	195.79	1142.01	167.81	0	1.78	0.83
Lactic acid	4.073	234	C00186	3770.82	607.07	7400.43	1641.85	0	1.96	0.97
L-proline	6.601	259	C00148	0	0	533.07	223.85	0	N/A	4.16
Malate	8.354	350	C00149	7179.06	2685.22	858.13	192.6	0	0.11	-3.06
Glyceryl palmitate	15.412	474	CID14900	5520.62	795.92	3839.53	416.87	0	0.69	-0.52
Propanedioic acid	5.65	248	C00383	3452.82	301.86	1798.13	770.04	0	0.52	-0.94
L-norvaline	2.93	261	C01826	18978.35	2814.32	13346.05	1311.83	0.01	0.7	-0.5
myo-Inositol	12.808	612	C00137	48121.61	7148.45	108637.77	31868.82	0.01	2.25	1.17
Decanoic acid	7.99	244	C01571	335.76	53.36	223.92	56.68	0.02	0.66	-0.58
Glycerol	6.397	309	C00116	3800.83	563.09	2875.28	235.88	0.02	0.75	-0.4
D-fructose	11.386	569	C00095, C02336	1673.29	977.08	0	0	0.02	0	-3.06
Glutamine	9.406	363	C00064	1095.55	258.77	1657.6	331.32	0.02	1.51	0.59
Galactitol	10.102	614	C01697	1346	128.59	1144.45	86.22	0.03	0.85	-0.23
Methylmaleic acid	6.322	262	C02226	741.39	55.92	386.7	233.69	0.03	0.52	-0.93
Hexanoic acid	4.162	188	C01585	1781.98	388.98	1221.7	235.65	0.04	0.68	-0.54
L-tryptophan	2.787	232	C00078	1413.5	243.11	1053.95	171.19	0.04	0.74	-0.42
Threonate	9.007	424	C01620	1418.64	604.8	601.31	170.53	0.05	0.42	-1.23

Table A.13. TR43477 leaf metabolites list. (cont.)

Metabolite	**RT**	**MW**	**KEGG/ Pubchem ID**	**Cont. Av.**	**Cont. SD**	**Tre. Av.**	**Tre. SD**	***p*-value**	**FC**	**log2 FC**
Succinate	6.723	262	C00042	555.54	329.51	155.81	96.15	0.07	0.28	-1.83
L-asparagine	9.812	348	C00152	188.59	155.92	0	0	0.07	0	-3.06
D-3-aminoisobutanoate	6.298	319	C01205	825.34	110.02	1197.33	415.83	0.14	1.45	0.53
Boric acid	3.26	278	C12486	2492.8	563.01	2136.34	233.4	0.29	0.85	-0.22
L-phenylalanine	9.468	309	C00079	88.72	108.67	22.41	44.82	0.3	0.25	-1.98
Anthranilic acid	9.351	281	C00108	4279.43	3973.83	2047.6	1297.12	0.33	0.47	-1.06
D-mannitol	11.57	614	C00392	199.03	244.24	65.93	131.86	0.37	0.33	-1.59
L-isoleucine	6.575	275	C00407	0	0	22.49	44.99	0.37	N/A	4.16
Cinnamic acid	12.935	396	C00423	505.83	154.51	578.63	134.14	0.49	1.14	0.19
Sucrose	15.943	918	C00089	307511.04	230593	222704.28	79886.83	0.51	0.72	-0.46
Glycine	6.697	291	C00037	2053.47	3258.32	966.42	159.74	0.54	0.47	-1.08
Sorbitol	12.973	614	C00794	1363.99	253.69	1270.91	154.51	0.55	0.93	-0.1
D-glucose	11.783	540	C00031	2152.6	427.67	1955.54	541.02	0.58	0.9	-0.13
Citrate	10.946	480	C00158	619.47	221.43	555.37	64.2	0.6	0.89	-0.15
D-L-arabinose	10.414	438	C00259	1319.82	620.32	1428.6	251.08	0.75	1.08	0.11
GABA	5.957	347	C00334	2769.07	210.83	2891.37	973.93	0.81	1.04	0.06
L-aspartic acid	8.62	349	C00049	537.95	182.69	517.7	118.36	0.85	0.96	-0.05

Table A.14. TR43477 root metabolites list. RT: Retention time; MW: Molecular Weight; Cont: Control; Tre: Treatment; Av: Average; SD: Standard deviation; FC: Fold change. Average values display the mean area of the representative peak in the spectrum.

Metabolite	**RT**	**MW**	**KEGG/ Pubchem ID**	**Cont. Av.**	**Cont. SD**	**Tre. Av.**	**Tre. SD**	***p*-value**	**FC**	**log2 FC**
Glyceryl palmitate	15.417	474	CID14900	4175.37	270.09	2214.49	143.39	0	0.53	-0.91
D-3-aminoisobutanoate	6.3	319	C01205	2264.49	172.02	1284.24	127.71	0	0.56	-0.81
Glutamine	9.408	363	C00064	1370.69	600.86	5690.54	995.69	0	4.15	2.05
L-threonine	7.479	335	C00188	429.26	110.71	981.18	139.17	0	2.28	1.19
Citrate	10.95	480	C00158	7001.48	5143.24	51447.78	10810.82	0	7.34	2.87
Sucrose	15.95	918	C00089	50587.51	14252.43	173264.34	33351.35	0	3.42	1.77
Hexadeconoic acid	12.3	328	C00249	4575.96	547.24	2703.61	284.49	0	0.59	-0.75
GABA	5.96	347	C00334	2265.46	143.33	1788.87	115.25	0	0.78	-0.34
Octadeconoic acid	13.494	356	C01530	4330.35	584.8	2297.78	254.04	0	0.53	-0.91
Dihydroxymandelic acid	7.715	356	C05580	928.07	54.27	583.24	103.37	0	0.62	-0.67
L-aspartic acid	8.62	349	C00049	1467.22	843.13	5594.88	1281.21	0	3.81	1.93
myo-Inositol	12.81	612	C00137	1962.13	615.14	33402.53	8810.46	0	17.02	4.08
L-isoleucine	6.575	275	C00407	0	0	316.76	92.5	0	N/A	4.16
L-valine	5.791	261	C00183	0	0	723.61	222.1	0	N/A	4.16
L-norvaline	2.929	261	C01826	20110.62	1693.04	13974.64	2435.22	0	0.69	-0.52

Table A.14. TR43477 root metabolites list. (cont.)

Metabolite	**RT**	**MW**	**KEGG/ Pubchem ID**	**Cont. Av.**	**Cont. SD**	**Tre. Av.**	**Tre. SD**	***p*-value**	**FC**	**log2 FC**
L-proline	6.601	259	C00148	0	0	604.05	215.19	0	N/A	4.16
Boric acid	3.261	278	C12486	1583.15	309.32	819.88	121.06	0	0.51	-0.94
L-tryptophan	2.79	232	C00078	1503.56	173.48	1112.37	125.45	0	0.73	-0.43
L-lysine	11.601	434	C00047	69.99	58.5	272.13	94.26	0	3.88	1.95
Galactitol	10.105	614	C01697	1084.57	178.64	690.86	41.61	0.01	0.63	-0.65
L-asparagine	9.82	348	C00152	464.35	612.85	2403.98	949.01	0.01	5.17	2.37
Decanoic acid	7.994	244	C01571	376.21	95.92	185.08	58.4	0.01	0.49	-1.02
L-serine	7.225	321	C00065	479.88	177.23	1693.08	603.03	0.01	3.52	1.81
Lactic acid	4.074	234	C00186	5137.61	1357.38	2546.46	517.38	0.01	0.49	-1.01
Myristic acid	10.99	300	C06424	28449.63	4087.22	20774.07	2583.1	0.01	0.73	-0.45
D-fructose	11.386	569	C00095, C02336	663.75	206.09	4078.24	2617.23	0.05	6.14	2.61
D-glucose	11.787	540	C00031	682.91	315.4	294.86	81.17	0.06	0.43	-1.21
Anthranilic acid	9.351	281	C00108	3234.03	1260.88	2093.58	679.84	0.16	0.64	-0.62
Glycerol	6.398	308	C00116	3491.24	299.51	3742.95	215.63	0.21	1.07	0.1
Nonanoic acid	7.132	230	C01601	890.12	277.74	685.05	185.05	0.25	0.76	-0.37
Sorbitol	12.974	614	C00794	547.76	162.68	435.97	73.65	0.26	0.79	-0.32
Hexanoic acid	4.163	188	C01585	1507.3	661.56	1124.21	96.61	0.31	0.74	-0.42
Galactonic acid	12.235	628	C00880	1563.38	451.09	1305.5	156.09	0.32	0.83	-0.26

Table A.14. TR43477 root metabolites list. (cont.)

Metabolite	**RT**	**MW**	**KEGG/ Pubchem ID**	**Cont. Av.**	**Cont. SD**	**Tre. Av.**	**Tre. SD**	***p*-value**	**FC**	**log2 FC**
Benzoic acid	6.055	194	C00180	651.2	136.35	576.6	79.44	0.37	0.88	-0.17
Fumaric acid	7.028	260	C00122	319.96	142.1	392.28	87.53	0.41	1.22	0.29
Glycine	6.698	291	C00037	758.7	539.11	532.83	133.23	0.45	0.7	-0.5
L-phenylalanine	9.468	309	C00079	447.97	296.06	574.49	113.81	0.46	1.28	0.35
Malic acid	8.36	350	C00149	20148.01	16133.15	25140.88	8505.91	0.6	1.24	0.31
D-mannitol	11.57	614	C00392	4449.23	4483.86	5812.63	3089.46	0.63	1.3	0.38
Succinate	6.723	262	C00042	1345.78	883.85	1591.57	498.89	0.64	1.18	0.24
D-gluconic acid	12.36	628	C00257	632.91	157.64	664.34	54.28	0.72	1.04	0.06
Threonate	9.006	424	C01620	563.99	162.87	521.27	165.1	0.72	0.92	-0.11
(R)-3-Hydroxybutanoate	7.403	248	C01089	336.11	92.98	317.35	118	0.8	0.94	-0.08
Glucose oxime	11.696	627	C02264	1124.95	863.1	1153.9	524.56	0.95	1.02	0.03

Table A.15. Ion contents and their statistical data for leaf tissues.

Tissue/	**ILC**		**ILT**		**TLC**		**TLT**		***p*-value (Condition or Genotype)**			
Ion	Avg (μg/g)	SEM	Avg (μg/g)	SEM	Avg (μg/g)	SEM	Avg (μg/g)	SEM	ILC vs. ILT	TLC vs. TLT	ILC vs. TLC	ILT vs. TLT
Na	3200.56	711.50	2630.8	266.42	955.9	43.95	4536.40	318.10	0.531548	0.000470	0.047587	0.003630
Mg	6912.6	423.753	6978.2	139.16	6744.6	294.62	6403.2	176.21	0.900617	0.405283	0.779220	0.052927
K	3220.4	198.52	4895.2	99.95	2604.20	113.28	4222	213.25	0.0005556	0.000919	0.050198	0.045284
Ca	6465.8	291.40	6431.4	148.82	7287.4	243.28	6982.2	120.98	0.928167	0.354681	0.090074	0.034319
Mn	251.24	23.74	230	11.64	130.06	3.91	107.81	5.06	0.500350	0.015596	0.009546	0.000223
Fe	115.99	12.89	83.34	14.14	103.94	13.12	85.26	8.73	0.165834	0.324456	0.574183	0.920976
Zn	82.91	7.74	81.96	3.85	258.82	8.08	266.3	12.24	0.925291	0.662294	0.000001	0.000069
Mo	13.11	1.50	10.42	0.43	1.21	0.21	1.24	0.13	0.186713	0.910741	0.001858	0.000013
B	33.92	4.32	26.68	0.83	47.10	4.25	38.91	3.41	0.210658	0.217989	0.087716	0.030703
Cu	8.44	0.30	6.67	0.12	9.58	0.92	7.04	0.20	0.003961	0.067807	0.340778	0.210593

Table A.16. Ion contents and their statistical data for root tissues.

Tissue/	**ILC**		**ILT**		**TLC**		**TLT**		***p*-value (Condition or Genotype)**			
Ion	Avg (μg/g)	SEM	Avg (μg/g)	SEM	Avg (μg/g)	SEM	Avg (μg/g)	SEM	ILC vs. ILT	TLC vs. TLT	ILC vs. TLC	ILT vs. TLT
Na	3933.2	286.98	11902	213.9	4146	422.22	14354.76	941.21	0.0000001	0.000137	0.720240	0.079241
Mg	9533	373.79	8969.80	217.32	10781.6	854.08	8088.4	187.21	0.285407	0.046213	0.280206	0.025641
K	6098.8	108.89	2937.6	23.38	6368.6	202.81	7293	222.85	0.000007	0.025503	0.334053	0.000055
Ca	1548.2	116.7	1195	27.86	1173.40	42.95	1089.40	24.16	0.052008	0.175876	0.042440	0.034105
Mn	133.94	7.97	90.64	5.61	344.5	68.25	177.41	24.89	0.005084	0.094286	0.050369	0.033796
Fe	1031.8	127.32	704.52	77.29	1644.96	619.72	740.7	98.48	0.092639	0.263811	0.431357	0.802912
Zn	1674.8	80.12	1143.40	31.28	1214.12	64.93	1184.2	44.42	0.002360	0.743602	0.004328	0.522796
Mo	140.04	15.41	171.9	8.35	10.14	2.53	7.63	1.02	0.153725	0.446274	0.001412	0.000051
B	2.68	0.5	3.81	0.51	2.74	0.17	6.22	0.52	0.191954	0.002626	0.920176	0.018254
Cu	67.14	1.55	85.11	0.89	72.44	3.28	100.76	4.56	0.000076	0.002522	0.241887	0.035853

APPENDIX B: SUPPLEMENTARY INFORMATION FOR THE KNOCKDOWN STUDY

Table B.1. Ion contents of the composite plants. M: Mean; SD: Standard deviation; ppt: parts per thousand.

Sample	Control M. (ppt)	Control SD	Treatment M. (ppt)	Treatment SD	log_2FC
Na-Leaf					
Blank	30.72	18.72	3823.33	631.09	6.95
HumFer	66.34	45.49	4276.33	651.06	6.01
SucPho	32.78	6.52	4604.36	977.17	7.13
Na - Root					
Blank	297.61	47.53	3470.88	284.24	3.54
HumFer	308.64	53.04	2951.97	473.98	3.25
SucPho	206.99	34.12	4006.9	345.03	4.27
K - Leaf					
Blank	4197.62	402.9	5248.53	218.94	0.32
HumFer	4278.77	354.14	5764.76	346.85	0.43
SucPho	3581.98	291.02	6951.51	370.64	0.95
K - Root					
Blank	4618.98	1006.36	2975.92	213.06	-0.63
HumFer	4752.33	653.69	2937.41	239.93	-0.69
SucPho	2309.2	260.48	4415.77	468.31	0.93
Ca - Leaf					
Blank	2339.7	288.84	2841.23	507.56	0.28
HumFer	1960.86	131.91	1983.84	163.81	0.01
SucPho	4243.24	410.78	1944.59	224.26	1.12
Ca - Root					
Blank	1500.39	445.43	1618.42	143.51	0.1
HumFer	1514.56	168.04	1358.57	121.37	-0.15
SucPho	1997.09	203.43	1012.11	87.56	-0.98

Table B.1. Ion contents of the composite plants. (cont.)

Sample	Control M. (ppt)	Control SD	Treatment M. (ppt)	Treatment SD	log_2FC
Mg - Leaf					
Blank	285.21	42.61	256.58	29.11	-0.15
HumFer	298.49	30.34	264.3	21.55	-0.17
SucPho	217.61	18.78	367.24	28.91	0.75
Mg - Root					
Blank	982.42	600.97	1527.62	557.3	0.63
HumFer	670.31	300.42	654.02	269.46	-0.03
SucPho	770.31	317.93	277.15	20.26	-1.47

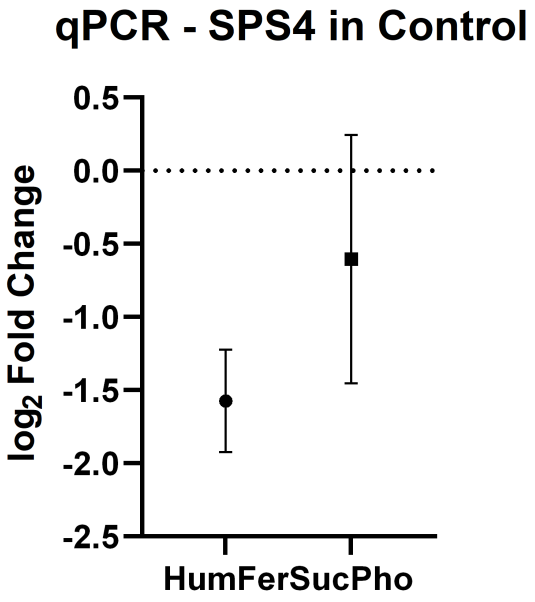

Figure B.1. RT-qPCR evaluation of *pvSPS4* expression in control conditions for HumFer and SucPho roots. Values represent±SEM.

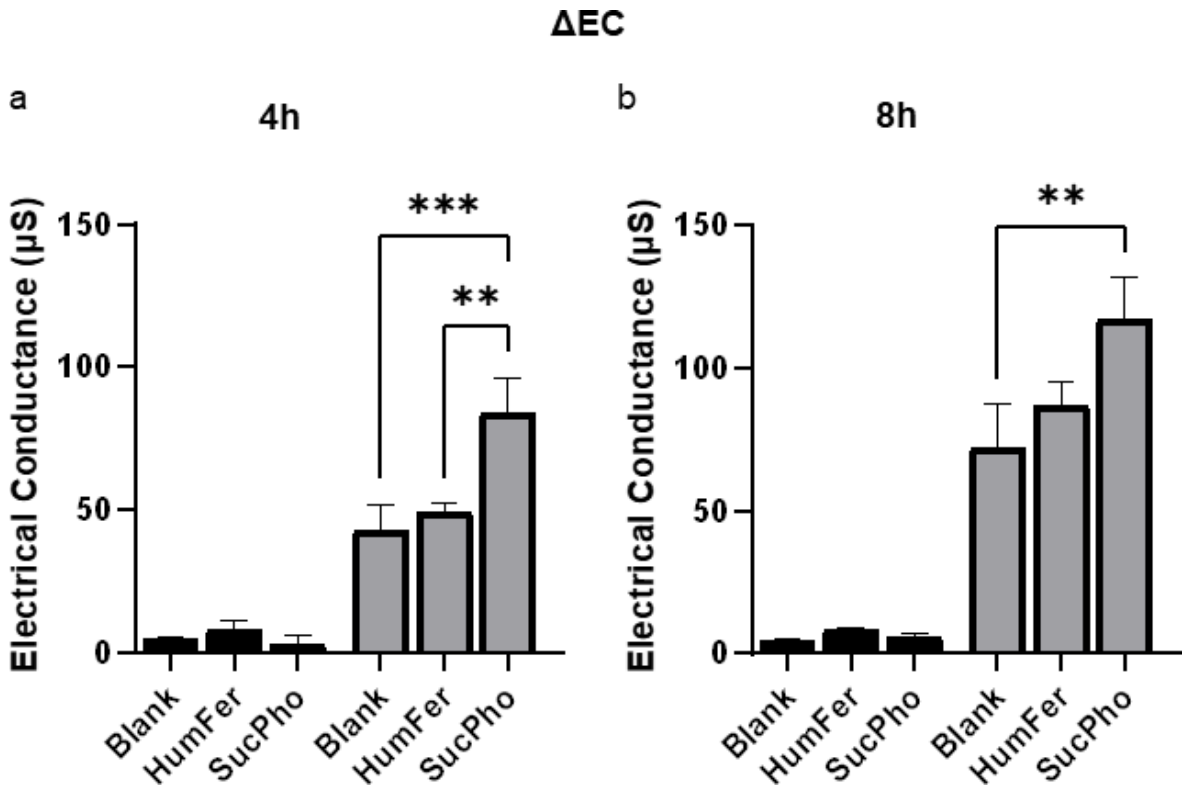

Figure B.2. Examination of the changes in electrical conductivity after 4 hours (a) and 8 hours (b) of sampling. Values represent±SEM.

APPENDIX C: COPYRIGHT INFORMATION

Permission to reproduce FAO copyright material (Figure 1.1) is granted at no charge, including the right to publish, reproduce, publicly display and distribute the whole or any part of the material in this and all revisions and any subsequent editions of this work; in any ancillary aids that may be prepared to accompany this work, including promotion and publicity uses; and in all forms of media now known or later developed.

FAO remains the copyright holder of the material, and retains the right to reproduce, translate, publish, and disseminate the whole or any part of it in print and electronic formats, and to grant others the right to do the same, as well as to incorporate material derived from the material in any subsequent work.